UNI
BASEL

Artificial Phosphate Transferases and Hydrogen Tranferases Based on Biotin-Streptavidin Technology

Inauguraldissertation

Zur

Erlangung der Würde eines Doktors der Philosophie

vorgelegt der

Philosophisch-Naturwissenschaftlichen Fakultät
Der Universität Basel

von

Thibaud Rossel

aus Prêles, Bern

Basel, 2011

Genehmigt von der Philosophisch-Naturwissenschaftlichen Fakultät auf Antrag von Prof. Dr.

Thomas R. Ward und Prof. Dr. Helma Wennemers

Basel, den 29 März 2011

Prof. Dr. Martin Spiess

Dekan

To my family

Table of contents

CV 177

Acknowledgements

Ruben Cal, Jennifer Zampese, Valérie Jullien, Gaëlle Contesse, Lauriane Contesse, Charlène Contesse, Rocio Palmadés and all the others.

Finally, the most important, I would like to thank my family for their unconditional support during all these years.

I finish by addressing my gratitude to a special person, Stéphanie Gfeller for sharing a piece of my life during this PhD.

Abstract

Enzymes have been the subject of numerous studies and have been extensively used to catalyse difficult chemical reactions. By extension, artificial metalloenzymes that bridge the gap between organometallic catalysis and enzymatic catalysis are attracting increasing attention in the scientific community due to their optimization potential by chemical and genetic methods. The active site of such artificial systems are based on the versatility of organometallic complexes, whereas the molecular scaffold, that provides the enantioselectivity as in natural enzymes, generates the second coordination sphere. The first part of this thesis presents new artificial metallohydrolases incorporating Ce(IV) as the active catalyst. The interest in this new class is motivated by the possibility to create new highly selective artificial nucleases for novel biomedical applications. The use of chiral substrates mimicking DNA or RNA coupled with colorimetric assay techniques allows developing high throughput screening methods to identify novel active and selective artificial metalloenzymes. The knowledge acquired by the creation of novel artificial hydrolases allows transposing the technology to a new class of artificial metalloenzymes such transfer hydrogenases. The second part of this thesis presents the incorporation of catalytically active biotinylated complexes within streptavidin, creating artificial metalloenzymes for the transfer hydrogenation of prochiral ketones. The optimization of the second coordination sphere, based on a crystal structure of the active hybrid catalyst and successive rounds of saturation mutagenesis at selected positions termed "designed evolution", afforded highly active and selective catalysts for the reduction of challenging ketone substrates. The well-defined active site of the hybrid catalysts can be redesigned for the reduction of novel substrates such as imines to create the first example of an artificial imine reductase.

Résumé

Les enzymes sont d'excellents catalyseurs qui ont fait l'objet de nombreuses études et qui ont été extensivement utilisées dans l'accélération de réactions chimiques difficiles. Par extension, les métalloenzymes artificielles qui tirent avantage de la catalyse organométallique et enzymatique attirent de plus en plus l'attention de la communauté scientifique de par leur excellent potentiel d'optimisation donné par leur diversité chimique et biologique. Le site actif de ces systèmes artificiels est basé sur la versatilité du complexe organométallique alors que l'échafaudage moléculaire fournit l'énantioselectivité à travers la seconde sphère de coordination, comme chez les enzymes naturelles. La première partie de la thèse présente de nouvelles hydrolases artificielle incorporant un Ce(IV) comme catalyseur actif. L'usage de substrat chiraux imitant l'ADN ou l'ARN couplé à des techniques d'analyse colorimétriques permet de développer des méthodes de criblage à haut débit pour identifier des nouvelles métallohydrolases artificielles actives et sélectives. Les connaissances accumulées par la création de nouvelles hydrolases artificielles permettent de transposer la technologie à une nouvelle classe de métalloenzymes artificielles telles que les transferts hydrogénases. La deuxième partie de la thèse présente l'incorporation de complexes biotinylés actifs au sein de la streptavidine engendrant une métalloenzyme artificielle pour le transfert hydrogénant de cétones prochirales. L'optimisation de la seconde sphère de coordination basée sur la structure cristalline du catalyseur hybride actif et des cycles de mutagénèse par saturation à des positions sélectionnées permet le design d'un protocole d'évolution pour générer des catalyseurs hautement actifs et sélectifs pour la réduction de substrats difficiles. Le site actif bien défini du catalyseur hybride peut être ré-optimisé pour la réduction de nouveaux substrats tels que les imines. Ceci permet d'obtenir le premier exemple d'une imine réductase artificielle.

List of abbreviations

$\subset$	included in
Å	Angström
ADH	Alcohol dehydrogenase
ATH	Asymmetric Transfer Hydrogenation
Ar	Arene
Avi	Avidin
BAPA	Bis(2-amino-pyridinyl-6-methylamine)
Biot	Biotin(yl)
B_4F	Biotin-4-fluoresceine
BINAP	2,2'-Bis(diphenylphosphino)-1,1'-binaphthyl
BINOL	1,1'-bi-2-naphthoL
BSA	Bovine serum albumin
BNPP	Bis (4-nitrophenyl phosphate)
CAN	Ceric Ammonium Nitrate
CLEAs	Cross-Linked Enzyme Aggregates
CTAB	Cetyl trimethylammonium bromide
Dex	Dextran
DMF	Dimethylformamide
DMSO	Dimethylsulfoxide
DNA	Deoxyribonucleic acid
DTPB	1,1,4,7,7-pentakis(1H-benzimidazol-2-ylmethyl)-1,4,7-triazaheptane
ds-DNA	double stranded DNA
ss-DNA	single stranded DNA
EDTA	Ethylenediaminetetraacetic acid
ee	enantiomeric excess
eq.	equivalent(s)
E	Enzyme
EP	Enzyme-Product
ES	Enzyme-Substrat
ESI	Electron Spray Ionisation
Et	Ethyl
Et_3N	Triethylamine
Glu	Glutaraldehyde
HABA	4-hydroxyazobenzene-2-carboxylic acid
HPLC	High Performance Liquid Chromatography
HXTA	5-methyl-2-hydroxy-1,3-xylene-α,α-diamine-N,N,N',N'-tetraacetic acid
HPNP	2-hydroxypropyl-*para*-nitrophenylphosphate
HTS	High Throughput Screening
IDA	Iminodiacetic acid
L-DOPA	L-3,4-dihydroxyphenylalanine
M	Metal
Me	Methyl
min.	minute(s)

MOPS	3-(*N*-morpholino)propanesulfonic acid
MOV	Mervein-Pondorf-Verley
MPGNs	Monolayer Protected Gold Nanoparticules
MS	Mass Spectrometry
NMR	Nuclear Magnetic Resonance
P	Product
PCR	Polymerase Chain Reaction
PDB	Protein Data Bank
PEI	Polyethylene imine
PNA	Peptide Nucleic Acid
RMS	Root Mean Square
r.t.	room temperature
Sav	Streptavidin
SDS	Sodium dodecylsulfate
TACN	1,4,7-triazacyclononane
TAMEN	N,N′-Tetra(4-antipyryl-methyl)-1,2-diaminoethane)
t_1, t_2	Retention times (min.)
Temp.	Temperature
TH	Transfer hydrogenation
TOF	Turnover frequency
TON	Turnover number
TS	Transition State
TsDPEN	*N*-(*p*-toluenesulfony1)-1,2-diphenylethylenediamine
WT	Wild-Type

Chapter 1:
Introduction

«Douter de tout ou tout croire sont deux solutions également commodes, qui l'une et l'autre nous dispensent de réfléchir »

Henri Pointcarré

Chapter 1: Introduction

1. General introduction to catalysis[1]

Catalysis stems from the Greek meaning, "down and loosen". Barzelius coined the term catalysis in 1836, proposing that beside the "affinity force", a new force is operative that he termed the "catalytic force". At that time, affinity was known as a driving force but there was no understanding at the molecular level of reaction rates. However, catalysis has already been exploited thousands years before in the fermentation process. In the Middle Ages, sulfuric acid was produced by burning sulfur with nitric acid in humid air without knowing that nitric acid catalyzed the reaction. At the end of the eighteenth century, the decomposition of several substances by metal oxides was described by different scientists. In 1834, Faraday proposed that reactants have to absorb simultaneously on the surface of a compound to react but didn't give further explanations. Finally Ostwald proposed that a catalyst does not influence the thermodynamic equilibrium of reactants and products but affects the rate of chemical reactions. Ostwald won the Nobel Prize in chemistry in 1909 for his work.

A catalyst is an entity, which is able to accelerate a chemical reaction by decreasing the energy of its transition state. The catalyst is not chemically changed at the end of the reaction and can be recovered and reused for other cycles. Catalysis plays a major role in many chemical processes such as plastic production, organic synthesis of fine chemicals, medicine applications, energy production or environmental protection. Some famous catalytic processes were described and used extensively in industry such as:

- The Haber-Bosch chemical process that transforms nitrogen into ammonia[2] using iron oxide as a catalyst. Fritz Haber received the Nobel Prize in chemistry in 1918 and Carl Bosch in 1931 for the discovery of this process and its optimization.

- The Fisher-Tropsch chemical process that transforms carbon monoxide and hydrogen into hydrocarbons using iron or cobalt as catalyst.[3]

- The three way catalyst used to purify car exhausts by oxydoreduction reactions using a so-called catalytic converter containing platinum metals as catalysts.[4]

Catalysis has been a major research area for decades and major efforts have been invested in this context to understand the molecular mechanism of such reactions. The Nobel Prize in chemistry was awarded to Noyori, Sharpless and Knowles in 2001, to Chauvin, Grubbs and Schrock in 2005 and to Heck, Negishi and Suzuki in 2010 for their research on catalytic systems, thus demonstrating that the field is still of great importance in chemistry and able to generate major discoveries used to solve scientific current problems.

1.2 Catalyst performances[5]

Catalysts participate in chemical reactions by changing the kinetics, while the overall thermodynamics are the same. The following factors can explain the effect of a catalyst on the reaction:

1) Stabilization of the transition state

2) Decrease of the entropy of the reactants by interactions that force their proximity and by favorable spatial orientation

3) Selective enhancement of one specific pathway over the competing undesired ones.

Different types of catalysts are presented in literature: homogeneous catalysts, heterogeneous catalysts and enzymatic catalysts.

1.2.1 Enzymes[5]

Enzymes are a class of macromolecules (see figure 1) that bind small molecules and affect reactions (see figure 1). In an enzymatic reaction, a complex between the substrate and the

enzyme is formed [ES], this [ES] complex passes through a transition state ($\Delta G^{\neq}_{cat,}$ figure 2) and converts to the enzyme product complex [EP] and finally to the free enzyme and free product. From the formulation of the reaction sequence, a rate law can be derived. In enzyme catalysis the first rate law that described the process was Michaelis and Menten's law in 1913; the corresponding mechanism is therefore named the Michaelis-Menten mechanism.
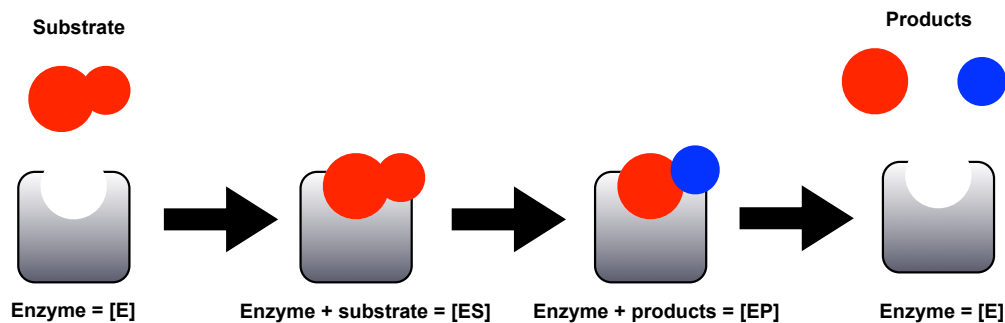
Figure 1 Reaction sequence

Enzyme Kinetics from binding and catalysis:

In the first step, the enzyme (E) and the substrate (S) associate in a rapid and reversible equilibrium to obtain an enzyme-substrate complex (ES) with a dissociation constant called K_s. A reaction occurs in the second step to obtain the product with a rate constant k_2.
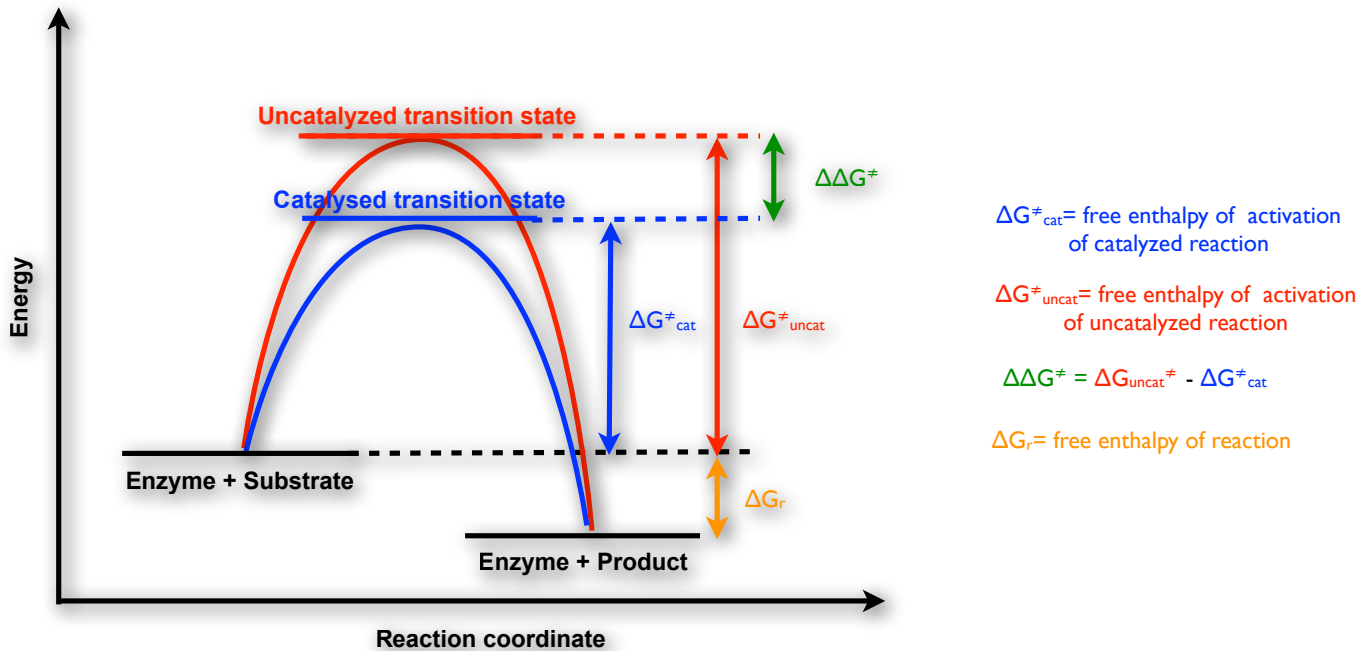
Figure 2 Free enthalpy reaction coordinate diagram for an enzyme reaction.

Other intermediates can take place in this reaction to form for example an enzyme-product complex. An apparent dissociation constant can be defined called K_M that represents the overall dissociation constant of all the enzyme-bound species. In the Michaelis-Menten equation, only an ES complex is involved and the binding step is considered to be fast therefore k_2 is assimilated as k_{cat} (the overall catalytic rate) and in this situation $K_M = K_S$. (See equation 1)

$$E + S \underset{}{\overset{K_M}{\rightleftharpoons}} ES \underset{}{\overset{k_{cat}}{\rightleftharpoons}} E + P \qquad v \text{ (initial reaction rate)} = \frac{[E]_0 [S] k_{cat}}{K_M + [S]} \text{ (Equation 1)}$$
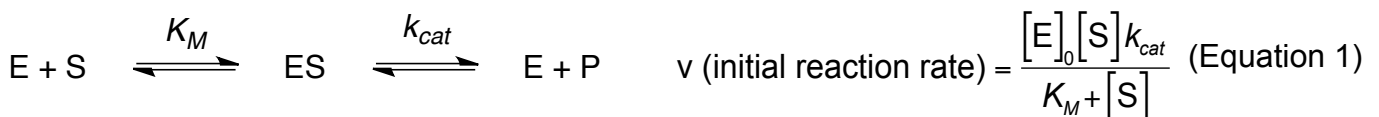
The activity of the enzyme is determined by the value of k_{cat} (moles of converted substrate per mole of catalyst per unit of time). k_{cat}/K_M is called the catalytic efficiency and describes the specificity of the enzyme for competing substrates and thus its general synthetic utility. Both high activity and low product inhibition must be optimised for applications in catalytic processes. Finally, two important parameters for a catalyst is the turnover over number (TON) which is the number of

moles of product per mole of catalyst before its inactivation (representative of the product inhibition) and the turnover number frequency (TOF) that represents the number of moles of product per mole of catalyst per hour. Both parameters must be as high as possible to obtain a good catalyst.

1.2.2 Homogeneous catalysis

Homogeneous catalysis is a sequence of reactions that involves a catalyst in the same phase as the reactants. Most commonly, a homogeneous catalyst is dissolved in a solvent with the reactants. Homogeneous asymmetric catalysis refers to the introduction of an asymmetric center in the prochiral substrate after reaction with the asymmetric catalyst.[6]

There are two types of homogeneous asymmetric catalysts:

- organometallic catalysts

- organocatalysts

The first type has found most applications in enantioselective synthesis.[7] A complementary method, which has attracted renewed interest in recent years, is enantioselective organocatalysis, in which the reaction is mediated by a small chiral organic molecule.[8a]

Homogeneous catalysis by transition metal complexes was extensively studied since the 1940's. G. Wilkinson provided a major contribution to the field with alkene hydrogenation using rhodium-based catalysts and this discovery had a major impact on the synthesis of organic compounds.[8b] Later on, Knowles[9] and Horner[10] modified Wilkinson's catalyst for the asymmetric hydrogenation of prochiral enamines. An important contribution was introduced when Kagan and Dang described DIOP, a biphosphine ligand bearing the chirality within the carbon skeleton for the asymmetric hydrogenation of dehydroamino acids.[11] In addition, Knowles made a significant discovery with

Introduction

the C_2-symmetric chelating P*-stereogenic biphosphine DIPAMP employed with Rh(I) for the industrial production of L-DOPA involved in the treatment of Parkinson's disease.[12] In the 1990's, the next breakthrough was Ru(II)-BINAP introduced by Noyori for the asymmetric hydrogenation of prochiral olefins and keto groups to produce enantiomerically enriched compounds with excellent enantioselectivity.[13] Finally, K.B. Sharpless developed chiral catalysts for asymmetric oxidation reactions.[14] R. Noyori, W.S. Knowles and K.B. Sharpless received the Nobel Prize in 2001 for their work on enantioselective catalysis.[15]

1.2.3 Heterogeneous catalysis

Heterogeneous catalysis concerns catalysis where the phase of the catalyst differs from that of the reactants. Many different phases can be exploited such as solid, liquid, gas phases but also immiscible liquids. Most of the heterogeneous catalysts are solids and react with liquid or gases. The reactants diffuse to the catalyst surface and react with it through the formation of a chemical bond. After the reaction, the products desorb from the surface and diffuse away. Heterogeneous catalysis is involved in important industrial chemical processes and energy production and has earned Nobel prizes to Fritz Haber in 1918, Carl Bosch 1931, Irving Langmuir in 1932, and Gerhard Ertl in 2007 (and few others).[6]

1.2.4 Artificial metalloenzymes

In the past decades, enantiomerically pure compounds have been obtained using different approaches: homogeneous catalysis with transition metal catalysis, organocatalysis or biocatalysis.[16] In this context, each field has evolved separately but efforts have been made to bridge the gap between these three domains. Artificial metalloenzymes are becoming of interest as they take the best features from the mentioned fields of catalysis. They consist of a hybrid catalyst

in which a catalytically active transition metal complex is incorporated into a host biomacromolecule, typically a protein[17] or DNA.[18]

It is widely assumed that the catalytic activity and selectivity of the transiton metal catalyst is almost exclusively controlled by the first coordination sphere provided by the chelating ligand. In contrast, enzymatic catalysis is known for its second coordination sphere interactions through hydrogen bonding or hydrophobic interactions. This provides a valuable contribution to activity and selectivity by complementing the transition state of the catalytic center.[19] Various approaches can be followed to create active and selective artificial metalloenzymes. One approach is the *de novo design* of such catalysts. It is based on the formation of a polypeptide not correlated to any natural protein. It would lead the possibility to obtain high activity and enantioselectivity from the start. One example of this system is the formation of alpha helical bundles used to mimic artificial heme proteins.[20] However the system suffers from poor knowledge of protein folding.

In contrast to the *de novo* design, some other systems have been developed such as creating active sites in existing native biomolecular scaffolds, like proteins or DNA. It presents the advantage of thermodynamic stability and tolerance to mutagenesis of the biomolecule.[21]

Introduction

Three key parameters for the formation of a highly efficient artificial metalloenzyme are: the transition metal containing cofactor, the biomolecular scaffold and the mode of attachment of the cofactor. The choice of the transition metal catalyst is guided by the desired catalytic activity. Futhermore, this activity must be orthogonal to the catalytic activity of the scaffold itself. The catalyst must also be tolerant to water as enzymes are active in water.[19, 22]

Chemical properties of the scaffold such as pH tolerance, temperature stability and resistance to organic solvents are crucial to obtain a robust artificial metalloenzyme. Furthermore, it is important to choose between an existing active site or a new active site created in the protein. The existing active site presents the advantage of being well defined and therefore can be re-engineered to optimize the performances of the catalytic system. The best example of such an artificial enzyme is the pioneer work of Wilson and Whitesides.[23] Avidin was used as a proteic scaffold because of its strong affinity for biotin and therefore for the biotinylated catalyst. In its deep pocket, both catalyst and substrate can be accommodated and the reaction outcome is partially dictated by the second coordination sphere around the catalyst given by the protein. However the system is limited by the need of a cavity able to accomodate both the catalyst and the substrate. Many systems were obtained with such an approach and some of the best examples are Avidin[23], Streptavidin[22a], Bovine Serum Albumin (BSA)[24] and apo-myoglobin.[25] All of them achieved good to high enantioselectivity. Some other Scaffolds like papaïn[26], cutinase[27], carbonic anhydrase[28] and tHisf as well.[29]

The alternative to active site redesign is to create a new active site in an existing biomolecular scaffold. The advantage of this approach is to extend the number of scaffolds that can be used. Some famous examples were given by the Roelfes-Feringa's system[31] in which the active site is created near the DNA groove by binding a transition metal complex to DNA. In this situation the

second coordination sphere is provided by the DNA allowing production of one enantiomer of the product.

Finally, a particular category of artificial metalloenzyme are proteins with a large vacant space *e. g.* the iron storage protein ferritin. The space allows the incorporation of metallic nanoparticles. In this context, the protein-encapsulated nanoparticles have been investigated for their catalytic properties. In this approach, the enantioselectivity is not necessarily important, as the hybrid system works more as a container or a reactor to grow nanoparticles of a certain size and shape that could be important for catalysis. Furthermore, the pores of the protein cage can be used to discriminate against substrates of different sizes.[32]

1.2.5 Anchoring strategies

In order to ensure the localization of the metal catalyst on the host scaffold, three strategies have been followed (see figure 3). The first is non-covalent and is based on anchoring through supra-molecular interactions. The second approach relies on covalent anchoring. The supra-molecular approach is based on strong and highly specific non-covalent interactions between biopolymers and small molecules or possibly ligands/inhibitors to generate artificial enzymes.[17] The perfect example of such a system is the biotin-streptavidin technology.[33] The third anchoring strategy is closely related to supramolecular anchoring but involves dative bonds, which refers to coordination between the catalytic metal ion and functionalities presented by the scaffold. Artificial metalloenzyme based on Iron or Manganese corrole in serum albumin[34] or Cr(III) Schiff base into apomyoglobin[25] are examples of this anchoring approach. These systems are used for enantioselective sulfoxidation and the metal-moiety presents the advantage of being precisely positioned in the scaffold.

a)   b)   c)

Figure 3 Anchoring strategies: supramolecular a) dative b) covalent c). M represents the catalytically active moiety.

The last strategy that can be envisaged is covalent anchoring. This method is based on the seminal work of Kaiser[35] where a cystein was used as the anchoring site. It allows site-selective anchoring. The system presents the advantage of having a precisely localized complex in the scaffold but it suffers from evolution limitation involving chemical modifications and non-trivial purification steps.

2. The biotin-streptavidin technology as a supramolecular anchoring strategy

The choice of a supramolecular anchor is important to create new artificial metalloenzymes. In this context, supramolecular anchoring seems to be more promising than the other systems because it allows separate variations, which can be further combined to generate consequent diversity. In addition, no chemical modification is needed after the incorporation of the catalyst precursor, ensuring the integrity of the catalytic moiety. As described previously, a strong interaction is

needed between the catalytic moiety and the scaffold. In this respect the biotin-streptavidin couple is a robust system to create artificial metalloenzymes with a high affinity between biotin or the biotinylated catalyst and (strep)avidin.[36]

2.1 Biotin-streptavidin affinity

The affinity constant of biotin for streptavidin is one of the strongest non-covalent interactions known in nature (K_a= $1.7 \cdot 10^{15}$ M^{-1} for avidin and K_a = $2.5 \cdot 10^{13}$ M^{-1} for Sav).[37] Derivatized biotinylated conjugates have a strong affinity for the protein even if slightly lower than biotin.[38]

2.2 Stability

Streptavidin has an excellent stability in the range of several minutes at 110°C (tetramer with 4 eq. of biotin), and an extreme resistance to pH variations (the denaturation of streptavidin requires 6M guanidinium chloride at pH = 1.5). The tetramer containing biotin is also resistant to high concentrations of organic solvents like ethanol (at 50% concentration) and to the presence of surfactants such as sodium dodecyl sulfate (SDS).[39]

2.3 Protein expression

Avidin[40] and streptavidin[38a, 40-41] can both be produced as recombinant proteins with high yields (about 200 mg per liter of E.coli culture for streptavidin). In addition, the two expressed proteins are easy to purify by affinity chromatography with immobilized iminobiotin.

2.4 Structural and functional informations

The exceptional properties of avidin and streptavidin are the reason for the wide interest of the scientific community for these proteins. The biotin (strep)-avidin system has been the subject of numerous practical applications and is an interesting model system for studying the affinity of macromolecules for small ligands. Many avidin and streptavidin variants, some including biotin

inside the binding pocket have been crystallized. Knowledge of the three dimensional structure of both avidin and streptavidin allows the comparison of their binding features towards biotin in more detail. Both proteins fold in an eight-stranded antiparallel β-barrel and their quaternary structure is composed of four identical barrels. Futhermore, each subunit of the protein has a single biotin-binding site (see figure 4). X-ray data has revealed that the residues responsible for the strong affinity are divided in two groups: the hydrophilic and the hydrophobic amino acids.[42]
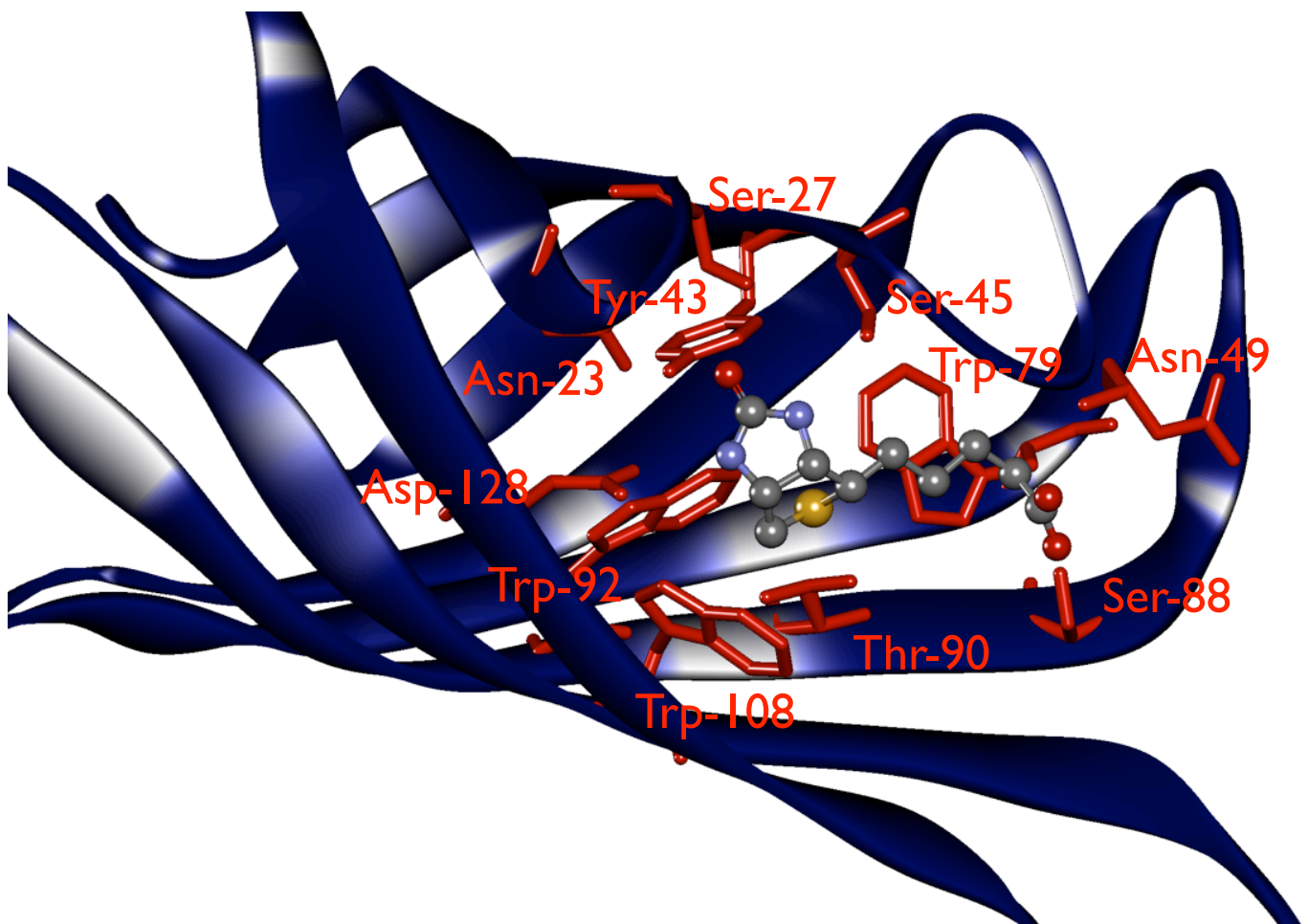
Figure 4 Streptavidin monomer (blue) binding biotin (ball and stick). Amino acids involved in biotin binding are displayed as sticks (Trp-120 not shown). PDB 1MK5.

2.5 Hydrophobic interactions of biotin⊂(strep)avidin

In avidin the residues responsible for the hydrophobic interactions of the amino acids with biotin are Trp-70, Phe-72, Phe-79, and Trp-97 from one monomer and Trp-110 from the adjacent monomer. Whereas in streptavidin (see figure 4 and 5b), these amino acids are Trp-79, Trp-92, Trp-108 from one monomer and Trp-120 from the adjacent monomer.[42b, 42e]

2.5 Hydrophilic interactions of biotin ⊂ (strep)avidin

For avidin (see figure 5a), three amino acid residues are involved in hydrophilic interactions: Asn-12, Ser-16 and Tyr-33. Each of them forms a hydrogen bond with the ureido oxygen of biotin. In addition, the ureido nitrogens of biotin are involved in hydrogen bond interactions with Thr-35 and Asn-118 while the sulfur of biotin interacts with Thr-77. The carboxylate of biotin forms five hydrogen bonds, with one oxygen of the carboxylate interacting with Ala-39, Thr-40 and Thr-38. The other oxygen is involved in hydrogen bonding with Ser-73 and Ser-75. The pattern of hydrogen bonding of biotin into streptavidin is similar to avidin. The oxygen of the ureido group is forming three hydrogen bonds with Asn-23, Ser-27 and Tyr-43. The ring nitrogen forms a hydrogen bond with Ser-45 and Asp-128. The biotin sulfur is interacting through a hydrogen bond with Thr-90. Finally, the carboxylate oxygens of the biotin valeric acid moiety form two hydrogen bonds, one with Asn-49 and the other with Ser-88.[42b, 42e]

2.6 Hydrogen bonding pattern in the loop L3,4

In avidin (see figure 5a), the loop L3,4 is three amino acids longer than the corresponding loop in streptavidin (residues 36-44 in avidin and 45-50 in streptavidin). In the apoproteins, the loop L3,4 in both avidin and streptavidin has an opened disordered conformation. When biotin is added to the apoprotein, the loop closes. The difference in length of the loop is the reason the hydrogen-bonding network is different with the carboxylic part of biotin. It is also believed that the presence

of Phe-72 and three additional hydrogen bonds are the reason of the stronger binding affinity of biotin to avidin in comparison with Streptavidin.[7a, 43]

a)   Avidin binding pocket with amino acids interactions around biotin
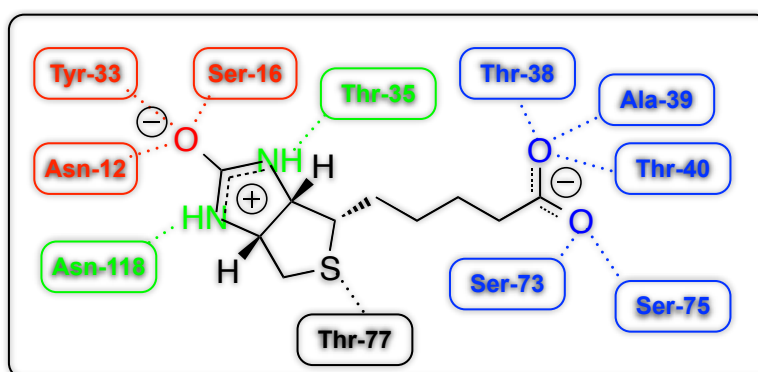
b)   Streptavidin binding pocket with amino acids interactions around biotin
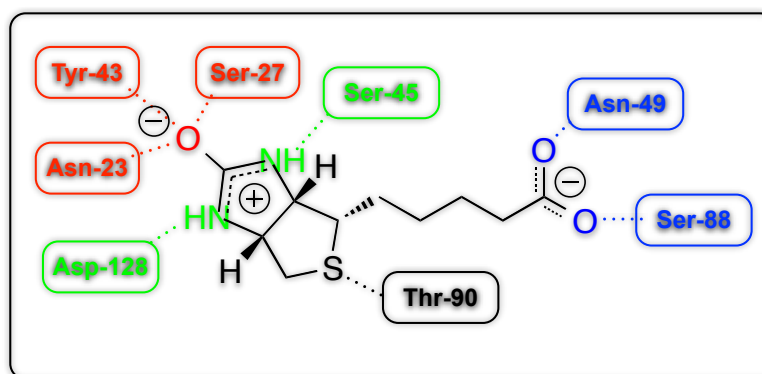
Figure 5 First coordination sphere hydrogen bonding of biotin ⊂ avidin and biotin ⊂ streptavidin.

3. Biological and chemical diversity

The chemogenetic approach[44] of artificial metalloenzymes has the potential for providing hybrid catalysts "made to order". The biological diversity is provided by the scaffold library based on proteins or DNA whereas the chemical diversity is provided by a catalyst library further anchored into the scaffold e. g. biotin-(strep)avidin system. Combination of the two libraries forms a hybrid

catalyst collection that can be screened for a specific reaction. The good one can be further improved for activity or selectivity.

The optimization of artificial metalloenzymes developed with biotin-streptavidin technology in the Ward group relies on the so-called "designed evolution".[45] (see figure 6).

Designed evolution incorporates rational decisions on scaffolds the corresponding elements, followed by rounds of screening to improve those elements that cannot be predicted.[46, 47]

The success of designed evolution protocols depends on two important decisions when applied to hybrid metalloenzymes. First, the appropriate homogeneous catalyst and second, the 2nd robust scaffold providing a well defined coordination sphere: *e. g.* avidin or streptavidin.[48]

If a crystal structure of the hybrid catalyst is available, amino acid close to the metal center (less than 10 Ångströms) can be selected and mutated to identify variants yielding good conversion and enantioselectivities towards a given substrate.[49] In this sense, the crystal structure guides the screening to identify rapidly the best variants (see figure 6).

In addition, all the results combined give an insight on the reaction mechanism and therefore allow the optimization of the second coordination sphere around the catalyst leading to genetic evolutionary approaches. (see figure 6)
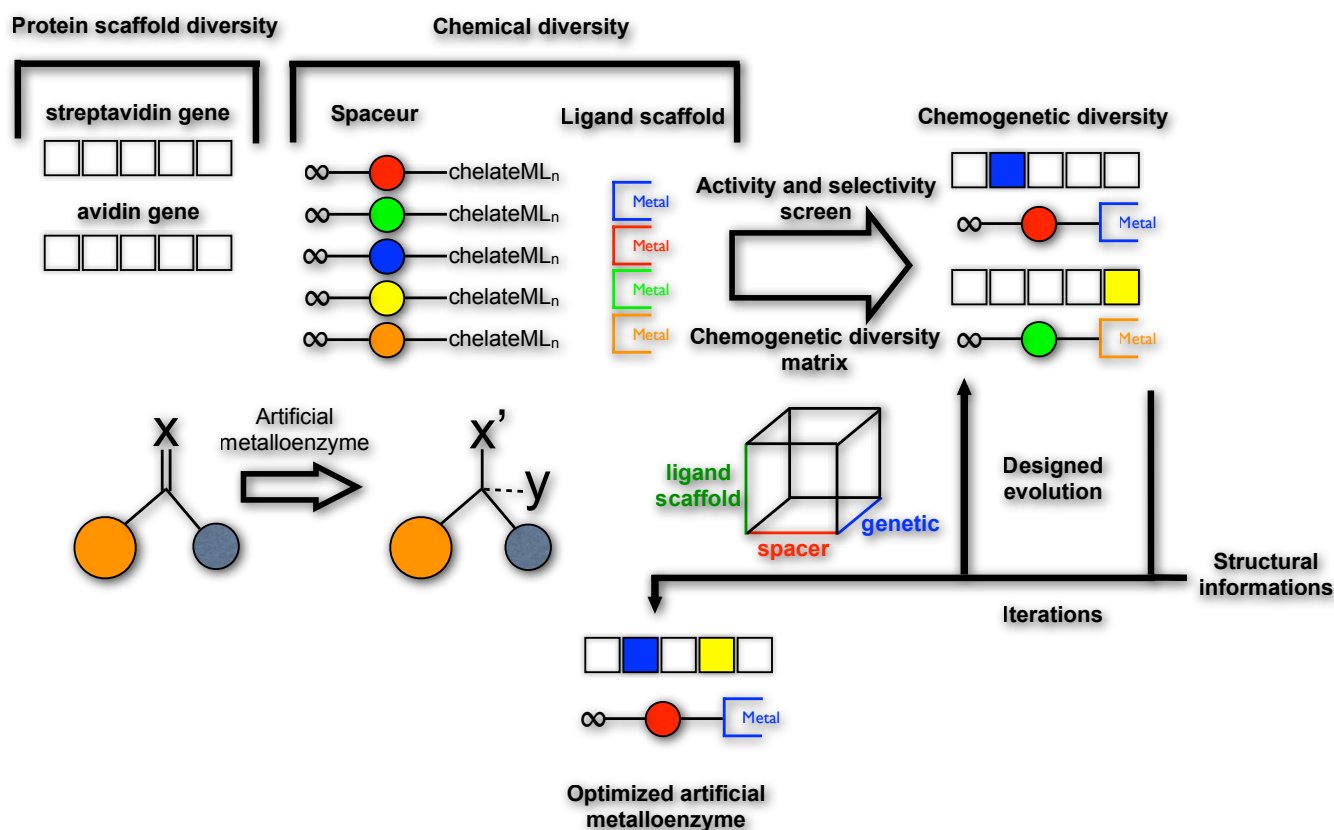
Figure 6 Designed evolution of an artificial metalloenzyme for asymmetric catalysis based on the biotin-(strept)avidin technology.

4. Enantioselectivity and chirality

The term "chiral" is used to describe an object that is not superimposable on its mirror image (see figure 7). By extension, in chemistry, "chiral" describes a molecule that is not superimposable to its mirror image. Chirality is a property of matter that can be found in biological systems from small molecules such as carbohydrates, amino acids and lipids to the layout of the entire organism.

Since life is based on chiral molecules, understanding and creating enantioselective processes is one of the most fascinating areas in organic chemistry.[6]
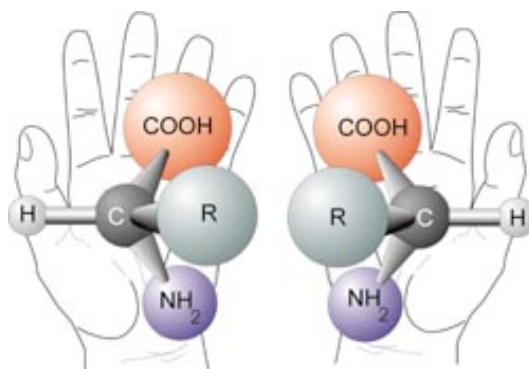
Figure 7 Pair of enantiomers of amino acids not superimposable on each other.

Chiral compounds have gained attention in many domains such as the pharmaceutical industry, biochemicals, pesticides, aroma and flavour compounds, dyes and pigments, polymers, and liquid crystals and others (see figure 8).
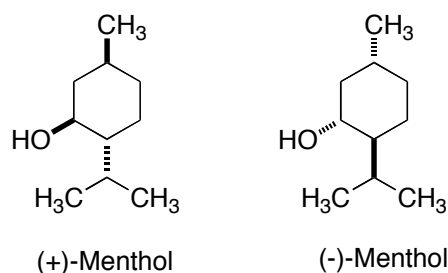
(+)-Menthol   (-)-Menthol

Figure 8 The two enantiomers of menthol display different tastes: the (+)-enantiomer has a sweet, fresh, minty, strong cooling effect taste while the (-)-enantiomer has a dusty, vegetable, less minty, less cooling taste.

A 1:1 mixture of two enantiomeres of a chiral compound is called a racemic mixture. The ratio between both enantiomers can be quantified with spectroscopic (NMR), polarimetric or

chromatographic techniques where the excess of one enantiomer over the other is given by the enantiomeric excess, *ee* (see equation 3)

$$ee = \frac{[R] - [S]}{[R] + [S]} \qquad \text{(equation 2)}$$

Different strategies can be exploited for the preparation of enantiopure compounds:[50]

1) Chemical modification of "chiral pool" molecules such as natural enantiopure molecules (amino acids, sugars, alkaloids, terpenes).

2) Resolution techniques (separation of diastereoisomers, enzymatic resolution).

3) Dynamic kinetic resolution allowing the transformation of a racemic starting material into a single enantiomer.

4.1 Enantioselectivity of homogeneous catalysts

Many non-biological metals have been used in synthetic chemistry as homogeneous catalysts. One of the best example is given by Wilkinson's catalyst [RhCl(PPh$_3$)$_3$] for the hydrogenation of olefins[8b] or the derived work of William S. Knowles for asymmetric hydrogenation.[9]

Knowles' discovery showed that transition metals could be placed within a chiral environment provided by enantiopure ligands to carry out asymmetric catalysis.

Many examples of asymmetric metal-catalysis have been given since the seminal work of Knowles. Some of the best examples are Noyori's Ru(II) Ts-DPEN derived complexes for the asymmetric transfer hydrogenation of ketones and imines[51] or Sharpless's work on the asymmetric dihydroxylation of alkenes[52] and asymmetric epoxydation of allylic alcohols.[53]

Introduction

4.2 Enantioselectivity of enzymes

In addition to enantioselective homogeneous catalysts, enzymes are a class of macromolecules that catalyse some of the most difficult biological reactions. A fundamental difference of enzymes compared to homogeneous catalysts is the presence of a well-defined second coordination sphere around the metal center providing improved efficiency and enantioselection. Furthermore, the presence of a narrow channel guides the substrate to the reaction center ensuring high enantioselectivity, which is particularly difficult to master in homogeneous catalysis (see figure 9).[54]

Enzyme   **Homogeneous catalyst**

Protein scaffold   Chiral ligand scaffold

Active site   Metal

Selectivity channel

Substrate   Substrate
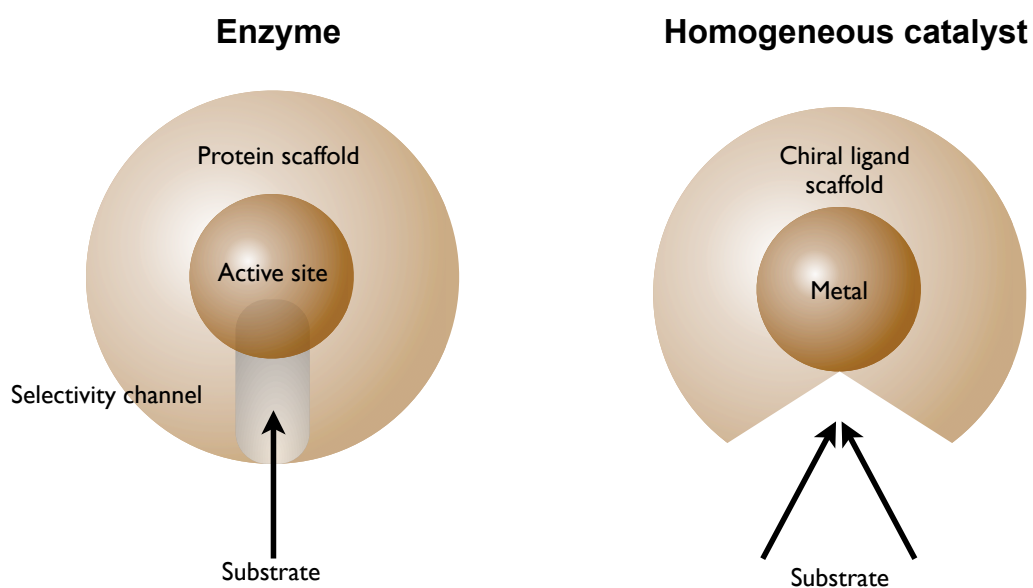
Figure 9 Comparison of enzyme versus homogeneous catalysts

A homogeneous catalyst can be modulated by changing the metal or the ligand in metal complex thus enhancing its performance. Enzymes can also be optimized with different techniques to improve their enantioselective properties. The approach is called *in vitro* evolution of enantioselective enzymes or "directed evolution".[55]

Introduction
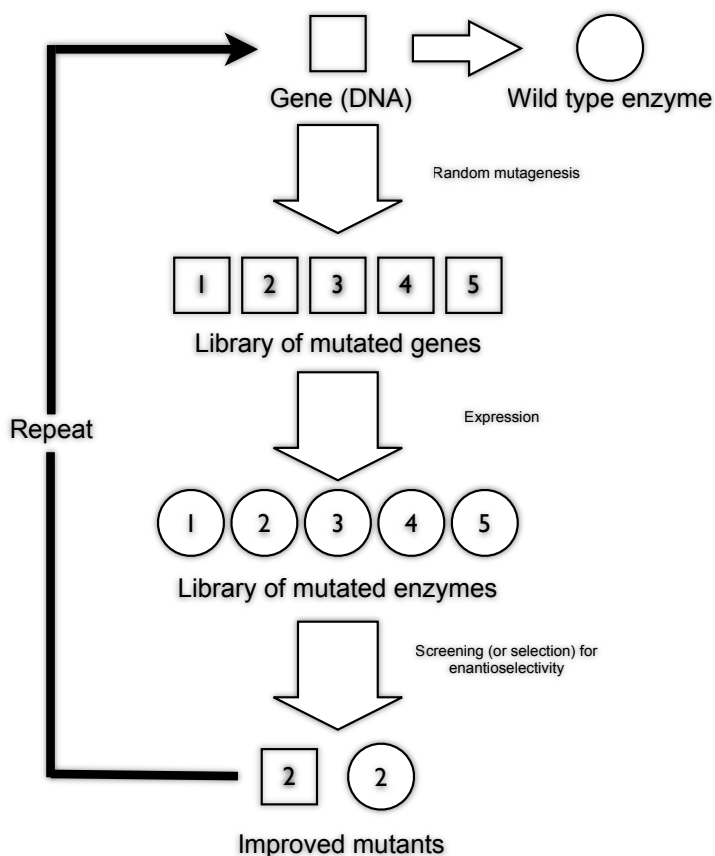
Figure 10 Directed evolution of an enantioselective enzyme

Directed evolution comprises an appropriate combination of gene mutagenesis and expression coupled with an efficient high throughput screening (HTS) system for evaluating enantioselectivity (enantiomeric excess assay). Cycles of evolution processes are called "Darwinistic" processes (see figure 10). The generation of a large library of different enzymes can be done by error-prone mutagenesis, saturation mutagenesis or DNA-shuffling. An example of such an evolution protocol was applied to a lipase where the catalytic properties were enhanced with such processes (see figure 11), allowing kinetic resolution of a chiral ester with an enantiodiscrimination factor higher than 51 (*E* value).[56]
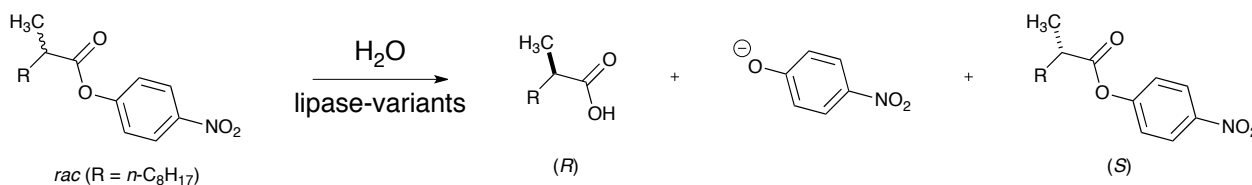
Figure 11 Kinetic resolution of a racemic mixture of chiral esters with lipase-variants

Notwithstanding recent progress in explaining the mechanism and selectivity of enzymes, It is difficult to routinely design or evolve enzymes that satisfy all requirements for a specific reaction. The challenge lies in the immenseness of biomolecular space, in the intrinsic constraints of biological molecules (such as a limited array of reactive groups) and in the added difficulty of controlling several characteristics simultaneously (for example, finding an enzyme with high thermal stability and high catalytic activity for the generation of an enantioenriched product).[57] These challenges are likely to slow the success of enzyme design and evolution. An alternative approach that can be exploited is the construction of hybrid catalysts obtained by the combination of a non biological catalyst entity and a biomolecular scaffold to generate an artificial metalloenzyme.[57]

4.3 Enantioselectivity of artificial metalloenzymes

The artificial metalloenzymes developed in the Ward group based on biotin-(strept)avidin have demonstrated that the chemogenetic fine tuning of the second coordination sphere can have dramatic effects on activity and selectivity.
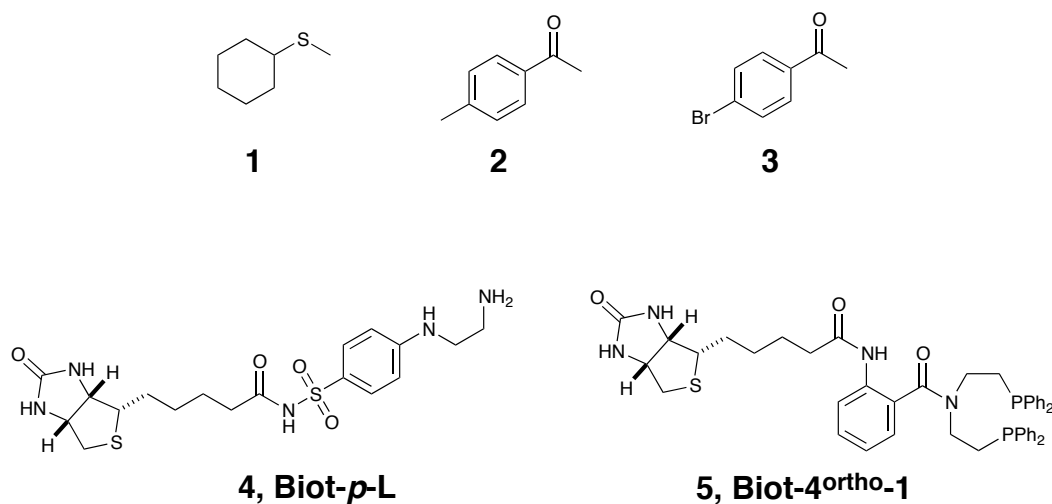
Figure 12 Ligands and substrates used in the Ward group

The first published example is the hydrogenation of acetamidoacrylic acid using diphosphine rhodium complexes [Rh(**Biot-4^{ortho}-1**)COD]$^+$ (**5,** figure 12) that yielded 94% ee in favor of the (*R*)-enantiomer by using a streptavidin isoform (S122G).[40]

A second example is the transfer hydrogenation of prochiral ketones using a biotinylated Ru-piano stool such as the [η^6-(*p*-Cymene*)*Ru(**Biot-*p*-L**)] (**4**) that afforded the (*R*)-enantiomer with the S112A streptavidin variant with a 91 % ee with *p*-methylacetophenone (**2**) whereas [η^6-(benzene)Ru(**Biot-*p*-L**)] ⊂ S112T variant afforded the (*S*)-enantiomer (55%) with *p*-bromoacetophenone (**3**).[58]

In addition to reduction reactions, oxidation reactions can also be optimized using the modulation of a biological scaffold through mutagenesis. Vanadyl-loaded streptavidin was successfully used for enantioselective sulfoxidation. The WT Sav afforded a 86% ee ((*R*)-enantiomer) using *t*-BuOOH as oxydant and VOSO$_4$ as vanadium source (cyclohexyl(methyl)sulfane as substrate, **1**)

whereas the Aviloop with VOSO$_4$ afforded a 90% ee ((R)-enantiomer) in the same catalytic conditions (cyclohexyl(methyl)sulfane as substrate, **1**).[33]

These examples demonstrate that genetic optimization is a powerful tool to improve or invert the enantioselectivity of artificial metalloenzymes. Hence, all entries provided by each hybrid variant allow insight on the reaction mechanism making wiser choices for the "designed evolution".

5. Comparison natural enzymes with artificial metalloenzymes

Natural and artificial metalloenzymes can be compared through their reaction scope.

5.1 Enzymes classification

Nomenclature of enzymes was first proposed in 1992.[59] In this context, natural enzymes are classified according to the committee of the international union of biochemistry and molecular biology and are divided into 6 classes given by an E.C. number (see figure 13):

1. Oxidoreductases (EC 1)

2. Transferases (EC 2)

3. Hydrolases (EC 3)

4. Lyases (EC 4)

5. Isomerases (EC 5)

6. Ligases (EC 6)

Each class of enzyme is further divided into subclasses, depending on the reaction type, cofactor, substrate type, etc.
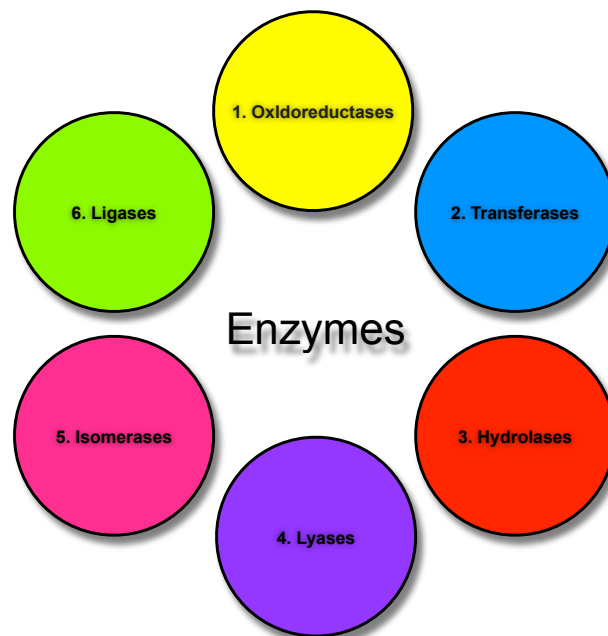
Figure 13 Enzymes classification

5.2 Artificial enzyme classification

Despite increasing descriptions of different types of artificial metalloenzymes, to date no classification has been proposed. The natural enzymes classification could be extended to artificial metalloenzymes. The same classes can be conserved and applied to artificial enzymes. Table 1 classifies and reviews some of the best artificial metalloenzymes as well as natural enzymes for comparison based on the enzyme nomenclature. It is interesting to mention that no artificial lyase has been described. Difficulties in such a classification relies on major differences between artificial systems and natural enzymes *e. g.* the type of anchoring strategy is not taken into consideration. Furthermore some sub-classes do not exist for the moment in the nomenclature such as chemical acceptors for the oxidoreductases but are replaced as suggested by a 99 (meaning: other). It is interesting to mention that streptavidin as a host is involved in 4 of the six

classes of enzymes as artificial metalloenzymes. This supports the versatility of the scaffold and the anchoring strategy to create artificial metalloenzymes.

Table 1 Comparison between artificial metalloenzymes based on biotin-streptavidin technology and natural enzymes

Enzyme type	Reaction type	Enzyme name	Metal-complex	Biomolecule host	Anchoring	E.C. number	Ref.
1. Oxydoreductases							
Artificial	Hydrogenation	Hydrogenase	Rh-Biotin	Streptavidin	Supramolecular	1.12.99	[20, 23, 36, 40, 60]
Artificial	Hydrogenation	Hydrogenase	Rh	Papain	Covalent	1.12.99	[26b, 49a, 61]
Artificial	Hydrogenation	Hydrogenase	Rh-diphosphine	Antibody	Supramolecular	1.12.99	[62]
Artificial	Hydrogenation	Hydrogenase	Pd	Apo-ferritin	Supramolecular	1.12.99	[63]
Artificial	Transfer hydrogenation	Transfer hydrogenase	Ru, Ir, Rh-Biotin	Streptavidin	Supramolecular	1.12.99	[33]
Artificial	Oxydation	Alcohol oxydase	Ru, Ir, Rh-Biotin	Streptavidin	Supramolecular	1.1.99	[22a]
	Oxydation	Alcohol oxydase	Zn-Cu exchange	Carboxypeptidase	Dative	1.1.99	[64]
Artificial	Sulfoxidation	Sulfoxidase	V	Streptavidin	Dative	1.8.99	[33]
Artificial	Sulfoxidation	Sulfoxidase	Mn, Fe-corrole	BSA	Dative	1.8.99	[34]
Artificial	Sulfoxidation	Sulfoxidase	Cr, Mn-Schiff base	Myoglobine	Covalent	1.8.99	[32a, 32c, 65]
Artificial	Sulfoxidation	Sulfoxidase	MO_4^{n-}: M=V,Mo,Re, Se,W	Hydrolases, ferritin	Dative	1.8.99	[66]
Artificial	Dihydroxylation	Dihydroxylase	OsO_4	Streptavidin	Dative	1.14.99	Submitted
Artificial	Dihydroxylation	Dihydroxylase	OsO_4	BSA	Dative	1.14.99	[24]
Artificial	Epoxydation	Epoxydase	Mn-Schiff base	Papain	Covalent	1.14.99	[61a]
Artificial	Epoxydation	Epoxydase	Zn-Mn exchange	Carbonic anhydrase	Dative	1.14.99	[28, 67]
Artificial	Peroxydation	Peroxidase	Se	Subtilisin	Covalent	1.11.1	[68]
Artificial	Peroxydation	Peroxidase	Fe-phophycene	Myoglobin	Dative	1.11.1	[69]

Artificial	Peroxydation	Peroxidase	Fe-hemin	DNA-RNA	Supramolecular	1.11.1	[70]
Natural	Meerwein-Pondorrf-Verley reduction	Alcoholdehydro genase	Zn			1.1.1.1	[71]
Natural	Epoxydation	Squalene epoxydase	-			1.14.99.7	[72]
Natural	Oppenauer oxidation	Alcohol dehydrogenase	Zn			1.1.1.1	[71]
Natural	Hydroxylation	Phenylalanine hydroxylase	Fe			1.14.16.1	[73]
Natural	Peroxidation	Cytochrome C Peroxidase	Fe			1.11.1.9	[74]
Natural	Sulfoxidation	Sulfite oxydase	Mo			1.8.3.1	[75]

2. Transferases

Artificial	Transfer	Acyl transferase	Se	Subtilisin	Covalent	2.3	[76]
Artificial	Transfer	Transaminase	Cu-pyridoxamine	Ribonuclease S	Supramolecular	2.3	[77]
Natural	Transfer	Methyltransferase				2.1.1.1	[78]
Natural	Transfer	Acyltransferase				2.3.1.1	[79]

3. Hydrolases

Artificial	Phosphodiester hydrolysis	Phosphodiesterase	Ce-HXTA	Streptavidin	Supramolecular	3.1.4	This work
Artificial	Hydrolysis	Esterase and amidase	Cu-phenantroline	Adipocyte lipid-binding protein	Covalent	3.1.4 and 3.4.13	[80]
Artificial	Hydrolysis	Endonucleases	Cu-phenantroline	DNA-binding proteins	Covalent	3.1.4	[81]
Artificial	Hydrolysis	Endonucleases	Zn	Peptide fragement with Rh intercalator	Covalent	3.1.4	[82]
Artificial	Hydrolysis	Endonucleases	Eu, Ce,Cu	Helix-Turn-Helix/Ca-binding motif	Covalent	3.1.4	[83]
Artificial	Hydrolysis	Endonucleases	Ce	Zinc finger protein	Covalent	3.1.4	[84]
Artificial	Hydrolysis	Nucleases	Zr	Peptide nucleic acid	Covalent	3.1.21	[85]
Artificial	Hydrolysis	Nucleases	Ce	Complementary peptide nucleic acid		3.1.21	[86]
Natural	Hydrolysis	Phosphodiesterase	Zn, Fe			3.1.4.3	[87]

Natural	Hydrolysis	Carboxylic ester Hydrolase	Zn			3.1.1	[88]
Natural	Hydrolysis	Amidase				3.5.1.4	[89]
Natural	Hydrolysis	Exonuclease	Mg			3.1.11-16	[90]
Natural	Hydrolysis	Endonuclease	Mn			3.1.21-31	[91]

4. Lyase

Natural		Decarboxylase				4.1.1.1	[92]
Natural		Aldolase	Zn			4.1.2.2	[93]
Natural		Oxacide lyase				4.1.3.1	[94]

5. Isomerase

Artificial	Isomerisation	Isomerase	Rh	CA	Covalent	5.2.1	[28]
Natural	Isomerisation	Racemase				5.1.1.1	[95]
Natural	Isomerisation	Isomerase				5.2.1.1	[96]

6. Ligase

Artificial	Methatesis	Methatesase	Ru-Biotin	Streptavidn	Supramolecular	6.4.1	Not published
Artificial	Allylic alkylation	Allylic alkylase	Pd-Biotin	Streptavidin	Supramolecular	6.4.1	[97]
Artificial	Diels-Alder	Diels-Alderase	Cu-phtalocyanine	BSA	Dativ	6.4.1	[26b]
Artificial	Diels-Alder	Diels-Alderase	Cu-bidentate diimines	DNA	Supramolecular	6.4.1	[18, 31, 98]
Artificial	Hydroformylation	Hydroformylase	Rh	HSA	Dative	6.4.1	[99]
Artificial	Friedel Craft	Friedel Craftase	Cu	DNA	Covalent	6.4.1	[100]
Artificial	Allylic amination	Allylic aminase	Ir	DNA	Covalent	6.3.1	[101]
Natural	synthetase	Tyrosine-tRNA ligase				6.1.1	[102]
Natural	synthetase	Acetate- Coa ligase				6.2.1.1	[103]

6. Goal of thesis

Artificial metalloenzymes based on biotin-streptavidin offer a new perspective for protein engineering by combining chemical and genetic modifications to create new activities and to fine-tune the selectivity. The object of this thesis is the development of efficient hybrid catalysts for challenging hydrolysis and reduction reactions (see figure 13). Hence, the work is divided in two parts, dealing with two different reactions: phosphate transfer, and transfer hydrogenation of carbonyl and imine compounds. The first part relies on the discovery of a selective artificial metalloenzyme for the hydrolysis of a chiral RNA mimic substrate (hydrolase). The goal of the following studies is the implementation of a high throughput screening protocol for the identification of an active and selective artificial metallohydrolases. The second part deals with the implementation of a robust protocol for the chemogenetic optimization of an artificial transfer hydrogenases (Oxydoreductase). This project started in a previous PhD thesis in Thomas Ward's laboratory (PhD thesis of Dr. Anca Pordea) and aimed to exploit the influence of the second coordination sphere to create an artificial keto-reductase for the reduction of challenging substrates, such as dialkylketones. This concept was further extended to create the first artificial imine reductase.

7. Bibliography

[1] B. Linström, L. J. Petterson, *CATTECH* **2003**, *7*, 130.

[2] J. N. Galloway, E. B. Cowling, *AMBIO* **2002**, *31*, 64.

[3] a)M. E. Dry, *Catal. Today* **2002**, *71*, 227; b)A. Igelsia, *Appl. Catal., A* **1997**, *161*, 59.

[4] D. Chatterjee, O. Deutschmann, J. Warnatz, *Faraday Discuss.* **2001**, *119*, 371.

[5] A. J. Kirby, F. Hollfelder, *From Enzyme Models to Model Enzymes*, Royal Society of Chemistry, Cambridge, **2009**.

[6] P. W. Atkins, L. Jone, *Chemistry, Molecules, Mater and Change*, 4th ed., W. H. Freeman, **1997**.

[7] a)H. U. Blaser, F. Spindler, M. Studer, *Appl. Catal.* **2001**, *221*, 119; b)H. U. Blaser, B. Pugin, F. J. Spindler, *J.Mol.Cat.A: Chemical* **2005**, *231*, 1; c)A. Thayer, *Chem.Eng.News.* **2006**, *84*, 15.

[8] a)P. I. Dalko, L. Moisan, *Angew. Chem. Int. Ed.* **2001**, *40*, 3726; b)D. Evans, J. A. Osborn, F. H. Jardine, G. Wilkinson, *Nature* **1965**, *208*, 1203.

[9] W. S. Knowles, M. J. Sabacky, *Chem. Commun.* **1968**, *22*, 1445.

[10] L. Horner, H. Siegel, H. Büthe, *Angew. Chem. Int. Ed.* **1968**, *7*, 942.

[11] a)T. P. Dang, H. B. Kagan, *Chem. Commun.* **1971**, *10*, 481; b)H. B. Kagan, T. P. Dang, *J. Am. Chem. Soc.* **1972**, *94*, 6429.

[12] a)B. D. Vineyard, W. S. Knowles, M. j. Sabacky, G. L. Bachman, D. F. Weinkauff, *J. Am. Chem. Soc.* **1977**, *99*, 5946; b)W. S. Knowles, *J. Chem. Edu.* **1986**, *63*, 222.

[13] a)R. Noyori, M. Ohta, Y. Hsiao, M. Kitamura, T. Ohta, H. Takaya, *J. Am. Chem. Soc.* **1986**, *118*, 7117; b)T. Ohta, H. Takaya, M. Kitamura, K. Nagai, R. Noyori, *J. Org. Chem.* **1987**, *52*, 3176; c)M. Kitamura, T. Ohkuma, S. Inoue, N. Sayo, H. Kumobayashi, S. Akutagawa, R. Ohta, H. Tayaka, R. Noyori, *J. Am. Chem. Soc.* **1988**, *110*, 629; d)R. Noyori, T. Ohkuma, T. Kitamura, H. Tayaka, N. Sayo, H. Kumobayashi, S. Akutagawa, *J. Am. Chem. Soc.* **1987**, *109*, 5856.

[14] K. B. Sharpless, *Angew. Chem. Int. Ed.* **2002**, *41*, 2024.

[15] R. Noyori, *Angew. Chem. Int. Ed.* **2008**, *41*.

[16] J. Seayad, B. List, *Organic & Biomolecular Chemistry* **2005**, *3*, 719.

[17] J. Steinreiber, T. R. Ward, *Coord. Chem. Rev.* **2008**, *252*, 751.

[18] G. Roelfes, *Mol. Biosyst.* **2007**, *3*, 126.

[19] F. Rosati, G. Roelfes, *ChemCatChem* **2010**, *2*, 916.

[20] W. F. DeGrado, C. M. Summa, V. Pavone, F. Nastri, A. Lombardi, *Annu. Rev. Biochem.* **1999**, *68*, 779.

[21] a)V. Nanda, R. Koder, *Nature Chem.* **2009**, *2*, 15; b)L. Jiang, E. A. Althoff, F. R. Clemente, L. Doyle, D. Rothlisberger, A. Zanghellini, J. L. Gallaher, J. L. Betker, F. Tanaka, C. F. B. III, D. Hilvert, K. N. Houk, B. L. Stoddard, D. Baker, *Science* **2008**, *319*, 1387.

[22] a)C. M. Thomas, C. Letondor, N. Humbert, T. R. Ward, *J. Organomet. Chem.* **2005**, *690*, 4488; b)C. M. Thomas, T. R. Ward, *Chem. Soc. Rev.* **2005**, *34*, 337.

[23] M. Wilson, G. Whitesides, *J. Am. Chem. Soc.* **1978**, *100*, 306.

[24] T. Kokubo, T. Sugimoto, T. Uchida, S. Tanimoto, M. Okano, *J. Am. Chem. Soc. Commun.* **1983**, 769.

[25] M. Ohashi, T. Koshiyama, T. Ueno, M. Yanase, H. Fujii, Y. Watanabe, *Angew. Chem. Int. Ed.* **2003**, *115*, 1035.

[26] a)L. Panella, J. Broos, J. Jin, M. Fraaije, D. Janssen, M. Jeronimus-Stratingh, B. Feringa, A. Minnaard, J. Vries, *Chem. Commun.* **2005**, *2005*, 5656; b)M. Reetz, M. Rentzsch, A. Pletsch, M. Maywald, P. Maiwald, J. J.-P. Peyraland, A. Maichele, Y. Fu, N. Jiao, F. Hollmann, R. Mondière, A. Taglieber, *Tetrahedron* **2007**, *63*, 6404.

[27] C. Kruithof, M. Casado, G. Guillena, M. Egmond, A. van der Kerk-van Hoof, A. Heck, R. Gebbink, G. van Koten, *Chem. Eur. J.* **2005**, *11*, 6869.

[28] K. Okrasa, R. Kazlauskas, *Chem. Eur. J.* **2006**, *12*, 1587.

[29] M. Reetz, M. Rentzsch, A. Pletsch, A. Taglieber, F. Hollmann, R. Mondière, N. Dickmann, B. Höcker, S. Cerrone, M. Haeger, *ChemBioChem* **2008**, *9*, 552.

[30] D. Coquière, J. Bobs, J. Beld, G. Roelfes, *Angew. Chem. Int. Ed.* **2009**, *48*, 5159.

[31] G. Roelfes, B. L. Feringa, *Angew. Chem. Int. Ed. Engl.* **2005**, *117*, 3230.

[32] a)T. Ueno, S. Abe, N. Yokoi, Y. Watanabe, *Coord. Chem. Rev.* **2007**, *251*, 2717; b)M. Uchida, M. T. Klem, M. Allen, P. Suci, M. Flenniken, E. Gillitzer, Z. Varpness, L. O. Liepold, M. Young, T. Douglas, *Adv. Mater.* **2007**, *19*, 1025; c)M. Ohashi, T. Koshiyama, T. Ueno, H. Yanase, H. Fujii, Y. Watanabe, *Angew. Chem. Int. Ed.* **2003**, *42*, 1005.

[33] M. Creus, A. Pordea, T. Rossel, A. Sardo, C. Letondor, A. Ivanova, I. Le-Trong, R. E. Stenkamp, T. R. Ward, *Angew. Chem. Int. Ed.* **2008**, *47*, 1400.

[34] A. Mahammed, Z. Gross, *J. Am. Chem. Soc.* **2005**, *127*, 2883.

[35] E. T. Kaiser, D. S. Lawrence, *Science* **1984**, *226*, 505.

[36] M. Skander, C. Malan, A. Ivanova, T. R. Ward, *Chem.Commun.* **2005**, 4815.

[37] M. Wilchek, E. A. Bayer, *Methods in Enzymology: Avidin-Biotin Technology, Vol. 184*, **1990**.

[38] a)E. A. Bayer, H. Benhur, M. Wilchek, *Methods Enzymol.* **1990**, *184*, 80; b)A. Loosli, U. E. Rusbandi, J. Gradinaru, K. Bernauer, C. W. Schlaepfer, M. Meyer, S. Mazurek, M. Novic, T. R. Ward, *Inorg. Chem.* **2006**, *45*, 660.

[39] a)M. Gonzalez, C. E. Argarana, G. D. Fidelio, *Biomol. Eng.* **1999**, *16*, 67; b)N. M. Green, *Adv. Protein Chem.* **1975**, *29*, 85; c)T. Sano, M. W. Pandori, X. Chen, C. L. Smith, C. R. Cantor, *J.Biol.Chem* **1995**, *270*, 28204.

[40]   J. Collot, J. Gradinaru, N. Humbet, M. Skander, A. Zocchi, T. R. Ward, *J. Am. Chem. Soc.* **2003**, *125*, 9030.

[41]   T. Sano, C. R. Cantor, *Proc. Natl. Acad. Sci. U.S.A* **1990**.

[42]   a)R. W. Dixon, R. J. Radmer, B. Kuhn, P. A. Kollman, J. Yang, C. Raposo, C. S. Wilcox, L. A. Klumb, P. S. Stayton, C. Behnke, I. Le Trong, R. Stenkamp, *J.Org. Chem.* **2002**, *67*, 1827; b)P. C. Weber, J. J. Wendoloski, M. W. Pantoliano, F. R. Salemme, *J. Am. Chem. Soc.* **1992**, *114*, 3197; c)O. H. Laitinen, V. P. Hytonen, H. R. Nordlund, M. S. Kulomaa, *Cell. Mol. Life Sci.* **2006**, *63*, 2992; d)P. C. Weber, D. H. Ohlendorf, J. J. Wendoloski, F. R. Salemme, *Science* **1989**, *243*, 85; e)O. Livnah, E. A. Bayer, M. Wilchek, J. L. Sussman, *Proc. Natl. Acad. Sci. U.S.A* **1993**, *90*, 5076.

[43]   T. Hamada, T. Fukuda, H. Imanishi, T. Katsuki, *Tetrahedron* **1996**, *52*, 515.

[44]   D. Haring, M. D. Distefano, *Bioconjugate Chem.* **2001**, *12*, 385.

[45]   I. P. Petrounia, F. H. Arnold, *Curr. Opin. Biotechnol.* **2000**, *11*, 325.

[46]   U. T. Bornscheuer, M. Pohl, *Curr. Opin. Biotechnnol.* **2001**, *5*, 137.

[47]   M. M. Altamirano, J. M. Blackburn, C. Aguayo, A. R. Fersht, *Nature* **2002**, *417*, 468.

[48]   a)D. A. Drummond, B. L. Iverson, G. Georgiou, F. H. Arnold, *J. Mol. Biol.* **2005**, *350*, 806; b)S. G. Peisajovih, L. Rockah, D. S. Tawfik, *Nat. Genet.* **2006**, *38*, 168.

[49]   a)M. T. Reetz, J. D. Carballeira, J. Peyralans, H. Hobenreich, A. Maichele, A. Vgel, *Chem.-Eur.J.* **2006**, *12*, 6031; b)K. L. Morley, R. J. Kazlauskas, *Trends Biotechnol.* **2005**, *23*, 231.

[50]   H. B. Kagan, *L'actualité chimique* **2003**, 10.

[51]   a)R. Noyori, S. Hashiguchi, *Acc.Chem.Res.* **1997**, *30*, 97; b)R. Noyori, T. Ohkuma, *Angew. Chem. Int. Ed.* **2001**, *40*, 40.

[52]   a)H. C. Kolb, K. VanNieuwenhse, B. Sharpless, *Chem. Rev.* **1994**, *94*, 2483; b)K. B. Sharpless, W. Amberg, Y. L. Bennani, G. A. Crispino, J. Hartung, K. J. Sung, H. L. Kwong, K. Morikawa, Z. M. Wang, *J.Org.Chem.* **1992**, *57*, 2768.

[53]   a)T. Katsuki, K. B. Sharpless, *J. Am. Chem. Soc.* **1980**, *102*, 5974; b)Y. Gao, J. M. Klunder, R. M. Hanson, H. Masamune, S. Y. Ko, K. B. Sharpless, *J. Am. Chem. Soc.* **1987**, *109*, 5765.

[54]   R. MacKinnon, *Angew. Chem. Int. Ed.* **2004**, *43*, 4265.

[55]   a)J. C. Moore, F. H. Arnold, *Nat. Biotechnol.* **1996**, *14*, 432; b)F. H. Arnold, *Acc. Chem. Res.* **1998**, *31*, 125.

[56]   M. Reetz, *Proc. Natl. Acad. Sci. U. S. A.* **2003**, *101*, 5716.

[57]   M. Creus, T. R. Ward, *Org. Biomol. Chem.* **2007**, *5*, 1835.

[58]   C. Letondor, A. Pordea, N. Humbert, A. Ivanova, S. Mazurek, M. Novic, T. R. Ward, *J. Am. Chem. Soc.* **2006**, *128*, 8320.

[59]   E. C. Webb, *Enzyme Nomenclature*, 1 ed., Academic Press, San Diego, California, **1992**.

[60]   a)J. Collot, N. Humbert, M. Skander, G. Klein, T. R. Ward, *J. Organomet. Chem.* **2004**, *689*, 4868; b)G. Klein, N. Humbert, J. Gradinaru, A. Ivanova, F. Gilardoni, U. E. Rusbandi, *Angew. Chem. Int. Ed.* **2005**, *44*, 7764; c)U. E. Rusbandi, C. Lo, M. Skander, A. Ivannova, M. Creus, N. Humbert, T. R. ward, *Adv. Synth. Catal.* **2007**, *349*, 1923.

[61]   a)M. Reetz, *Tetrahedron* **2002**, *58*, 6595; b)J. G. de Vries, L. Lefort, *Chem. Eur. J.* **2006**, *12*, 4722.

[62]   H. Yamaguchi, T. Hirano, H. Kiminami, D. Taura, A. Harada, *Org. Biomol. Chem.* **2006**, *4*, 3571.

[63]   T. Ueno, T. Suzuki, T. Goto, T. Matsumoto, K. Nagayama, Y. Watanabe, *Angew. Chem. Int. Ed.* **2004**, *43*, 2527.

[64]   K. Yamamura, E. T. Kaiser, *J. Chem. Soc. Commun.* **1976**, 1587.

[65]   T. Ueno, T. Koshiyama, M. Ohashi, K. Kondo, M. Kono, A. Suzuki, T. Yamane, Y. Watanabe, *J. Am. Chem. Soc.* **2005**, *127*, 6556.

[66]   a)F. van de Velde, L. Konemann, F. van Rantwijk, R. A. Sheldon, *Chem. Commun.* **1998**, 1891; b)F. van de Velde, I. W. C. E. Arends, R. A. Sheldon, *Top Catal.* **2000**, *13*, 259.

[67]   A. Fernandes-Gacio, A. Codina, J. Fastrez, O. Riant, P. Soumillion, *ChemBioChem* **2006**, *7*, 1013.

[68]   I. M. Bell, M. L. Fisher, Z. P. Wu, D. Hilvert, *Biochemistry* **1993**, *32*, 3754.

[69]   T. Hayashi, D. Murata, M. Makino, H. Sugimoto, T. Matsuo, H. Sato, Y. Shiro, Y. Hisaeda, *Inorg.Chem.* **2006**, *45*, 10530.

[70]   a)P. Travascio, Y. Li, D. Sen, *Chem. Biol.* **1998**, *5*, 505; b)P. Travascio, A. J. Bennet, D. Y. Wang, D. Sen, *Chem.Biol.* **1999**, 779.

[71]   H. Jörnvall, *Eur. J. Biochem.* **1977**, *72*, 443.

[72]   a)S. Yamamoto, K. Bloch, *J. Biol. Chem.* **1970**, *245*, 1670; b)E. J. Corey, W. E. Russey, O. de Montellano, *J. Am. Chem. Soc.* **1966**, *88*, 4750.

[73]   O. A. Andersen, T. Flatmark, E. Hough, *J. Mol. Biol.* **2001**, *314*, 266.

[74]   A. M. Altschul, R. Abrams, T. R. Hogness, *J. Biol. Chem.* **1940**, *136*, 777.

[75]   R. M. MacLeod, W. Farkas, I. Fridovitch, P. Handler, *J. Biol. Chem.* **1961**, 1841.

[76]   Z. Wu, -P, D. Hilvert, *J. Am. Chem. Soc.* **1989**, *111*, 4513.

[77]   R. S. Roy, B. Imperiali, *Protein Eng.* **1997**, *10*, 691.

[78]   G. L. Cantoni, *J. Biol. Chem.* **1951**, *189*, 203.

[79]   W. K. Maas, G. D. Vovelli, F. Lipmann, *Prot. Natl. Acad. Sci. U. S. A.* **1953**, *39*, 1004.

[80]   a)D. Qi, C.-M. Tann, D. Haring, M. D. Distefano, *Chem. Rev.* **2001**, *101*, 3081; b)R. R. Davies, M. D. Distefano, *J. Am. Chem. Soc.* **1997**, *119*, 11643.

[81]   a)M. M. Meijler, O. Zelenko, D. S. Sigman, *J. Am. Chem. Soc.* **1997**, *119*, 1135; b)C. B. Chen, L. Milne, R. Landgraf, D. M. Perrin, D. S. Sigman, *ChemBioChem* **2001**, 735.

[82]   a)M. P. Zitzsimons, J. K. Barton, *J. Am. Chem. Soc.* **1997**, *119*, 3379; b)K. D. Copeland, M. P. Fitzsimons, R. P. Houser, J. K. Barton, *Biochemistry* **2002**, *41*, 343.

[83] a)J. T. Welch, W. R. Kearney, S. J. Franklin, *Proc. Natl. Acad. Sci. U. S. A.* **2003**, *100*, 3725; b)S. W. Wong-Deyrup, Y. Kim, S. J. Franklin, *J. Biol. Inorg. Chem.* **2006**, *11*, 17; c)S. Lim, S. J. Franklin, *Protein Sci.* **2006**, *15*, 2159; d)S. B. Shields, S. J. Franklin, *Biochemistry* **2004**, *43*, 16086.

[84] a)A. Nomura, Y. Sugiura, *J. Am. Chem. Soc.* **2004**, *126*, 15374; b)T. Nakatsukasa, Y. Shiraishi, S. Negi, M. Imanishi, S. Futaki, Y. Sugiura, *Biochem. Biophys. Res. Commun.* **2005**, *330*, 247.

[85] F. H. Zelder, A. A. Mokhir, R. Kramer, *Inorg. Chem.* **2003**, *42*, 8618.

[86] a)Y. Kitamura, M. Komiyama, *Nucleic Acids Res.* **2002**, *30*, e102; b)W. Chen, Y. Kitamura, J. M. Zhou, J. Sumaoka, M. Komiyama, *J. Am. Chem. Soc.* **2004**, *126*, 10285; c)W. Chen, M. Komiyama, *ChemBioChem* **2005**, *6*, 1825; d)Y. Yamamoto, A. Uehara, A. Watanabe, H. Aburatani, M. Komiyama, *ChemBioChem* **2006**, *7*, 673; e)Y. Yamamoto, M. Mori, Y. Aiba, T. Tomita, W. Chen, J. M. Zhou, A. Uehara, Y. Ren, Y. Kitamura, M. Komiyama, *Nucleic Acids Res.* **2007**, *35*, e53; f)K. Ito, H. Katada, N. Shigi, M. Komiyama, *Chem. Commun.* **2009**, 6542.

[87] R. G. Sheiknejad, P. n. Srivasta, *J. Biol. Chem.* **1986**, *261*, 7544.

[88] J. Burch, *Biochem. J.* **1954**, *58*, 415.

[89] H. G. Bray, S. P. James, I. M. Raffan, W. V. Thorpe, *Biochem. J.* **1949**, *44*, 618.

[90] a)R. B. Kelley, M. R. Atkinson, J. A. Huberman, A. Kornberg, *Nature* **1969**, *224*, 495; b)C. C. Richarson, A. Kornberg, *J. Biol. Chem.* **1964**, *239*, 242.

[91] a)M. Kunitz, *Science* **1948**, *108*, 19; b)M. Privat de Garilhe, M. Laskowski, *J. Biol. Chem.* **1955**, *215*, 269.

[92] T. P. Singer, J. Pensky, *J. Biol. Chem.* **1952**, *196*, 375.

[93] F. C. Charalampous, G. C. Mueller, *J. Biol. Chem.* **1953**, *201*, 161.

[94] B. A. McFadden, W. V. Howes, *J. Biol. Chem.* **1963**, *238*, 1737.

[95] W. A. Wood, I. C. Gunsalus, *J. Biol. Chem.* **1951**, *190*, 403.

[96] E. J. Behrman, R. Y. Stanier, *J. Biol. Chem.* **1957**, *228*, 923.

[97] J. Pierron, C. Malan, M. Creus, J. Gradinaru, I. Hafner, A. Ivanova, A. Sardo, T. R. Ward, *Angew. Chem. Int. Ed.* **2008**, *120*, 713.

[98] G. Roelfes, A. J. Boersma, B. L. Feringa, *Chem. Commun.* **2006**, 635.

[99] a)M. Marchetti, G. Mangano, S. Paganelli, C. Botteghi, *Tetrahedron Lett.* **2000**, *41*, 3717; b)C. Bertucci, C. Botteghi, D. Giunta, M. Marchetti, S. Paganelli, *Adv. Synth. Catal.* **2002**, *344*, 556; c)S. Crobu, M. Marchetti, G. Sanna, *J. Inorg. Biochem.* **2006**, 1514.

[100] A. Boersma, B. Feringa, G. Roelfes, *Angew. Chem. Int. Ed.* **2009**, *48*, 3346.

[101] P. Fournier, R. Fiammengo, A. Jäschke, *Angew. Chem. Int. Ed.* **2009**, *48*, 4426.

[102] E. H. Allen, E. Glassman, R. S. Schweet, *J. Biol. Chem.* **1960**, *235*, 1061.

[103] T. C. Chou, F. Lipmann, *J. Biol. Chem.* **1952**, *196*, 89.
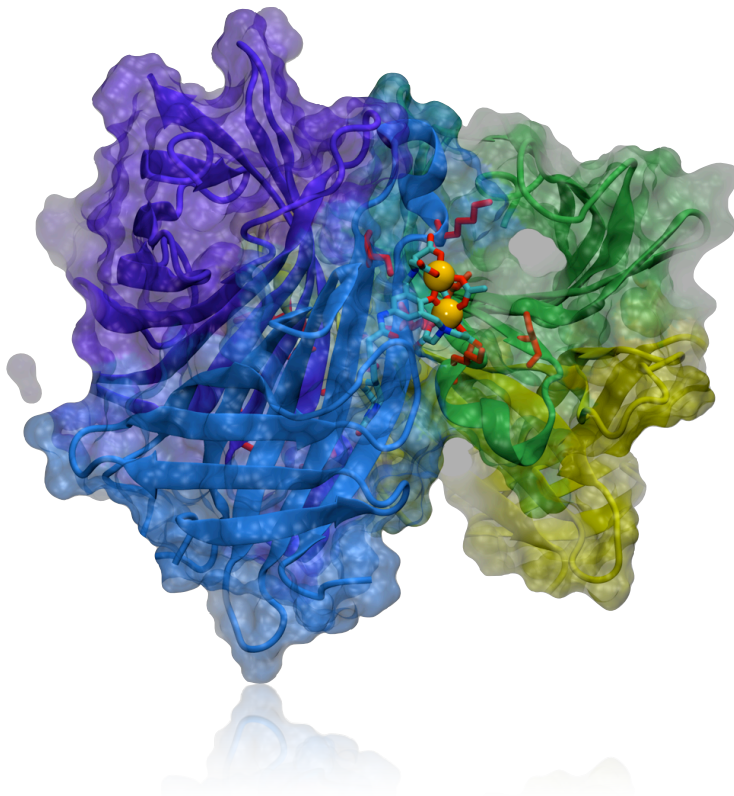
Chapter 2:

Artificial Phosphate Transferases

« Le plus beau sentiment du monde, c'est le sens du mystère. Celui qui n'a jamais connu cette émotion, ses yeux sont fermés »

Albert Einstein

Chapter 2: Artificial phosphate transferases

1. Abstract

Introduction of a biotinylated Ce(IV) complex within streptavidin affords an artificial metallohydrolase. Combining both chemical and genetic optimization strategies allows the improvement of both the activity and the selectivity of the hybrid catalyst for the phosphate transfer of enantiopure 2-hydroxypropyl-*para*-nitrophenylphosphate (HPNP), a model phosphodiester (k_{obs}/k_{uncat} > 50 and estimated E > 65 (R) and -27 (S)).

2. Introduction

Creating new artificial hydrolases is of particular interest especially for selective DNA and RNA cleavage.[1] Phosphodiester bonds are remarkably stable with a half-life of ca. 130 000 years.[2] In natural nucleases, the stability of the negatively charged backbone of nucleic acid molecules towards nucleophilic attack is overcome through coordination to Lewis acid metals (Zn(II), Ca(II), Mg(II), Fe(II)). These metals activate both the P–O bond for cleavage and the nucleophilicity of coordinated water.[1a] Lanthanide ions, which are hard Lewis acids with high coordination numbers and fast ligand exchange rates are ideally suited to mimick the reactivity of these biological metal cofactors.[1a, 3]

Many catalysts for the hydrolysis of phosphodiester substrates have been developed by mimicking enzymes found in nature such as alkaline phosphatase and purple acid phosphatase (see figure 1).[4] Alkaline phosphatase bears a dinuclear zinc center whereas purple acid phosphatase possesses a dinuclear iron center.

Purple acid phosphatase   **Alkaline phosphatase**
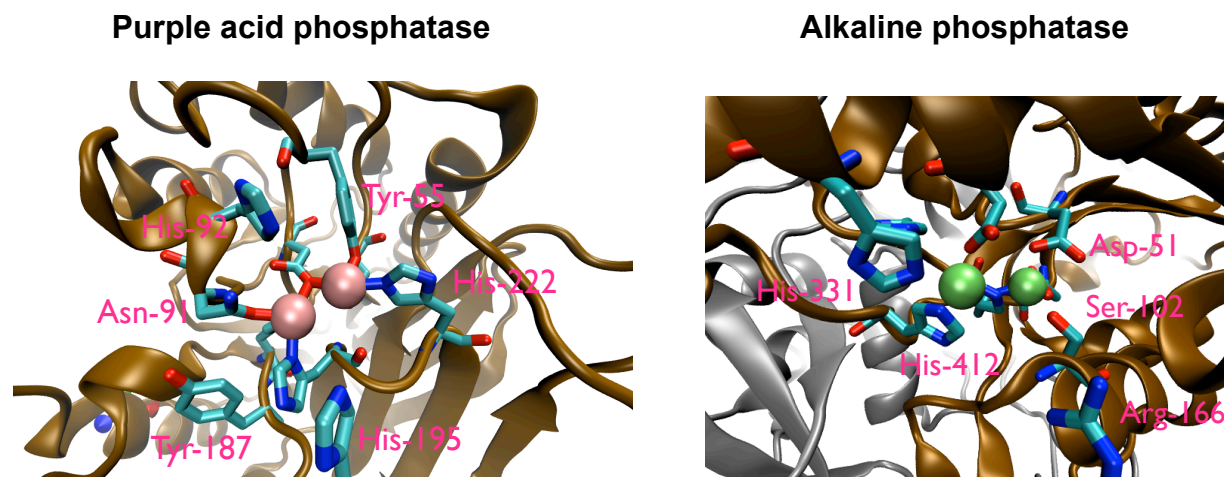
Figure 1 Close up view of the active sites of purple acid phosphatase and alkaline phosphatase. Both bear a dinuclear metal center (iron or zinc) coordinated by histidines, aspartate and glutamate. Coordination of a tyrosine to the metal center (Tyr-55) in purple acid phosphatase generates a charge transfer transition yielding a purple color to the enzyme. For alkaline phosphatase, an arginine presents the substrate to the metal center via Coulomb interactions and a serine acts as a transient nucleophile towards the phosphorus atom of the substrate.

To mimic these natural enzymes, chemists have developed a variety of catalysts able to perform phosphodiester hydrolysis on model substrates such as HPNP (2-hydroxypropyl-*para*-nitrophenylphosphate) or BNPP (bis-nitrophenylphosphate) (see figure 2), single stranded DNA (ss-DNA), double stranded DNA (ds-DNA) or supercoiled DNA (plasmid). The hydrolysis of phosphodiesters was investigated with lanthanide salts, mono and dinuclear metal complexes. Some of the best catalysts are reviewed in the next paragraphs.

The trivalent lanthanides ions[3b] accelerate the hydrolysis of DNA under saturation kinetics conditions up to k_{cat} = 1.0 · 10^{-4} s^{-1}. Ce(IV) is a 20 to 1000 times more efficient than any other trivalent lanthanide. It displays comparable efficiency toward ss-DNA and ds-DNA.[5] However,

aqueous lanthanides salts are toxic. To overcome this problem, stable and highly active complexes needs to be developed. Theses hydrolytic complexes are divided in two groups: the mononuclear complexes and the dinuclear complexes.

BNPP, 1

HPNP, 2
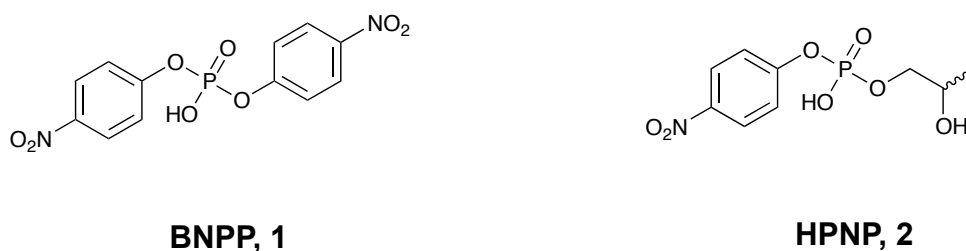
Figure 2 Schematic representation of BNPP and HPNP

A few mononuclear complexes were described as artificial nucleases. The Co(III) complex of the polyamine ligand TAMEN (**3**) cleaves plasmid DNA with a k_{cat} = 5 · 10^{-5} s^{-1} , in this case the cleavage is hydrolytic.[6] Fuji and co-workers reported a TACH/Cu(II)[7] (**4,** figure 3) complex promoting the hydrolytic cleavage of plasmid DNA. Saturation kinetic were observed with a k_{cat} = 1.2 · 10^{-3} s^{-1}. Such reactivity ranks among the highest to date for mononuclear complexes.

In addition to mononuclear complexes, dinuclear complexes were described for the cleavage of phosphodiesters and DNA cleavage. In 1996, Schneider and co-workers described a 30-membered azacrown macrocyle able to bind to Eu(III) or Pr(III) ions[3b] (**6**). These complexes promoted plasmid DNA nicking with a k_{cat} = 2.8 · 10^{-4} s^{-1}. More effective are the dinuclear Er(III) complexes of a Schiff base containing macrocycles (**7**) reported by Zhu and coworkers[8] able to hydrolyse plasmid DNA with a maximum rate constant of k_{cat} = 1.1 · 10^{-3} s^{-1}. A few complexes mimicking the active site Trof purple acid phosphatase incorporating a dinuclear iron center were described. An example is given by Liu and co-workers that developed an Iron/DTPB[9] complex (**8**) able to cleave supercoiled DNA with a k_{cat} = 2.1 · 10^{-3} s^{-1} which is the best system to date for the

hydrolytic cleavage of DNA. Very few bimetallic systems based on zinc and copper have been described: Scrimin and coworkers developed a binuclear Zn(II)-binding heptapeptide[10] able to cleave plasmid DNA with a k_{cat} = 1.1 · 10^{-5} s^{-1}. Finally, a very efficient dicerium complex composed of a polyaminocarboxylate ligand HXTA (**5**) was reported by Que and coworkers.[2] The catalyst displays an acceleration of k_{cat} = 1.4 · 10^{-4} s^{-1} for the cleavage of ds-DNA.

Mononuclear and dinuclear complexes present a good acceleration towards model substrates such as BNPP, HPNP (see figure 2) or DNA-substrates. In contrast, all of them suffer from product inhibition and therefore most of the time the turnover number of the catalyst is not mentioned or is very small.[11] In addition, not all kinetic parameters (k_{cat}/k_{uncat}, K_M, V_{max}, k_{cat}/K_M) are clearly reported in the literature for each catalyst. This renders difficult the comparison between all systems.

TAMEN with Co(III), 3　　　**TACH with Cu(II), 4**　　　**HXTA with Ce(IV), 5**

with Eu(III) or Pr(III), 6　　　**with Er(III), 7**　　　**DTPB with Fe(III), 8**
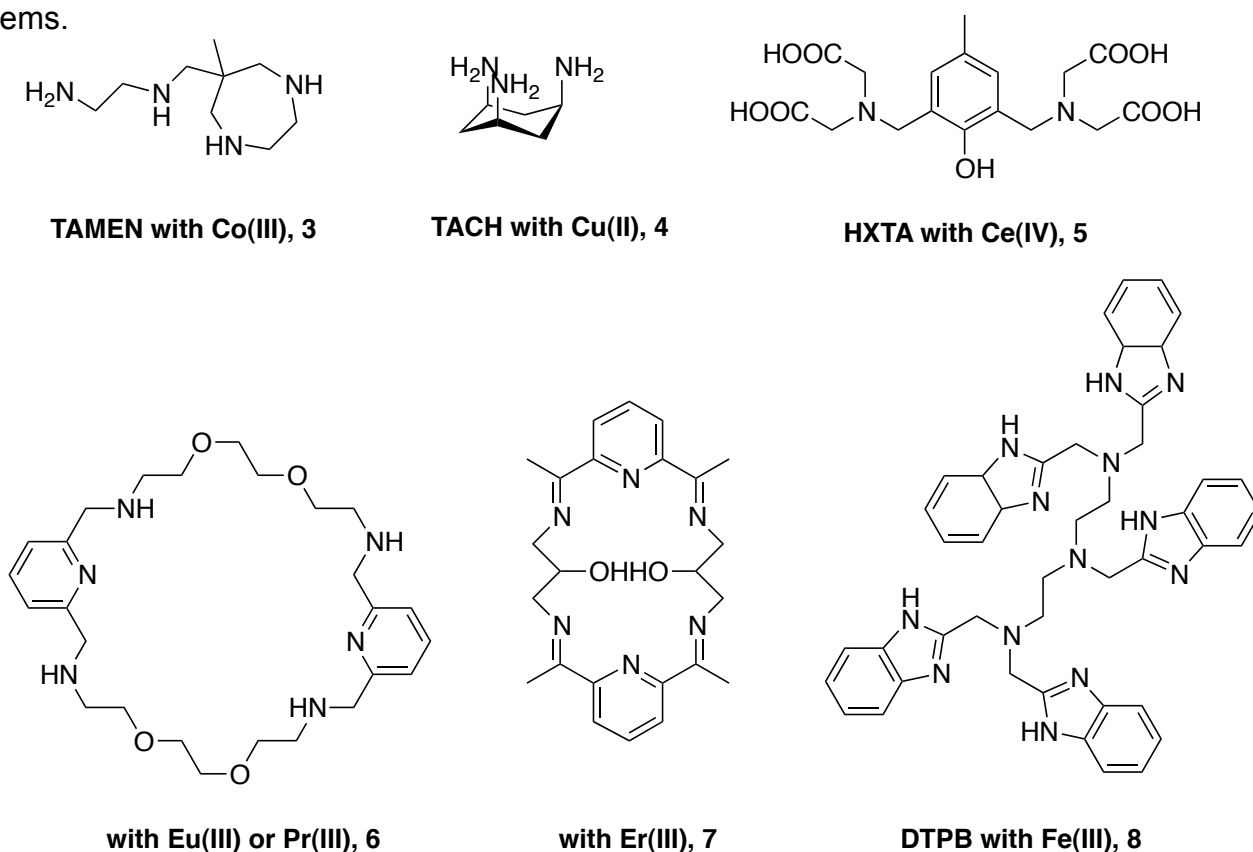
Figure 3 Some of the most efficient metal-ligand combinations for DNA hydrolysis

Anchoring artificial hydrolases to a macromolecular scaffold (protein or DNA) provide a second coordination sphere around the organometallic complex thus mimicking natural enzymes. The second coordination sphere may ameliorate the turnover number and or the selectivity of the catalyst. Some of the best examples of catalysts comprising a second coordination sphere are reviewed below.

Hollfelder et al.[11-12] have developed a highly active polymer system called "synzymes" for the hydrolysis of HPNP. The system works with or without metal. It consists of a derivatization of polyethylene imine (PEI) with alkyl (C_2-C_{12}) benzyl and guanidinium groups (see figure 4). The system without metal gives rise to catalysts with a rate acceleration (k_{cat}/k_{uncat}) of up to 10^4 for intramolecular transesterification of HPNP. The synzymes exhibit saturation kinetics (K_M = 250 µM, k_{cat} = 0.5 min^{-1}) and up to 2340 turnovers per polymer molecule. Addition of a metal (especially zinc) to the polymers creates metal containing synzymes and accelerate the phosphate transfer by 10^8 (k_{cat}/k_{uncat}) with a K_M in the range of 2.5 to 8 mM, the k_{cat} of the system increases to 0.09 s^{-1}. In the metal coordinated synzymes, the polymer around the metal can be viewed as a second coordination sphere thus mimicking the active site of a natural enzyme.

a)

b)
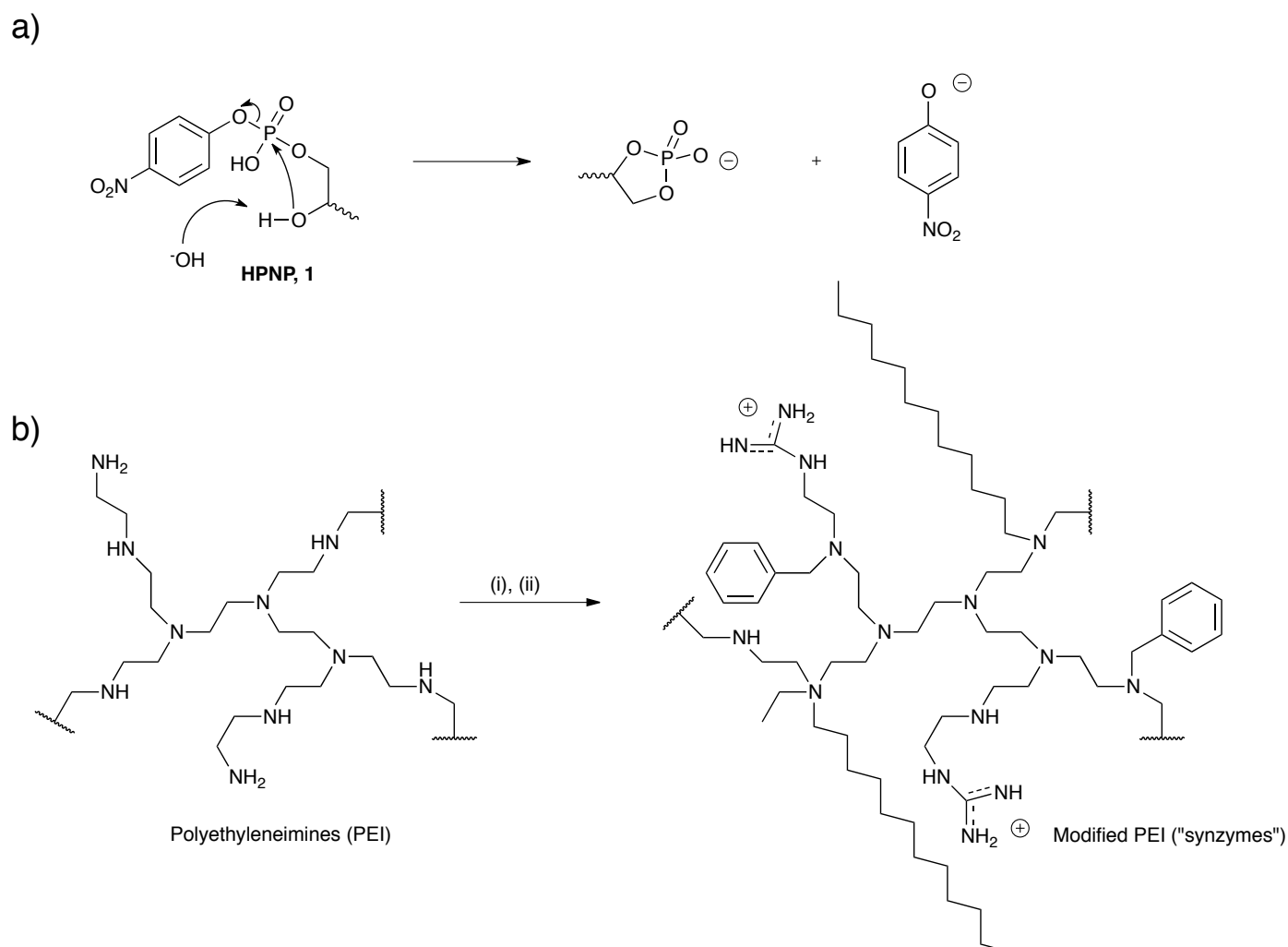
Figure 4 HPNP transesterification reaction a) b) Derivatization scheme to modify PEI to give "synzymes". Polymer amine groups reacted (in DMF, 30°C) with varying amounts of (i) praxadine (1*H*-pyrazole-1-carboximide hydrochloride) and (ii) iodoalkanes (C$_2$-C$_{12}$) or benzylbromide b)

Another example is the work of Komiyama et al.[13] They used an artificial restriction DNA cutter (ARCUT) composed of Ce(IV)/EDTA complex (molecular scissors) in combination with pseudo-complementary PNA (pcPNA) strands (see figure 5). The PNA strands are highly selective towards specific sequences of DNA thus allowing recognition *in vivo*.
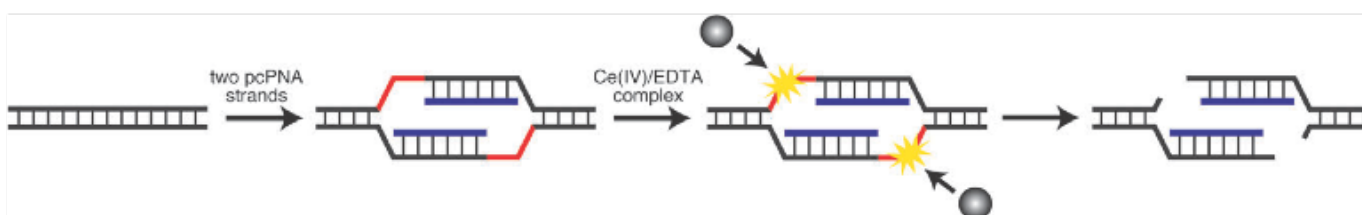
Figure 5 Schematic diagram of site-specific cleavage of double-stranded DNA by ARCUT. By adding two pcPNA strands (blue line) to double-stranded DNA (black line), ss-DNA portions (red lines) are formed within the invasion complex. These single-stranded portions are selectively hydrolysed by Ce(IV)/EDTA complex (gray circles).

Krämer et al.[14] described a family of PNA-metal chelators conjugates whose Zr(IV) complexes selectively cleave ss-DNA oligonucleotides (see fig 6). The use of a large excess of free Zr(IV), due to the low metal affinity for the ligand (TRIS) subunit led to substantial non-specific cleavage. However, the scission occurred with remarkable regiospecificity at the P-O3' bond.
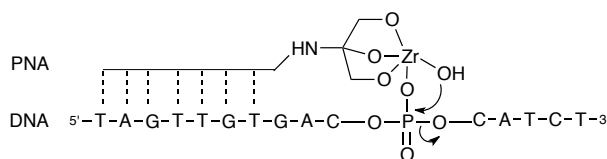
Figure 6 Proposed model for hydrolytic DNA scission by PNA-Zr(IV) conjugate.

Barton and coworkers[15] have developed a mononuclear Zn(II)-binding peptide, tethered to a rhodium complex as a major groove intercalator (see figure 7). This system allows plasmid cleavage with a rate constant of k_{obs} = 2.5 · 10^{-5} s^{-1} at pH = 6 and 37 °C. In contrast to the system described above, this system has a similar activity toward ds-DNA.
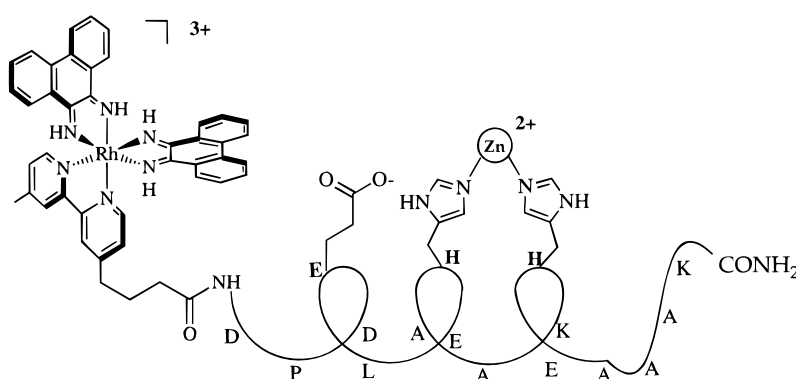
Figure 7 Schematic illustration of intercalator-peptide conjugates. The conjugate combines DNA-binding and reactive moieties: the rhodium intercalator binds in the major groove with high affinity and the tethered peptide binds divalent cations to promote hydrolysis of the phosphodiester linkage.

Examples of selective bimetallic systems based on Cu(II) and Zn(II) with a good activity were reported by Scrimin and coworkers.[10, 16] (see figure 8). They have described a Zn(II)-binding heptapeptide wich cleaves plasmid DNA with a first order rate constant of k_{cat} = 10^{-5} s^{-1} at pH = 7 and 37°C. The peptide has a 3$_{10}$-helical conformation and the two chelating TACN moieties face each other at a distance of about 6 Å. The substrate is believed to interact with both metal centers thus mimicking artificial dinuclear nucleases.
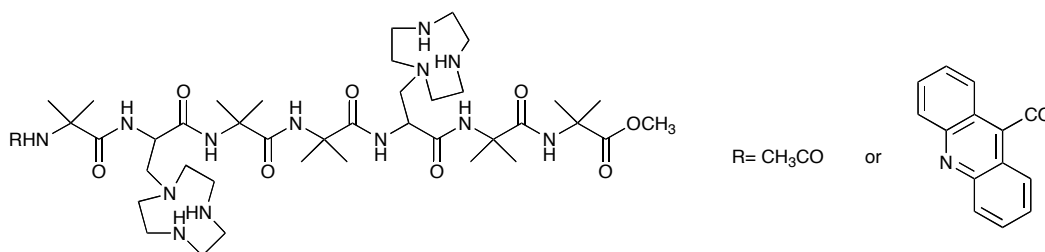
Figure 8 A Zn(II)-binding heptapeptide cleaves plasmid DNA with first order rate constant of 10^{-5} s^{-1} at pH = 7 and 37 °C.

To exploit dendrimers as scaffold, Scrimin et al. developed metallodendrimers as transphosphorylation catalysts.[16a] For this purpose, they functionalized a third generation DAB (polypropylene imine) dendrimers with triazacyclononane moieties. The metal loaded dendrimer cleaves HPNP with a k_{cat} = 8.72 · 10^{-3} s^{-1} and a k_{obs} = 1.55 · 10^{-2} s^{-1} (see figure 9). The triazacyclononane macrocycle is an excellent ligand for ions such as Zn(II) and Cu(II) and complexes and these metal ions are effective catalysts for the cleavage of phosphodiesters.
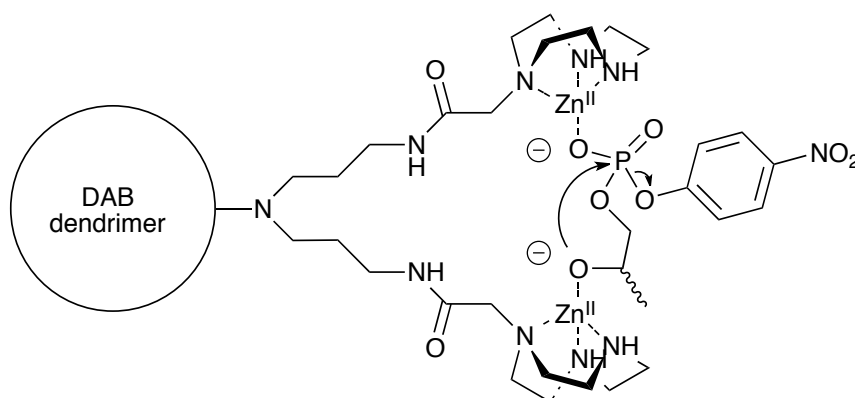
Figure 9 DAB dendrimers able to perform catalysis on phosphodiester substrates.

Following similar design principles, they developed a nanoparticle-based catalyst for phosphodiester and DNA hydrolysis.[16c] The catalyst was obtained by self-assembling multiple copies of a ligand bearing a thiol anchor on gold nanoparticules (see figure 10). High activity and a

new mode of action emerged from the multivalent nature of the catalyst. Zn(II) complexes of BAPA (bis(2-amino-pyridinyl-6-methyl)amine) relies on two Lewis acids for the activation of the substrate and on hydrogen bonding to achieve increased hydrolytic activity toward phosphate diester with a k_{obs} of $3.6 \cdot 10^{-5}$ s^{-1}.

BAPA
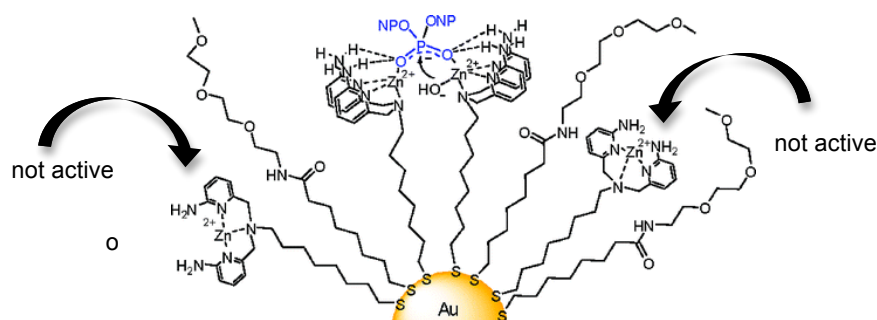
Figure 10 Nanoparticle-based catalyst for phosphodiester and DNA hydrolysis. The catalyst is obtained by self-assembling multiple copies of the thiolated ligand on the surface nanoparticules (MPGNs).

Finally, Scrimin et al. studied the nuclease mechanism by exploring the role of proximal ammonium groups on phosphate diester cleavage (see figure 11). The hydrolytic activity of complexes based on the BAPA allowed easy investigation of the substituent effect.

They designed new ligands (**11**) where an ammonium group is located behind the active nucleophile in the spirit of a Lysine group present in nucleases. The ammonium group helps the formation of the nucleophile and decrease the pK_a by 2 orders of magnitude compared to ligand (**10**).

The maximum reactivity shifted closer to physiological values and the reactivity is increased due to electrostatic effects exerted by positive charge stabilization of the transition state. The pK_a

decrease appears also for ligand (**12**) but no charge interaction with the substrate was present. The catalytic efficiency is given for BNPP k_{cat}/K_M = 0.097 M^{-1} s^{-1} for complex (**10**) (see figure 11) compared to k_{cat}/K_M = 0.022 M^{-1} s^{-1} for complex (**11**) (see figure 11) and k_{cat}/K_M = 0.0015 M^{-1} s^{-1} for (**12**).
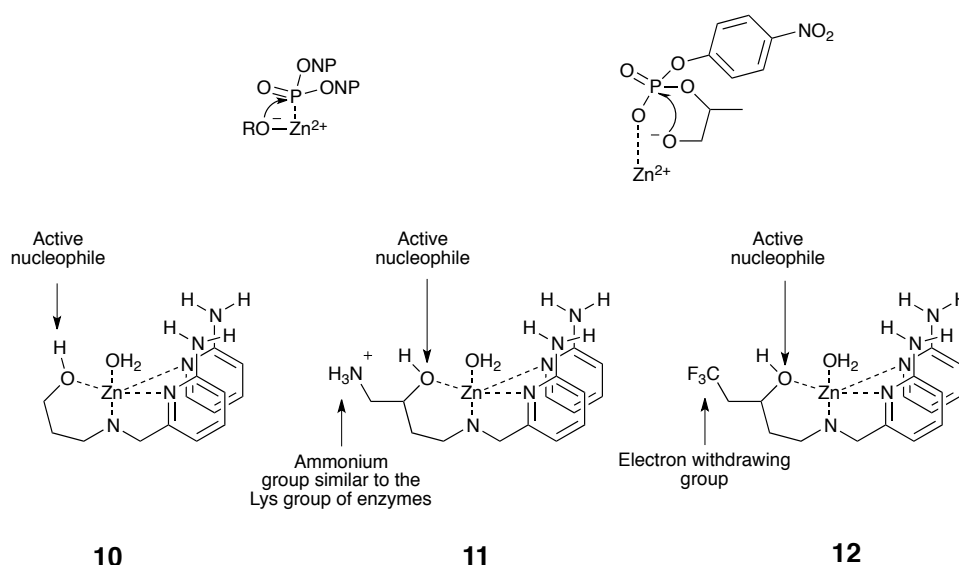
Figure 11 Ligands designed by Scrimin et al. with an ammonium group located behind the nucleophile reminiscent of the Lys group in nucleases.

The reaction of HPNP (**1**) with metal complexes is an intramolecular transesterification where the nucleophile is the substrate's hydroxyl groups. As a consequence, HPNP (**1**) reactivity is not affected by the activity (or even by the absence) of metal-bound nucleophiles and provided a good indication of the ability of the catalyst to stabilize the transition state. The catalytic efficiency is given for HPNP by k_{cat}/K_M = 0.26 M^{-1} s^{-1} for complex (**10**) (see figure 11) compared to k_{cat}/K_M = 0.70 M^{-1} s^{-1} for complex (**11**) (see figure 11) and k_{cat}/K_M = 0.22 M^{-1} s^{-1} for (**12**).

Sugiura and coworkers[17] have exploited the DNA binding affinity of zinc finger motifs to prepare a sequence selective DNA cleavage catalyst (see figure 12). They obtained zinc finger peptides with hydrolytic activity $k_{cat}/K_M = 502 \cdot 10^{-2}$ M^{-1} s^{-1}.

Linkage of these three zinc-finger mutants resulted in a system with high affinity for the DNA duplex containing a GC box (K_d = 85 nM). The cleavage is moderately efficient but the system has a good selectivity.

Figure 12 Zinc finger peptide. Aminoacids bound to the zinc, cationic and anionic amino acids are denoted by bold black, red, and blue letters, respectively a) The three-tandem zinc finger protein for sequence selective ds DNA cleavage b).

Finally, Franklin et al.[18] have designed a 33-mer peptide incorporating a DNA recognition sequence and a metal ion binding site (see figure 13). The peptide folds in a HTH motif where the two helices have been derived from the DNA binding engrailed homeodomain and the turn produces the calcium binding site of calmodulin. Addition of Ce(IV) or Eu(III) allows formation of a peptide bearing a lanthanide which maintains the tertiary structure. The complex allows cleavage of both plasmids and ds-DNA with reactivity similar to the free metal ion. The complex is regioselective while cleaving only the P-O3' bonds and has a preference for T/C rich domains.

Figure 13 Computer-generated model of the interaction of chimeric peptides with DNA based on the HTH motif and EF-hand motifs from engrailed (red) and calmodulin (yellow), respectively. Crystal structure of engrailed homeodomain, cocrystallized with DNA 82HDD; gray and red ribbon, wit blue DNA and one EF-hand of calmoduline (1OSA; yellow ribbon, with coordinated Ca(II)), are overlaid to show the similarity of the folds. The peptides comprise α2 and α3 of engrailed and the Ca-binding loop of calmodulin.

Characteristics of natural enzymes are often their high substrate selectivity, provided by a well-defined second coordination sphere environment that can allow exquisite discrimination. It was anticipated that, thanks to its large biotin binding vestibule, streptavidin (Sav hereafter) may be well suited to accommodate biotinylated Lewis acids and thus provide a suitable host for the generation of artificial hydrolases.

3. Aims of the chapter

The aim of the chapter is the development of artificial phosphate transferase based on the biotin-streptavidin technology. Whereas redox artificial metalloenzymes[19] (hydrogenation, transfer hydrogenation, oxidation) and ligases[19b] (allylic alkylation) have been previously described, this is the first report of an artificial phosphate transferase based on biotin-streptavidin technology. In the annex this concept is extended to the hydrolysis of i) insoluble chiral phosphodiester leading to phospholipases like activity and ii) biotinylated ss-DNA leading to artificial restriction enzymes.

4. Results and discussion

To test the validity of this concept, enantiopure 2-hydroxypropyl-*para*-nitrophenylphosphate HPNP was selected as a substrate (see figure 14). Inspired by the report of Que[2] and Komiyama, Ce(IV)[5a, 13, 20] was selected as Lewis acid. There is ample evidence that, even in the presence of anionic donor atoms, these are powerful redox-innocent Lewis-acids capable of hydrolyzing model substrates, and single as well as double stranded DNA.[2] The synthesis of a series of biotinylated aminocarboxylic acids for coordination with Ce(IV) was carried out. The ligands are outlined in figure 15 (see experimental part).[21]
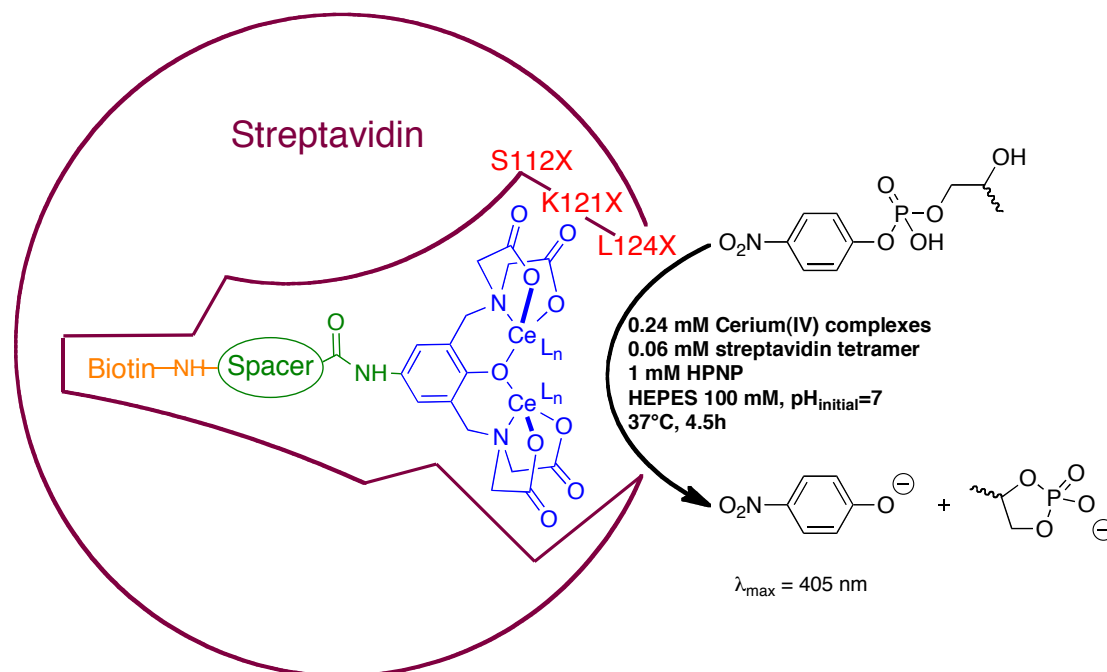
**Figure 14** Artificial metallohydrolases based on the biotin-avidin technology. Incorporation of a biotinylated Ce(IV) complex within streptavidin yields an artificial phosphodiesterase. Optimization can be achieved either by varying the nature of the spacer (oval) or the ligand combined with site-directed mutagenesis at select positions on the host protein.

To gain insight on the localization of the biotinylated Lewis acid within streptavidin, docking studies were performed on $\{(\textbf{Biot-HXTA})Ce_2(\mu\text{-}OAc)_2\}^+ \subset$ Sav. (Hereafter, the symbol $\subset$ is used for the incorporation of the biotinylated catalyst within Sav). For this purpose, the X-ray structure of $\{(\textbf{HXTA})Fe_2(\mu\text{-}OAc)_2\}^-$ (CSD refcode AJEKOP[22]) was derivatized with a biotin anchor and the $\{Fe_2(\mu\text{-}OAc)2\}^{4+-}$ fragment removed. The resulting biotinylated ligand **Biot-HXTA**-H_5 was docked within Sav using the AutoDock4[23] program and the $\{Ce_2(\mu\text{-}OAc)_2\}^{6+}$ fragment was introduced, The resulting structure is depicted in figure 15b.

a)

b)
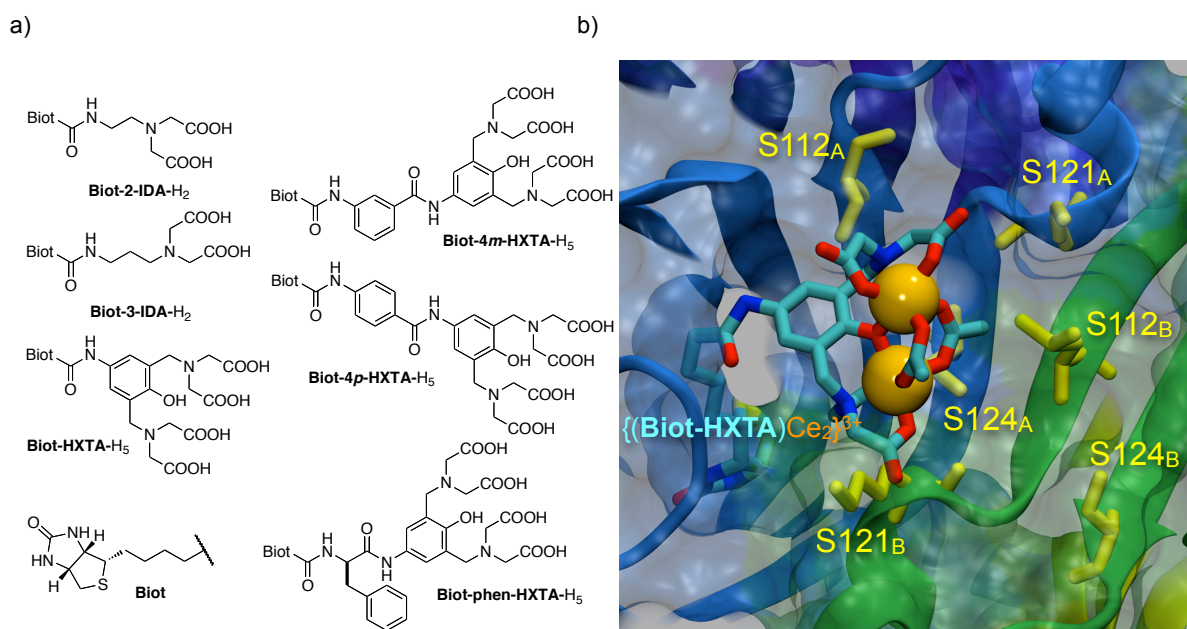
Figure 15 Structure of biotinylated aminocarboxylic acids used in this study a); close up view of the docked structure of {(**Biot-HXTA**)Ce$_2$(OAc)$_2$}$^+$ ⊂ Sav (only one complex displayed). Close-lying residues subjected to mutagenesis are highlighted in red b).

This structure reveals that, despite the size of the dinuclear complex, up to four biotinylated moieties can occupy the four binding sites of tetrameric Sav. This was confirmed by a HABA displacement titration[24] demonstrating the incorporation of four equivalents of {(**Biot-HXTA**)Ce$_2$}$^{3+}$ (Fig.16b). To determine the optimal pH, the rate of hydrolysis of (*rac*)-HPNP was determined in the presence of {(**Biot-HXTA**)Ce$_2$}$^{3+}$ ⊂ Sav at 37 °C, Fig. 1b. All subsequent studies were performed at pH 7.0 in HEPES (100 mM).
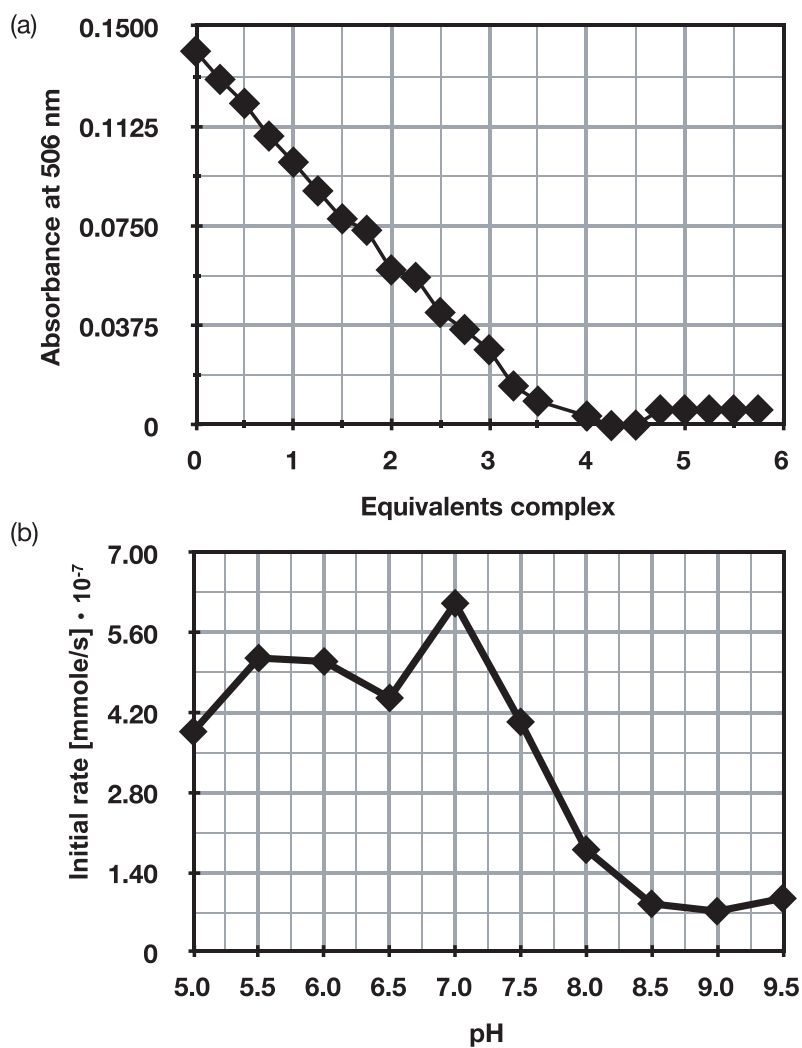
Figure 16 HABA-displacement titration, suggesting the incorporation of four $\{(\textbf{Biot-HXTA})Ce_2\}^{3+}$ within tetrameric streptavidin a) and initial rate (*rac*)-HPNP hydrolysis as a function of pH catalyzed by $\{(Biot\text{-}HXTA)Ce_2\}^{3+} \subset Sav$ b)

Based on the docked structure, positions S112, K121, and L124 were identified as close-lying and thus were subjected to site-directed mutagenesis to incorporate genetic diversity.

Mutants V47G and P64G, wich had proven versatile in other artificial metalloenzymes, were also included in the screening effort. A library of 23 Sav isoforms was combined with six complexes prepared in situ from ligands **Biot-2-IDA**-H_2, **Biot-3-IDA**-H_2, **Biot-HXTA**-H_5, **Biot-4m-HXTA**-H_5, **Biot-4p-HXTA**-H_5 and **Biot-phen-HXTA**-H_5. This chemogenetic n·m diversity matrix was screened in the presence of enantiopure HPNP.

The initial rates of hydrolysis (k_{obs}) were conveniently monitored using a 96 well-plate reader by recording the absorbance at 405 nm, diagnostic for the formation of nitrophenolate and the corresponding product of the reaction (the cyclized phosphonate).

Determination of the initial slopes for each catalyst $\subset$ Sav isoform was carried out for both HPNP enantiomers in separate wells, thus yielding both k_{obs} (Figure 17 a, Table 1) and the estimated E (ratio of $k_{obs}(R)/k_{obs}(S)$, figure 17b, Table 2). From these data, the following trends for k_{obs} were identified:
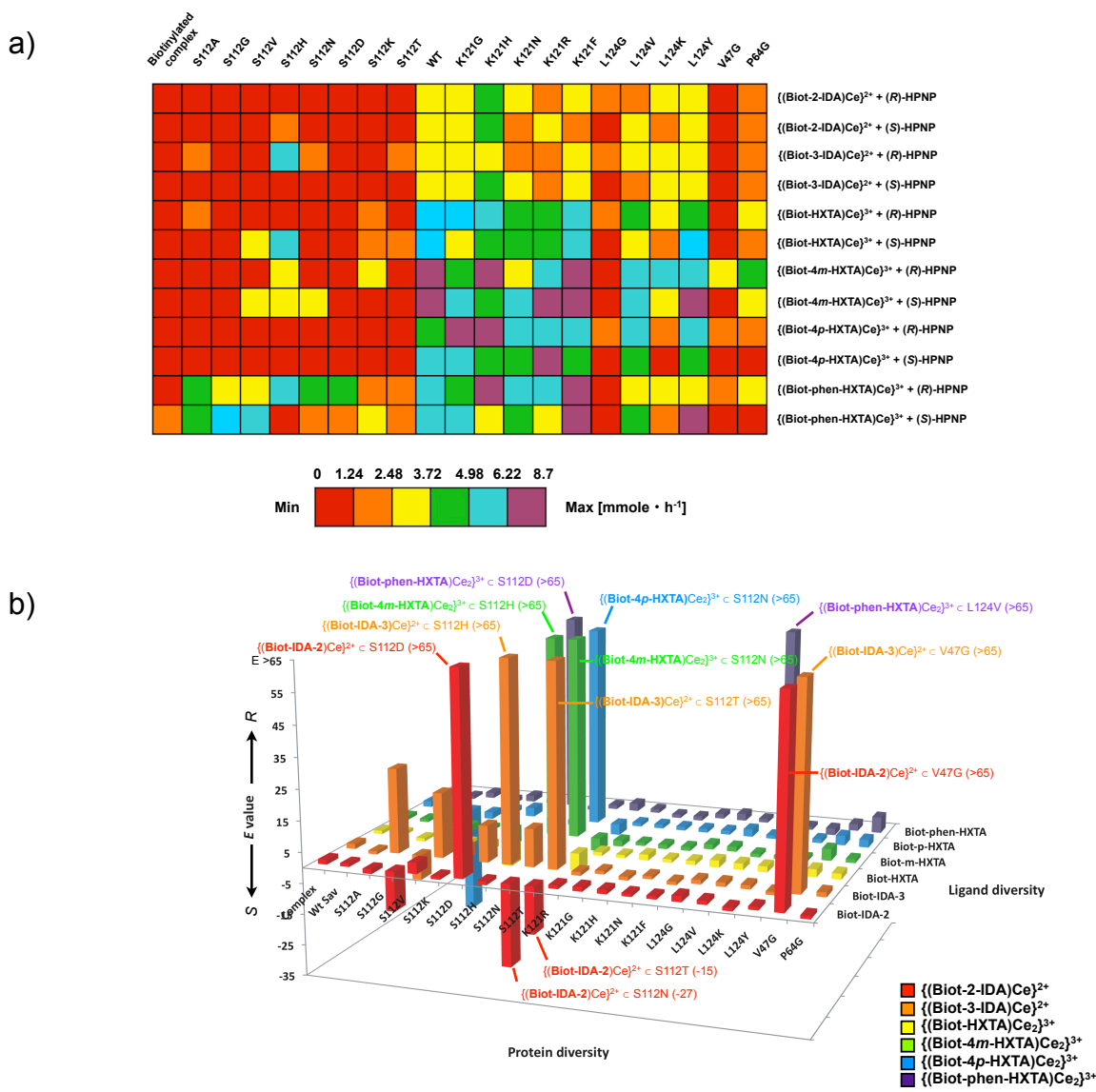
Figure 17 Graphical summaries of the results for the hydrolysis of HPNP catalyzed by artificial metallohydrolases: Initial rates k_{obs} for both HPNP enantiomers a) and estimated E b).

Table 1 Numerical summary of selected initial rates k_{obs} for the HPNP hydrolysis.

Entry	Ligand	Sav	k_{obs}/k_{uncat} (R)-HPNP	k_{obs}/k_{uncat} (S)-HPNP
1	{(**Biot-4m-HXTA**)Ce$_2$}$^{3+}$	–	8	8
2	{(**Biot-2-IDA**)Ce}$^{2+}$	S121G	25	18
3	{(**Biot-2-IDA**)Ce}$^{2+}$	S121F	26	27
4	{(**Biot-3-IDA**)Ce}$^{2+}$	S121G	23	20
5	{(**Biot-HXTA**)Ce$_2$}$^{3+}$	S121F	43	32
6	{(**Biot-4m-HXTA**)Ce$_2$}$^{3+}$	S121G	47	49
7	{(**Biot-4m-HXTA**)Ce$_2$}$^{3+}$	S121R	21	42
8	{(**Biot-4m-HXTA**)Ce$_2$}$^{3+}$	S124Y	45	49
9	{(**Biot-4p-HXTA**)Ce$_2$}$^{3+}$	S121N	51	38
10	{(**Biot-phen-HXTA**)Ce$_2$}$^{3+}$	WT	38	40
11	{(**Biot-phen-HXTA**)Ce$_2$}$^{3+}$	S121G	47	55
12	{(**Biot-phen-HXTA**)Ce$_2$}$^{3+}$	S121F	45	20

i) Compared to the uncatalyzed reaction at pH 7.0, rate accelerations (k_{obs}/k_{uncat}) > 50 fold were obtained. Compared to the biotinylated catalyst alone, incorporation within Sav results in > 7 fold rate accelaration (Table 1 entries 1 vs. 2-12). This suggests that the host protein has a tunable impact on the hydrolysis rate of the resulting artificial metallohydrolases.

ii) Mutation of S112 leads to a significant decrease in activity. We hypothesize that, in a biomimetic spirit, this serine may act as a transient nucleophile during hydrolysis.

iii) Dinuclear complexes derived from **HXTA** are more efficient (higher k_{obs}) than mononuclear complexes bearing an **IDA** moiety (Table 1, entries 2-5 vs. 6-12)

iv) Introduction of a spacer between the biotin anchor and **HXTA** contributes to the improvement of k_{obs}, thus yielding the most proficient artificial hydrolases (Table 1 entry 5 vs. 6-12).

v) Mutation at position K121 is most effective, yielding rate accelerations k_{obs}/k_{uncat} of up to 55-fold. Substitution of the positively charged lysine by a glycine (K121G) is most beneficial (Table 1 entries 2,4,6,11).

Table 2 Numerical summary of selected estimated E values ($k_{obs}(R)/k_{obs}(S)$) for the HPNP hydrolysis.

Entry	Ligand	Prot	estimated E
1	{(**Biot-2-IDA**)Ce}$^{2+}$	S112D	>65
2	{(**Biot-2-IDA**)Ce}$^{2+}$	V47G	>65
3	{(**Biot-2-IDA**)Ce}$^{2+}$	S112N	-27
4	{(**Biot-2-IDA**)Ce}$^{2+}$	S112T	-15
5	{(**Biot-3-IDA**)Ce}$^{2+}$	S112H	>65
6	{(**Biot-3-IDA**)Ce}$^{2+}$	V47G	>65
7	{(**Biot-4m-HXTA**)Ce$_2$}$^{3+}$	S112H	>65
8	{(**Biot-4m-HXTA**)Ce$_2$}$^{3+}$	S112N	>65
9	{(**Biot-4p-HXTA**)Ce$_2$}$^{3+}$	S112N	>65
10	{(**Biot-phen-HXTA**)Ce$_2$}$^{3+}$	S112D	>65
11	{(**Biot-phen-HXTA**)Ce$_2$}$^{3+}$	L124V	>65

Compared to the k_{obs} data summarized above, the estimated E data (Table 2) reveal distinct trends:

i) Both mononuclear, **IDA** and **HXTA**-derived metalloenzymes are equally effective for the preferential hydrolysis of one enantiomer of **HPNP** (Table 2 entries 1-4 vs. 5-10).

ii) The hydrolysis of (R)-**HPNP 1** is preferred in most cases. Only two combinations were identified which hydrolyze (S)-**HPNP** more efficiently (E -26 and -15 for $\{(\textbf{Biot-2-IDA})Ce\}^{2+} \subset$ S112N Sav and $\{(\textbf{Biot-2-IDA})Ce\}^{2+} \subset$ S112T Sav, respectively, Table 2, entries 2, 3).

iii) Mutation of S112 by more potent nucleophiles at pH 7 (ie. S112H and S112D) has a positive impact on selectivity (Table 2, entries 1, 4, 5, 8). For example, mutation S112H displays higher $k_{obs}(R)$ with $\{(\textbf{Biot-3-IDA})Ce\}^{2+}$ (and with $\{(\textbf{Biot-phen-HXTA})Ce_2\}^{3+}$) than equivalent combinations with other Sav mutants at this position. This rate acceleration for the (R)-**HPNP** gives rise to both high rates and high selectivity. These data lend support to docking studies, suggesting the proximity of position 112 to the biotinylated Lewis acids.

As a representative and promising example, $\{(\textbf{Biot-4}m\textbf{-HXTA})Ce_2\}^{3+} \subset$ K121G was subjected to Michaelis-Menten kinetic analysis, figure 18. For the recognized (R)-substrate, the K_M values (2.34 mM, (S)-**HPNP** 0.0091 mM) are comparable to natural enzymes, as well as some of the best man-made catalysts.
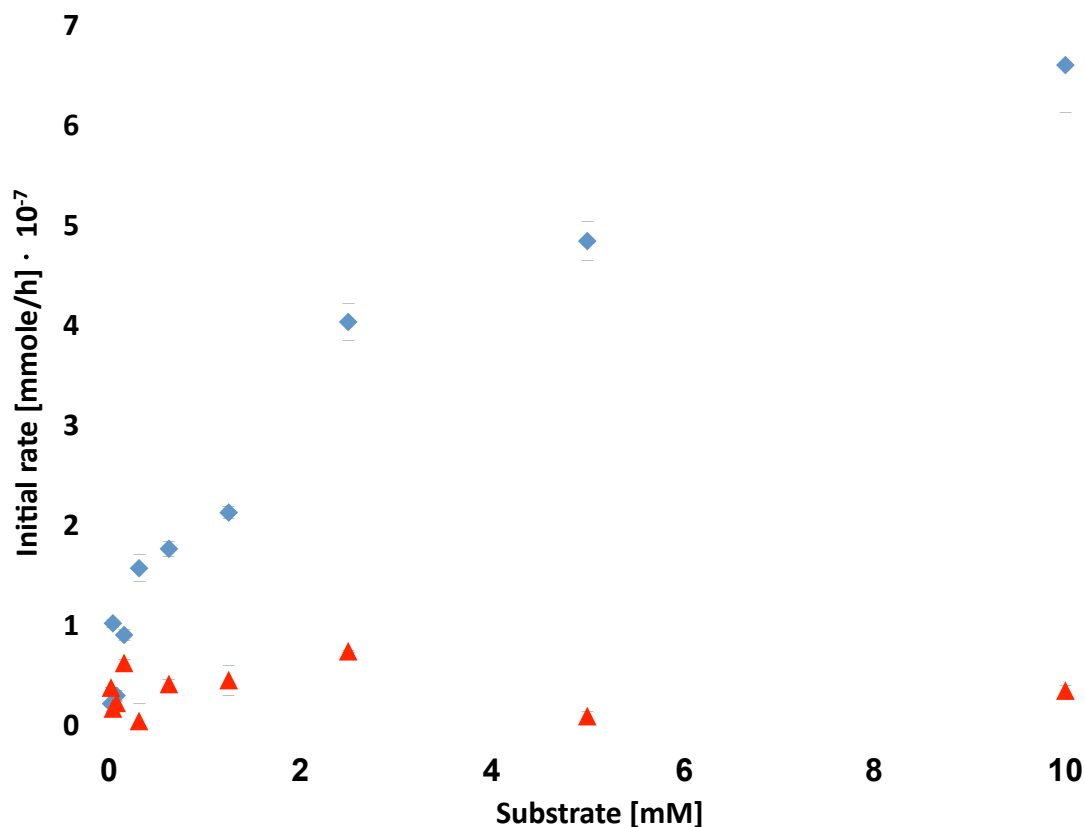
Enzyme	K_M [mM]	k_{cat} [s^{-1}]
Purple acid phosphatase	1.25	470
Alkaline phosphatase	90	80
Metal-coordinated synzyme	16.7	0.00145
Synzyme	1.25	0.00833
{(**Biot-4*m*-HXTA**)Ce$_2$} ⊂ K121G	2.34	0.000030

Figure 18 Saturation kinetics plot for the hydrolysis of (*R*)-**HPNP** (measured : full circles; fitted : solid blue line) and (*S*)-**HPNP** (measured: red full squares; fitted : solid red line) catalyzed by {(**Biot-4*m*-HXTA**)Ce$_2$}$^{3+}$ ⊂ K121G a) and parameters for selected natural and artificial metallonucleases b.

5. Conclusion

As was outlined in this work, the k_{obs} values and k_{cat} ($3 \cdot 10^{-5}$ s^{-1} and $1.41 \cdot 10^{-6}$ s^{-1} for both **HPNP** enantiomers) can be improved by combining chemical and genetic diversity. Relying on this strategy, it was shown for the first time that promising selectivities towards two enantiomers could be achieved.

6. Perspectives

As demonstrated by Que and coworkers, $\{(\textbf{HXTA})Ce_2\}^{3+}$ can hydrolyze ds-DNA. Incorporation of this fragment in a host protein offering extended contacts with DNA may allow selective hydrolytic cleavage of specific sequences. Current efforts are directed towards the recognition of oncogenic ds-DNA sequences using the strategy outlined above.

7. Experimental part

7.1. Synthesis

Synthesis of Biot-2-IDA
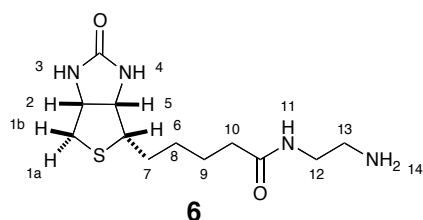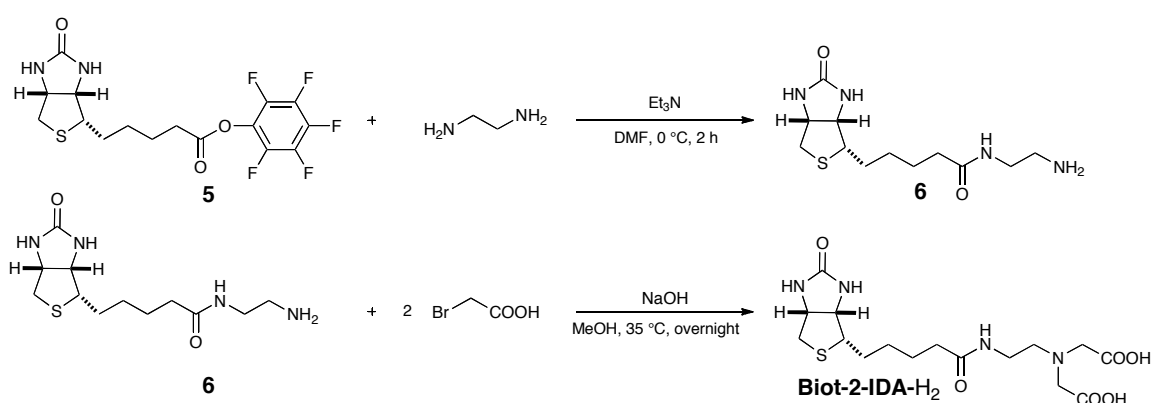
A solution of ethylenediamine (490 µL, 7.43 mmol) was slowly added at 0 °C to a solution of activated biotin **5**[25] (300 mg, 0.73 mmol) in DMF (20 mL) containing Et$_3$N (230 µL, 1.65 mmol). The mixture was stirred at RT for 2 days. The solvent was evaporated under reduced pressure. The residue was dissolved in hot MeOH (20 mL) and cooled overnight (5 °C). The white precipitate was filtered, washed with cold MeOH and cold acetonitrile and dried under reduced pressure to afford amine **6** (Yield: 72%).

^{1}H NMR (400.00 MHz, [D$_6$] DMSO, 20 °C): δ (ppm) = 1.25-1.67 (m, 6H, **H^7**, **H^8**, **H^9**), 2.10 (m, 2H, **H^{10}**), 2.59 (m, 1H, **H^{1a}**), 2.79-2.86 (m, 3H, **H^{1b}**, **H^{13}**), 3.08-3.19 (m, 1H, **H^6**), 3.23-3.28 (m, 2H, **H^{12}**), 4.13-4.16 (m, 1H, **H^5**), 4.32 (m, 1H, **H^2**), 6.40 (s, 1H, **H^3**), 6.45 (s, 1H, **H^4**), 8.03 (s, 1H, **H^{11}**); **^{13}C NMR** (100.58 MHz, [D$_6$] DMSO, 20 °C): δ (ppm) = 25.9, 28.9, 29.1, 36.0, 39.8, 40.0, 40.7, 56.3, 60.1, 61.9, 163.6, 173.6 ; **MS (ESI)**: ESI-MS for C$_{12}$H$_{22}$N$_4$O$_2$S (286.2 g/mol): 287.2 (100%) [M+H]$^+$.

Mp (°C) 211 (Dec.).

Biot-IDA-2-H$_2$
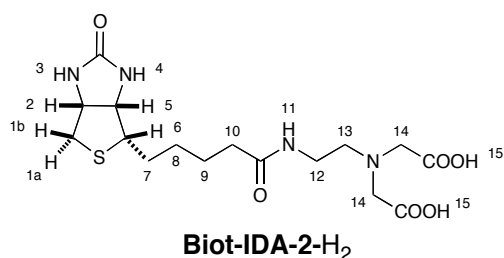
Amine 6 (500 mg, 1.75 mmol) was dissolved in MeOH (60 mL) and added to an aqueous solution of 2-bromoacetic acid (486 mg, 3.50 mmol, 9 mL) . The reaction was stirred for 2 h at 35 °C and NaOH (280 mg, 6.99 mmol dissolved in water 6 mL) was added. The solution was stirred for 1 day at RT. The pale brown precipitate was filtered and dried under reduced pressure. The solid obtained was dissolved in MeOH, precipitated with ether and filtered to afford **Biot-2-IDA**-H$_2$. (Yield: 87%).

^{1}H NMR (400.00 MHz, D$_2$O, 20 °C): δ (ppm) = 1.29-1.69 (m, 6H, **H^7, H^8, H^9**), 2.74 (m, 1H, **H^{1a}**), 2.97 (m, 1H, **H^{1b}**), 3.13 (m, 1H, **H^6**), 3.25-3.5 (m, 10H, **H^{10}, H^{12}, H^{13}, H^{14}**), 4.33-4.36 (m, 1H, **H^5**), 4.51-4.54 (m, 1H, **H^2**) **MS (ESI)**: ESI-MS for C$_{16}$H$_{26}$N$_4$O$_6$S (402.2 g/mol) : 401.2 (100%) [M-H]$^-$. Mp (°C) 121.

Synthesis of Biot-3-IDA
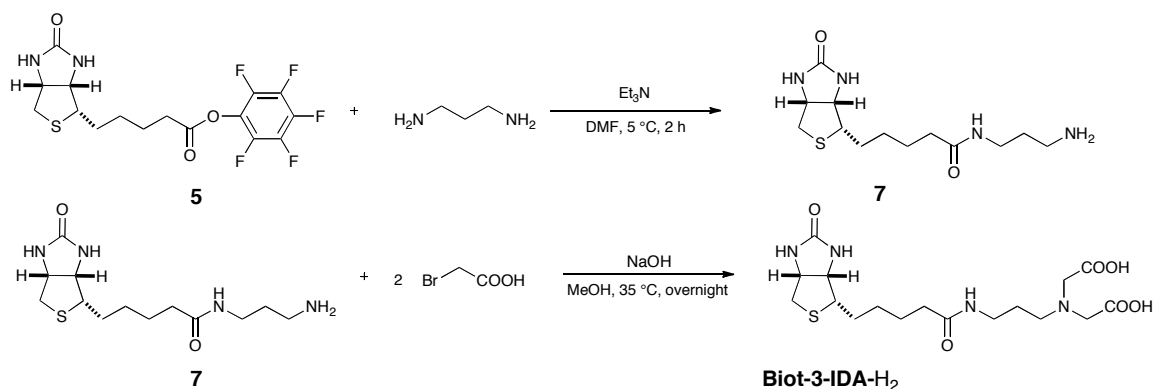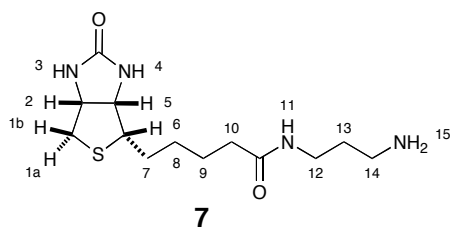
A solution of 1,3-propylenediamine (490 µL, 5.87 mmol) was slowly added at 0°C to a solution of activated biotin **5**[1] (300 mg, 0.73 mmol) in DMF (20 mL) containing Et$_3$N (230 µL, 1.65 mmol). The mixture was stirred at RT for 2 days. The solvent was evaporated under reduced pressure. The residue was dissolved in hot MeOH (20 mL) and cooled overnight (5 °C). The white precipitate was filtered, washed with cold MeOH and cold acetonitrile and dried under reduced pressure to afford amine **7** (Yield: 72%).

^{1}H NMR (400.00 MHz, [D$_6$] DMSO, 20 °C): δ (ppm) = 1.24-1.66 (m, 8H, **H^7,H^8,H^9,H^{14}**), 2.05 (t, 2H, **H^{10}**), 2.56-2.65 (m, 1H, **H^{1a}**), 2.80-2.85 (m, 1H, **H^{1b}**), 3.00-3.12 (m, 5H, **H^6, H^{12}, H^{13}**), 4.11-4.15 (m, 1H, **H^5**), 4.29-4.32 (m, 1H, **H^2**), 6.36 (s, 1H, **H^3**), 6.43 (s, 1H, **H^4**) ; **^{13}C NMR** (100.58 Hz, [D$_6$] DMSO, 20 °C): δ (ppm) = 24.4, 26.2, 28.9, 29.1, 30.2, 36.1, 37.1, 40.7, 56.3, 60.1, 61.9, 163.6, 172.8 ; **MS (ESI)**: ESI-MS for C$_{13}$H$_{24}$N$_4$O$_2$S (300.2 g/mol): 301.2 (100%) [M+H]$^+$. Mp (°C) 241 (Dec.).
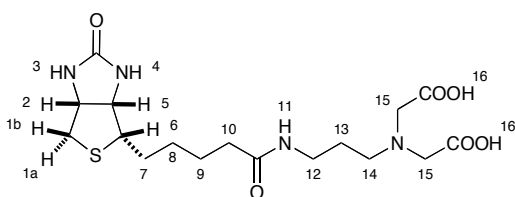
Amine 7 (552 mg, 1.84 mmol) was dissolved in MeOH (60 mL) and mixed with a solution of 2-bromoacetic acid (486 mg, 3.5 mmol) in water (9 mL). The reaction was stirred for 2 h at 35 °C and NaOH (280 mg, 6.99 mmol dissolved in water 6 mL) was added. The solution was stirred for 1 day at RT. The pale brown precipitate was filtered and dried under reduced pressure. The solid obtained was dissolved in MeOH, precipitated with ether and filtered to afford **Biot-3-IDA**-H$_2$ (Yield: 98%).

^{1}**H NMR** (400.00 MHz, D_2O, 20 °C): δ (ppm) = 1.25-1.9 (m, 6H, **H^7, H^8, H^9**), 2.1-2.23 (m , 2H, **H^{10}**), 2.74 (m, 1H, **H^{1a}**), 2.94 (m, 1H, **H^{1b}**), 3.13-3.29 (m, 7H, **H^6, H^{12}, H^{13}, H^{14}**), 3.79-3.86 (m, 4H, **H^{15}**), 4.31-4.37 (m, 1H, **H^5**), 4.52-4.55 (m, 1H ,**H^2**) ; **MS (ESI)**: ESI-MS for $C_{17}H_{28}N_4O_6S$ (416.2 g/mol): 415.5 (100%) [M-H]$^-$. Mp (°C) 77.

Synthesis of Biot-HXTA
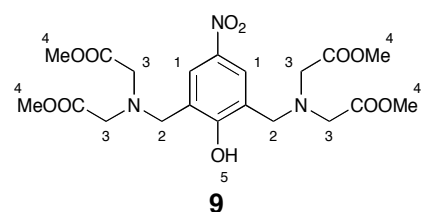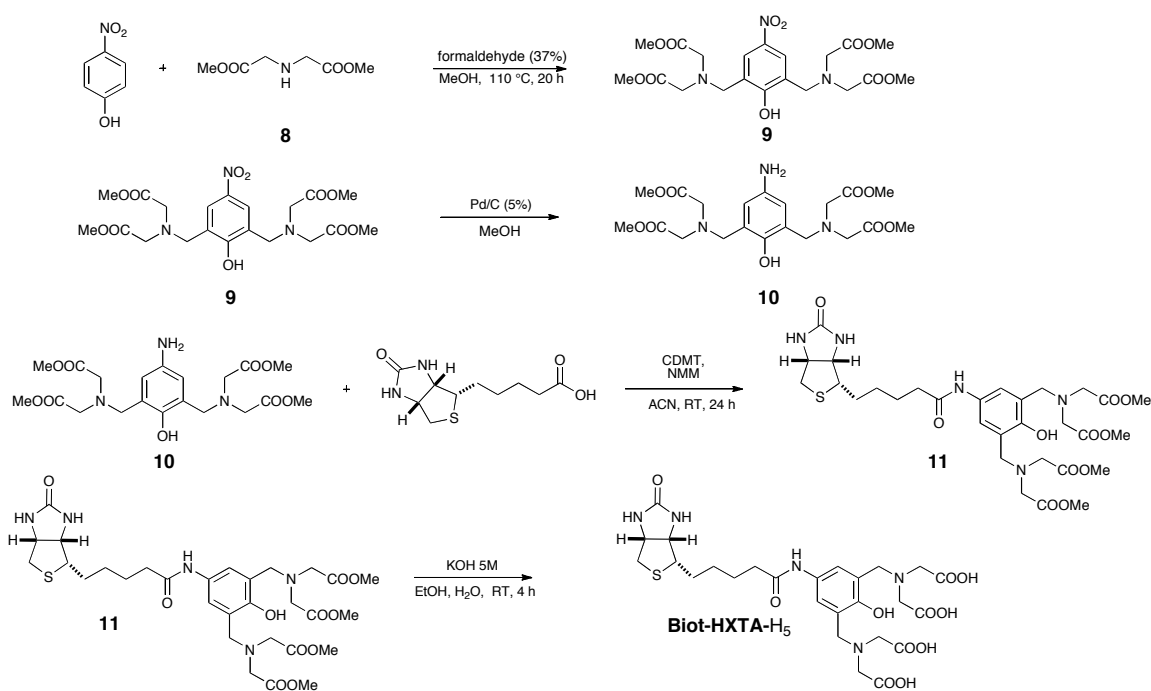
Amine **8** (3.56 g, 22.10 mmol) was added to a solution of aqueous formaldehyde 37 % (0.66 g, 21.84 mmol) and MeOH (12 mL). After evaporation of the solvent, another portion of MeOH (12 mL) was added to the reaction mixture and the solvent was again evaporated. 4-nitrophenol (0.76 g, 5.46 mmol) was added to the mixture and the solution was heated to 110 °C for 20 h. The slurry was dissolved in a minimal amount of dichloromethane and precipitated in an excess of ether. The

collected solid was filtered, washed with cold ether and dried under reduced pressure to afford the nitrophenol **9** (Yield: 19%).

^{1}H NMR (400.00 MHz, CDCl$_3$, 20 °C): δ (ppm) = 3.59 (s, 8H, **H^3**), 3.74 (s, 12H, **H^4**), 4.04 (s, 4H, **H^2**), 8.13 (s, 2H, **H^1**); **^{13}C NMR** (100.58 MHz, CDCl$_3$, 20 °C): δ (ppm) = 171.5, 161.8, 140.4, 126.1, 124.3, 55.6, 54.2, 52.1 ; **MS (ESI)**: ESI-MS for C$_{20}$H$_{27}$N$_3$O$_{11}$ (485.2 g/mol): 486.1 (100%) [M+H]$^+$ 508.13 (10%) [M+Na]$^+$. Mp (°C) 125.
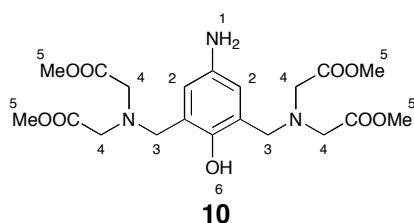
An autoclave containing a suspension of Pd/C (5%, 36.32 mg) in MeOH (18 mL) was filled with *p*-nitrophenol **9** (100 mg, 0.21 mmol). The autoclave was purged three times with nitrogen and filled with hydrogen (3 bars). The reaction was stirred at RT for 3 h, the pressure was carefully released and the suspension was filtered through a celite plug. The organic solvent was evaporated under reduced pressure to dryness to obtain the crude product, which was purified by flash chromatography (CH$_2$Cl$_2$/MeOH 3%) to yield aminophenol **10,** a brown air sensitive sticky solid (Yield: 78%).

^{1}H NMR (400.00 MHz, CDCl$_3$, 20 °C): δ (ppm) = 3.55 (s, 8H, **H^4**), 3.71 (s, 12H, **H^5**), 3.91 (s, 4H, **H^3**), 5.32 (s, 1H, **H^6**), 6.56 (s, 2H, **H^2)** , 8.82 (s, 2H, **H^1**); **^{13}C NMR** (100.58 MHz, CDCl$_3$, 20 °C): δ (ppm) = 171.8, 148.7, 138.5, 123.8, 117.2, 54.2, 54.1, 51.9; **MS (ESI)**: ESI-MS for C$_{20}$H$_{29}$N$_3$O$_9$ (455.2 g/mol): 456.1 (10%) [M+H]$^+$, 478.1 (100%) [M+Na]$^+$.

11
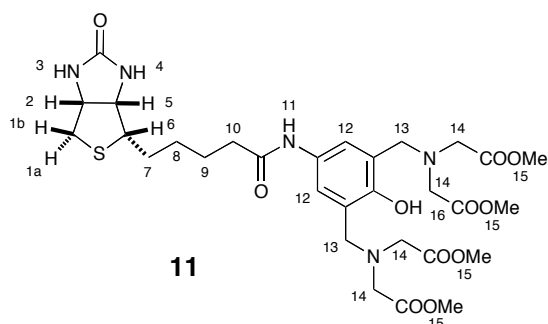
To a suspension of **biotin** (96 mg, 0.39 mmol) in acetonitrile (10 mL) aminophenol **10** (177 mg, 0.389 mmol) and 2-chloro-4,6-dimethoxy-1,3,5-triazine (CDMT) (72 mg, 0.41 mmol) were added. *N*-methymorpholine (0.064 mL, 0.58 mmol) was then added at RT. The solution was stirred at RT for 24 h. The crude product was purified by flash chromatography (AcOEt/MeOH 8:1) to obtain **11** as a white solid. (Yield: 18%).

^{1}H NMR (400.00 MHz, CD$_3$OD, 20 °C): δ (ppm) = 1.5-1.8 (m, 6H, **H^7**, **H^8**, **H^9**), 2.38 (m, 2H, **H^{10}**), 2.73 (m, 1H, **H^{1a}**), 2.95 (m, 1H, **H^{1b}**), 3.25 (m, 1H, **H^6**), 3.54 (s, 8H, **H^{14}**), 3.69 (s, 12H, **H^{15}**), 3.89 (s, 4H, **H^{13}**), 4.31 (m, 1H, **H^5**), 4.49 (m, 1H, **H^2**), 7.29 (s, 2H, **H^{12}**) ; **MS (ESI)**: ESI-MS for C$_{30}$H$_{43}$N$_5$O$_{11}$S (681.3 g/mol): 363.9 (100%) [M+2Na]$^{2+}$. Mp (°C) 95.

Biot-HXTA-H$_5$
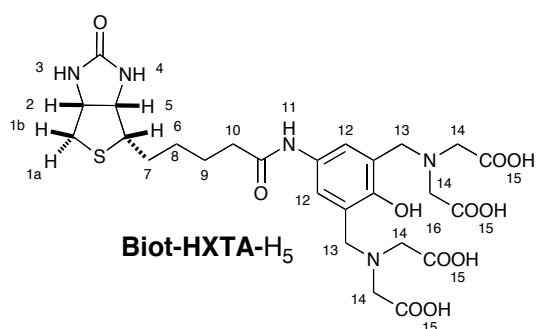
A 10 mL flask was charged with **tetraester 11** (42 mg, 0.062 mmol) and a solution of KOH in EtOH (3 mL, 0.5 M) was added. After 15 min a precipitate had formed. The reaction mixture was stirred for 2 h, water (1.3 mL) was added to dissolve the precipitate and the reaction was stirred for an additional 2 h. The solution was acidified with HCl (1 mL, 2 M). The solvent was removed under reduced pressure and the residue was dissolved in MeOH and filtered. The solvent was removed *in vacuo* to afford the biotinylated ligand **Biot-HXTA**-H$_5$ as a white powder (Yield: 35%).

^{1}H NMR (400.00 MHz, CD$_3$OD, 20 °C): δ (ppm) = 1.17-1.77 (m, 6H, **H^7**, **H^8**, **H^9**), 2.41 (m, 2H, **H^{10}**), 2.76 (m, 1H, **H^{1a}**), 2.97 (m, 1H, **H^{1b}**), 3.25 (m, 1H, **H^6**), 4.24 (s, 4H, **H^{13}**), 4.43 (m, 1H, **H^5**), 4.61 (m, 1H, **H^2**), 4.67 (s, 8H, **H^{14}**), 7.81 (s, 2H, **H^{12}**) ; **MS (ESI):** ESI-MS for C$_{26}$H$_{35}$N$_5$O$_{11}$S (625.2 g/mol): 624.3 (100%) [M-H]$^-$. Mp (°C) 271(Dec.).

Synthesis of Biot-4*m*-HXTA
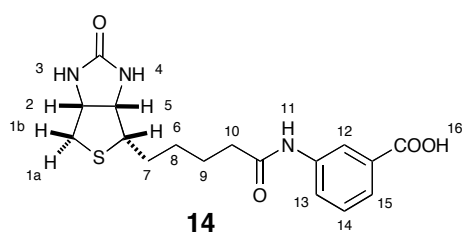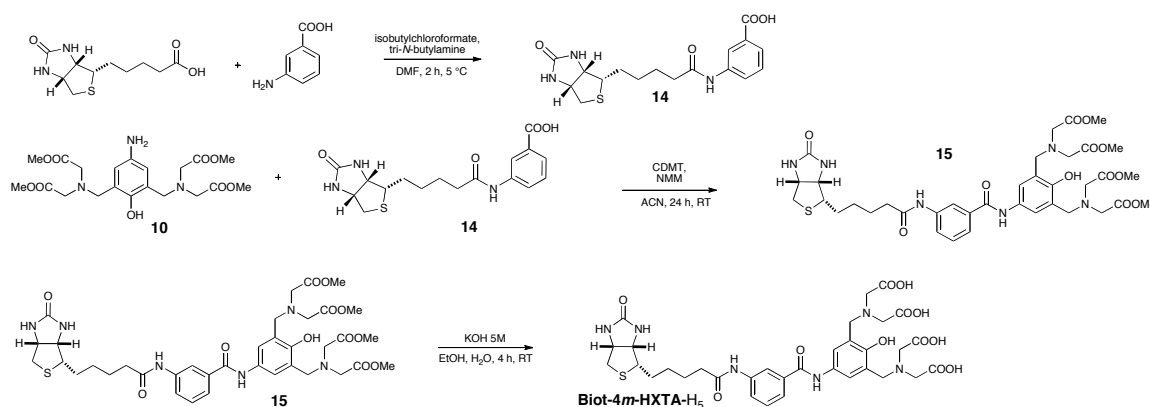
Isobutyl chloroformate (0.32 mL, 2.47 mmol) was added to a solution of biotin (496 mg, 2.03 mmol) in DMF (40 mL) containing tri-*N*-butylamine (0.64 mL, 2.69 mmol). After 10 min at RT, the mixture was slowly added at 5 °C to a suspension 3-aminobenzoic acid (561 mg, 4.1 mmol) in DMF (40 mL). After stirring at 5 °C for 2 h, the solvent was removed under reduced pressure and the crude precipitate was dissolved in warm aqueous EtOH (1:1, 36 mL total). The mixture was acidified with 2.0 M HCl to pH 2 and kept at 0 °C for 12 h. The resulting precipitate was filtered, washed with water and dried under reduced pressure to afford **14** as a pale yellow powder (yield: 65%).

^{1}H NMR (400 MHz, [D$_6$] DMSO, 20 °C): δ (ppm) = 1.30-1.70 (m, 6H, **H^7, H^8, H^9**), 2.34 (m, 2H, **H^{10}**), 2.61 (m, 1H, **H^{1a}**), 2.83 (dd, 1H, **H^{1b}**), 3.16 (m, 1H, **H^6**)**,** 4.16 (m, 1H, **H^5**), 4.32 (m, 1H, **H^2**), 6.38 (br, 1H, **H^4**), 6.46 (br, 1H, **H^3**), 7.42 (m, 1H, **H^{13}**), 7.61 (m, 1H, **H^{12}**), 7.84 (m, 1H, **H^{14}**), 8.25 (m, 1H, **H^{15}**), 10.15 (br, 1H, **H^{11}**), 12.80 (br, 1H; **H^{16}**); **^{13}C NMR** (100.58 MHz, [D$_6$] DMSO, 20 °C): δ (ppm) = 25.9, 29.0, 29.1, 37.1, 40.7, 56.3, 60.1, 61.9, 120.6, 124, 124.6, 129.8, 132.1, 140.4, 163.6, 168.1, 172.3; **MS (ESI)**: ESI-MS for C$_{17}$H$_{21}$N$_3$O$_4$S (363.13 g/mol) : 362.2 [M-H]$^-$. Mp (°C) 288 (Dec.).
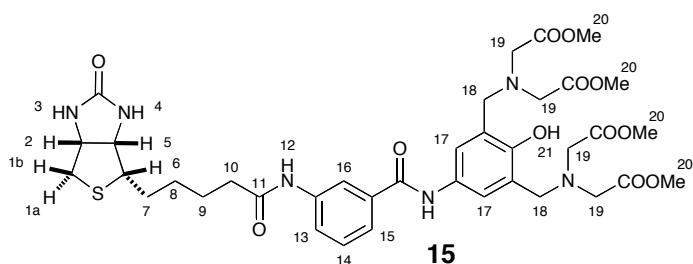
To a suspension of **carboxylic acid 14** (144, 0.39 mmol) in acetonitrile (10 mL), **amine 10** (177 mg, 0.38 mmol), 2-chloro-4,6-dimethoxy-1,3,5-triazine (72 mg, 0.41 mmol) and *N*-methymorpholine (0.093 mL, 0.596 mmol) were added. The solution was stirred at RT for 24 h. The crude tetraester **15** was purified by flash chromatography (AcOEt/MeOH 8:1) to obtain **18** as a white solid (Yield: 12%).

^{1}H NMR (500.00 MHz, CD$_3$OD, 20 °C): δ (ppm) = 1.47-1.94 (m, 6H, **H^7, H^8, H^9**), 2.43 (m, 2H, **H^{10}**), 2.70 (d, 1H, **H^{1a}**), 2.92 (m, 1H, **H^{1b}**), 3.30 (m, 1H, **H^6**), 3.57 (s, 8H, **H^{19}**), 3.70 (m, 12H, **H^{20}**), 3.93 (s, 4H, **H^{18}**), 4.31 (m, 1H, **H^5**), 4.49 (m, 1H, **H^2**), 7.44 (m, 3H, **H^{17}, H^{14}**), 7.61 (m, 1H**, H^{15}**), 7.73 (m, 1H, **H^{13}**), 8.08 (s, 1H, **H^{16}**) ; **MS (ESI):** ESI-MS for C$_{37}$H$_{48}$N$_6$O$_{12}$S (800.3 g/mol): 822.8 (25%) [M+Na]$^+$, 801.0 (100%) [M+H]$^+$. Mp (°C) 87.
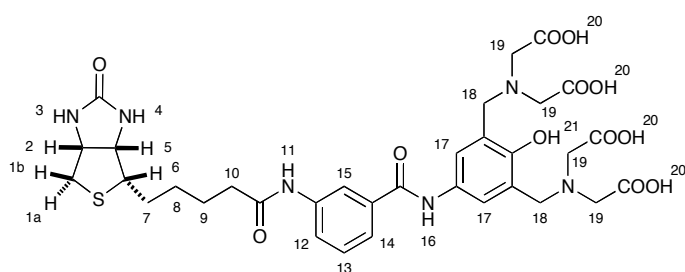
Biot-4*m*-HXTA-H$_5$

A 10 mL flask was charged with **tetraester 15** (50.4 mg, 0.067 mmol) and a solution of KOH in EtOH (3 mL, 0.5 M). After 15 min a precipitate was formed. The reaction mixture was stirred for 2 h, water (1.3 mL) was added to dissolve the precipitate and the reaction was stirred for an additional 2 h. The solution was acidified with HCl (1 mL, 2 M). The solvent was removed under reduced pressure and the residue was dissolved in MeOH and filtered. The solvent was removed *in vacuo* to afford the biotinylated ligand **Biot-4*m*-HXTA-**H$_5$ as a white powder (Yield: 20%).

^{1}H NMR (500.00 MHz, CD$_3$OD, 20 °C): δ (ppm) = 1.25-1.8 (m, 6H, **H^7**, **H^8**, **H^9**), 2.47 (m, 2H, **H^{10}**), 2.75 (m, 1H, **H^{1a}**), 2.97 (m, 1H, **H^{1b}**), 3.27 (m, 1H, **H^6**), 4.13 (s, 8H, **H^{19}**), 4.36 (m, 1H, **H^5**), 4.54 (s, 1H, **H^2**), 4.58 (s, 4H, **H^{18}**), 7.49-7.69 (m, 3H, **H^{12}**, **H^{13}, H^{14}**), 7.81 (s, 1H, **H^{15}**), 8.25 (s, 2H, **H^{17}**) ; MS (Maldi-TOF, neg) for C$_{33}$H$_{40}$N$_6$O$_{12}$S (744.2 g/mol): 742.7 (100%) [M-H]$^-$.

Synthesis of Biot-4*p*-HXTA
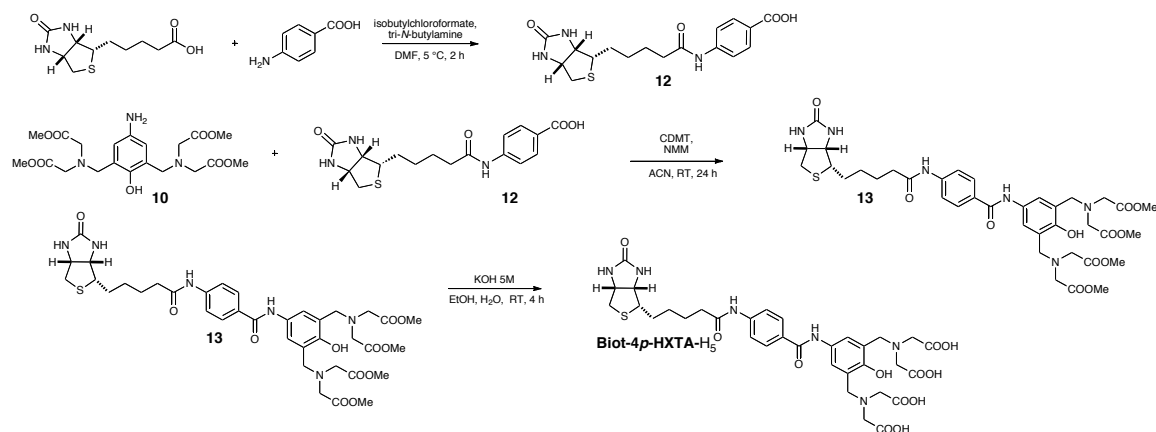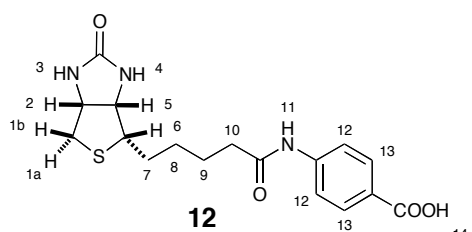
Isobutyl chloroformate (0.32 mL, 2.47 mmol) was added to a solution of biotin (496 mg, 2.03 mmol) in DMF (40 mL) containing tri-*N*-butylamine (0.64 mL, 2.69 mmol). After 10 min at RT, the mixture was slowly added at 5 °C to a suspension of 4-aminobenzoic acid (561 mg, 4.1 mmol) in DMF (40 mL). After stirring at 5 °C for 2 h, the solvent was distilled under reduced pressure and the crude precipitate was dissolved in warm aqueous EtOH (1:1, 36 mL total). The mixture was acidified with 2.0 M HCl to pH 2 and kept at 0 °C for 12 h. The precipitated product **12** was filtered, washed with water and dried under reduced pressure. (Yield: 74%).

^{1}H NMR (400.00 MHz, [D$_6$] DMSO, 20 °C): δ (ppm) = 1.30-1.70 (m, 6H, **H^7, H^8, H^9**), 2.36 (m, 2H, **H^{10}**), 2.61 (m 1H; **H^{1a}**), 2.84 (m, 1H, **H^{1b}**), 3.13 (m, 1H, **H^6**), 4.16 (m, 1H, **H^5**), 4.32 (m, 1H, **H^2**), 6.41 (br, 1H, **H^4**), 6.50 (br, 1H; **H^3**), 7.72 (d, *J* = 8.8 Hz, 2H, **H^{12}**), 7.89 (d, *J* = 8.8 Hz, 2H, **H^{13}**), 10.20 (br, 1H, **H^{11}**), 12.68 (br, 1H, **H^{14}**), **^{13}C NMR** (100.58 MHz, [D$_6$] DMSO, 20 °C): δ (ppm) = 25.8, 28.9, 29.1, 37.2, 40.7, 56.3, 60.1, 61.9, 119.1, 125.7, 131.2, 144.2, 163.7, 167.8, 172.6 ; **MS (ESI)**: ESI-MS for C$_{17}$H$_{21}$N$_3$O$_4$S (363.13 g/mol): 386.13 (100%) [M+Na]$^+$. Mp (°C) 285 (Dec.).
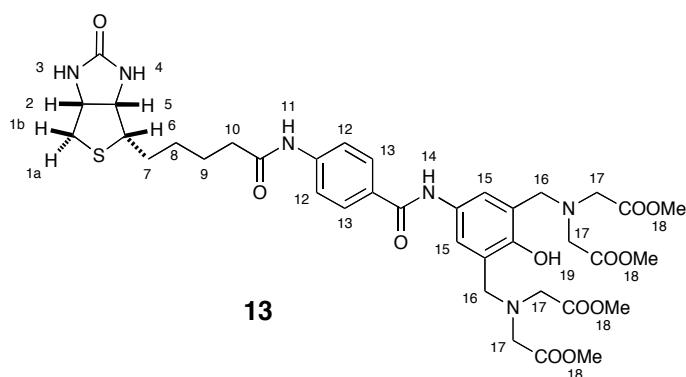
To a suspension of **carboxylic acid 12** (144 mg, 0.39 mmol) in acetonitrile (10 mL) aminophenol **10** (177 mg, 0.38 mmol), 2 chloro-4,6-dimethoxy-1,3,5-triazine (72 mg, 0.596 mmol) and *N*-methymorpholine (0.064 mL, 0.58 mmol) were added to the suspension. The

resulting solution was stirred at RT for 24 h. The crude product was purified by flash chromatography (AcOEt/MeOH 8:1) to yield the tetraester **13** as white solid (Yield: 10 %).

^{1}H NMR (400.00 MHz, CD$_3$OD, 20 °C): δ (ppm) = 1.5-1.8 (m, 6H, **H^7**, **H^8**, **H^9**), 2.46 (m, 2H, **H^{10}**), 2.73 (m, 1H, **H^{1a}**), 2.95 (m, 1H, **H^{1b}**), 3.25 (m, 1H, **H^6**), 3.60 (s, 8H, **H^{17}**), 3.74 (s, 12H, **H^{18}**), 3.96 (s, 4H, **H^{16}**), 4.35 (m, 1H, **H^5**), 4.52 (m, 1H, **H^2**), 7.45 (s, 2H, **H^{15}**), 7.75 (d, *J* = 8.8 Hz, 2H, **H^{13}**), 7.92 (d, *J* = 8.7 Hz, 2H, **H^{12}**); **MS (ESI):** ESI-MS for C$_{37}$H$_{48}$N$_6$O$_{12}$S (800.3 g/mol): 801.0 (100%) [M+H]$^+$, 822.8 (25%) [M+Na]$^+$.


Biot-4*p*-HXTA-H$_5$
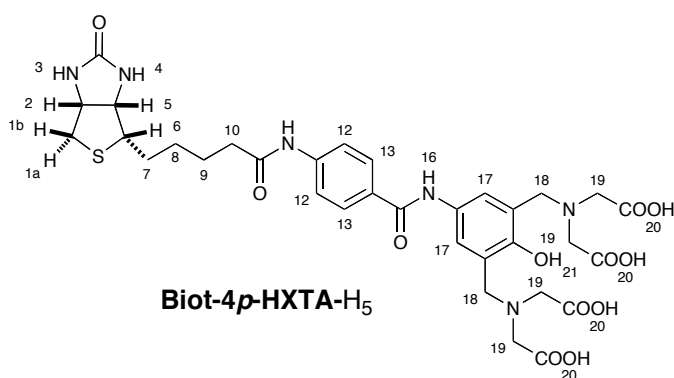
A 10 mL flask was charged with tetraester **13** (50.4 mg, 0.067 mmol) and a solution of KOH in EtOH (3 mL, 0.5 M) was added. After 15 min a precipitate formed. The reaction mixture was stirred for 2 h and water (1.3 mL) was added to dissolve the precipitate. The solution was stirred for an additional 2 h and the solution was acidified with HCl (1 mL, 2 M). The solvent was removed under reduced pressure, the residue was dissolved in MeOH and filtered. The solvent was removed *in vacuo* to afford the biotinylated ligand **Biot-4*p*-HXTA**-H$_5$ *as* a white powder (Yield: 23%).

^{1}H NMR (400.00 MHz, CD$_3$OD, 20 °C): δ (ppm) = 1.36-1.77 (m, 6H, **H^7**, **H^8**, **H^9**), 2.35 (m, 2H, **H^{10}**), 2.60-2.63 (m, 1H, **H^{1a}**), 2.83-2.86 (m, 1H, **H^{1b}**), 3.13 (m, 1H, **H^6**), 3.93 (s, 8H, **H^{19}**), 4.24 (m, 1H, **H^5**), 4.38 (s, 4H, **H^{18}**), 4.41 (m, 1H, **H^2**), 7.61 (s, 2H, **H^{17}**), 7.64-7.66 (d, *J* = 8.7 Hz, 2H, **H^{13}**), 7.82-7.84 (d, *J* = 8.7 Hz, 2H, **H^{12}**) ; **MS** (Maldi-TOF, neg) for C$_{33}$H$_{40}$N$_6$O$_{12}$S (744.2 g/mol): 742.7 (100%) [M-H]$^-$.

Synthesis of the Biot-phen-HXTA
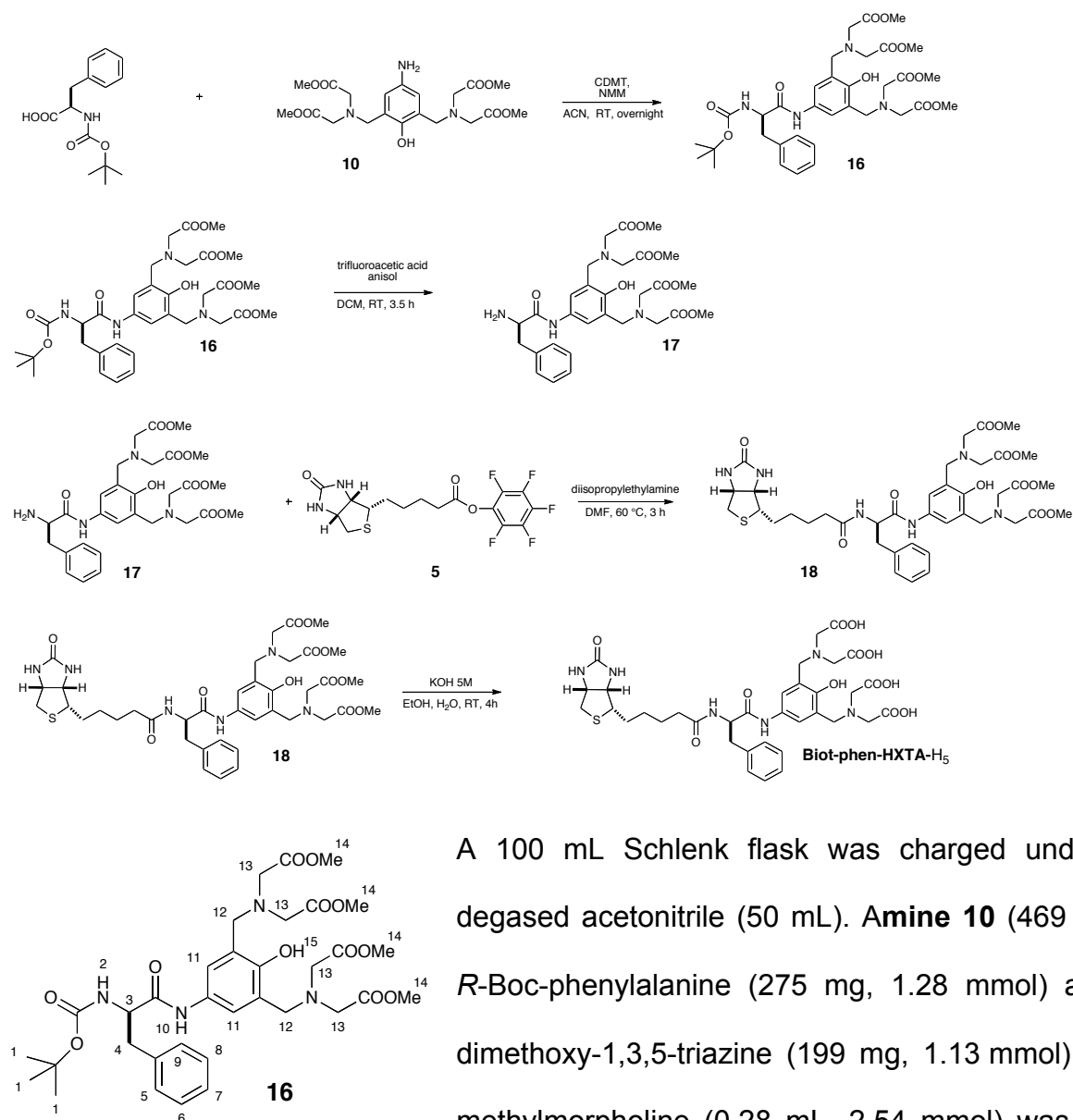
A 100 mL Schlenk flask was charged under nitrogen with degased acetonitrile (50 mL). A**mine 10** (469 mg, 1.03 mmol), *R*-Boc-phenylalanine (275 mg, 1.28 mmol) and 2-chloro-4,6-dimethoxy-1,3,5-triazine (199 mg, 1.13 mmol) were added. *N*-methylmorpholine (0.28 mL, 2.54 mmol) was added dropwise and the red reaction mixture was stirred overnight. The solvent was removed under reduced pressure and the crude product was dissolved in MeOH and adsorbed on silica. Column chromatography (CH₂Cl₂/MeOH, gradient from 0.00-3.00% MeOH) yielded the **Boc-protected amine 16** (Yield: 30 %) as a red oil.

¹**H NMR** (400.00 MHz, CDCl₃, 20 °C): δ (ppm) = 1.29 (s, 9H, **H¹**), 2.30-2.74 (m, 2H, **H⁴**), 3.25 (s, 16H, **H¹²**, **H¹⁴**), 3.36 (m, 1H, **H³**), 3.44 (s, 2H, **H⁴**), 3.62 (s, 8H, **H¹³**), 7.20-6.70 (m, 7H, **H⁵**, **H⁶**, **H⁷**, **H⁸**, **H⁹**, **H¹¹**) ; MS (ESI): ESI-MS for C₃₄H₄₆N₄O₁₂ (702.31 g/mol)**:** 703.1 (100%) [M+H]⁺, 724.9 (20%) [M+Na]⁺, 740.8 (4%) [M+K]⁺.
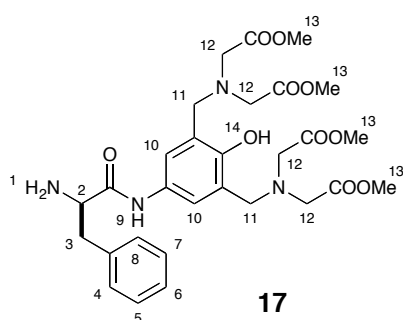
A 5 mL flask was charged with **Boc-protected amine 16** (218.2 mg, 0.31 mmol) and CH₂Cl₂ (0.5 mL). A solution of trifluoroacetic acid (0.46 mL, 6.05 mmol) and anisole (0.045 mL, 0.625 mmol) in CH₂Cl₂ (1 mL) was slowly added. The resulting dark red solution was stirred for 3.5 h at RT. The solvent was removed under reduced pressure to afford the crude **amine 17** (Yield: 100%) as a red oil which was used without further purification.

¹**H NMR** (400.00 MHz, CDCl₃, 20 °C): δ (ppm) = 3.51 (s, 12H, **H¹³**), 3.68 (s, 8H, **H¹²**), 4.32 (s, 4H, **H¹¹**), 6.69-7.40 (m, 10H, **H²,H³,H⁴,H⁵,H⁶,H⁷,H⁸,H¹⁰**) ; **MS (ESI):** ESI-MS for C₂₉H₃₈N₄O₁₀ (602.3 g/mol): 603.1 (100%) [M+H]⁺.
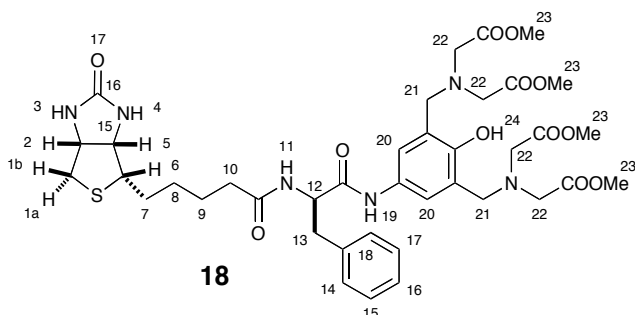
A 50 mL Schlenk flask was charged with degased DMF (5 mL) and activated biotin **5**[1] (127 mg, 0.31 mmol). A solution of **amine 17** (187 mg, 0.31 mmol) in DMF (20 mL) was added, the red solution was stirred and diisopropylethylamine (155 mg, 1.2 mmol) was added. The reaction mixture was stirred for 40 h at RT and then at 60 °C for 3 h. The solvent was removed under reduced pressure and the brown crude product was dissolved in

MeOH and adsorbed on silica. The crude product was purified by preparative TLC (Solvent: AcOEt 4/ MeOH 1) to afford pure tetraester **18** as a yellow solid (Yield: 8.25 %).

¹H NMR (500.00 MHz, CD₃OD, 20 °C): δ = 1.44-1.76 (m, 6H, **H⁷, H⁸, H⁹**), 2.5 (m,, 2H, **H¹⁰**), 2.86 (m, 1H, **H¹ᵃ**), 2.90 (m, 1H, **H¹ᵇ**), 3.25 (m, 3H, **H¹², H¹³**), 3.25 (m, 1H, **H⁶**) 3.50 (s, 8H, **H²²**), 3.66 (s, 12H, **H²³**), 3.81 (s, 4H, **H²¹**), 4.23-4.30 (m, 1H, **H⁵**), 4.40-4.50 (m, 1H, **H²**), 7.45 (m, 3H, **H¹⁵, H¹⁶, H¹⁷**), 7.61 (m, 1H, **H¹⁴**), 7.76 (m, 1H, **H¹⁸**), 8.1 (s, 2H, **H²⁰**) ; **MS (ESI):** ESI-MS for $C_{39}H_{52}N_6O_{12}S$ (828.3 g/mol): 829.5 (100%) [M+H]⁺, 851.4 (25%) [M+Na]⁺. Mp (°C) 88.5.

Biot-phen-HXTA-H₅
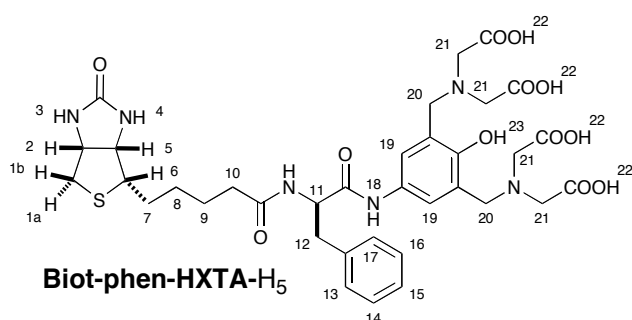
A 10 mL flask was charged with tetraester **18** (40 mg, 0.053 mmol) and a solution of KOH in EtOH (3 mL, 0.5 M) was added. After 15 min a precipitate formed. The reaction mixture was stirred for 2 h, water (1.3 mL) was added to dissolve the precipitate and the reaction stirred for an additional 2 h. The solution was acidified with HCl (1 mL, 2 M). The solvent was removed under reduced pressure and the residue was dissolved in MeOH and filtered. The solvent was removed *in vacuo* to afford the biotinylated ligand **Biot-phen-HXTA-H₅** as a white powder (Yield: 30%).

¹H NMR (400.00 MHz, CD₃OD, 20 °C): δ (ppm) = 1.51-1.79 (m, 6H, **H⁷, H⁸, H⁹**), 2.26 (m, 2H, **H¹⁰**), 2.71-2.74 (m, 1H, **H¹ᵃ**), 2.91-3.12 (m, 1H, **H¹ᵇ**), 3.18 (m, 1H, **H⁶**), 3.24 (m, 2H, **H¹²**), 4.14 (s, 8H, **H²¹**), 4.29 (m, 1H, **H¹¹**), 4.52 (m, 1H, **H⁵**) 4.56 (s, 4H, **H²⁰**), 4.70 (m, 1H, **H²**), 7.23-7.31 (m, 5H, **H¹³, H¹⁴, H¹⁵, H¹⁶, H¹⁷**), 7.63 (s, 2H, **H¹⁹**).; MS (Maldi-TOF, neg) for $C_{35}H_{44}N_6O_{12}S$ (772.3 g/mol): 770.7 (100%) [M-H]⁻. Mp (°C) 240 (Dec.).

Complexes: The formation of the {(**Biot-spacer-HXTA**)Ce$_2$}$^{3+}$ complex was conveniently monitored by the appearance of an absorption band at 472 nm upon addition of ceric ammonium nitrate to **Biot-spacer-HXTA**-H$_5$ at pH 8 as described by Que for the non-biotinylated analogue.[2]

7.2. Experimental procedure for catalysis

The catalysis was performed in a 96 well plate and the reactions were monitored with a thermostatted Tecan Safire-2 plate reader. The following solutions were added to each well by means of a 12 channel pipette:

i) biotinylated ligand (15 μL, 2.4 mM in HEPES 100 mM pH 7), ii) Ceric ammonium nitrate (15 μL, 4.8 mM for the HXTA ligands in water and 2.4 mM for the IDA ligands).

iii) streptavidin isoform (100 μL, 0.4 mM with 4 active sites in HEPES 100 mM pH 7).

iv) enantiopure **HPNP** substrate (7.5 μL, 10 mM, in HEPES 100 mM pH 7).

v) buffer (7.5 μL, HEPES 100 mM, pH 7).

The hydrolysis of the substrate was monitored at 37 °C for 4.5 h at 405 nm. The initial rate for each reaction was calculated using the Magellan software. The estimated *E* was determined as the ratio of the slopes of the measured initial rates for both **HPNP** enantiomers.

HPNP, 1

$Abs_{max} = 405$ nm
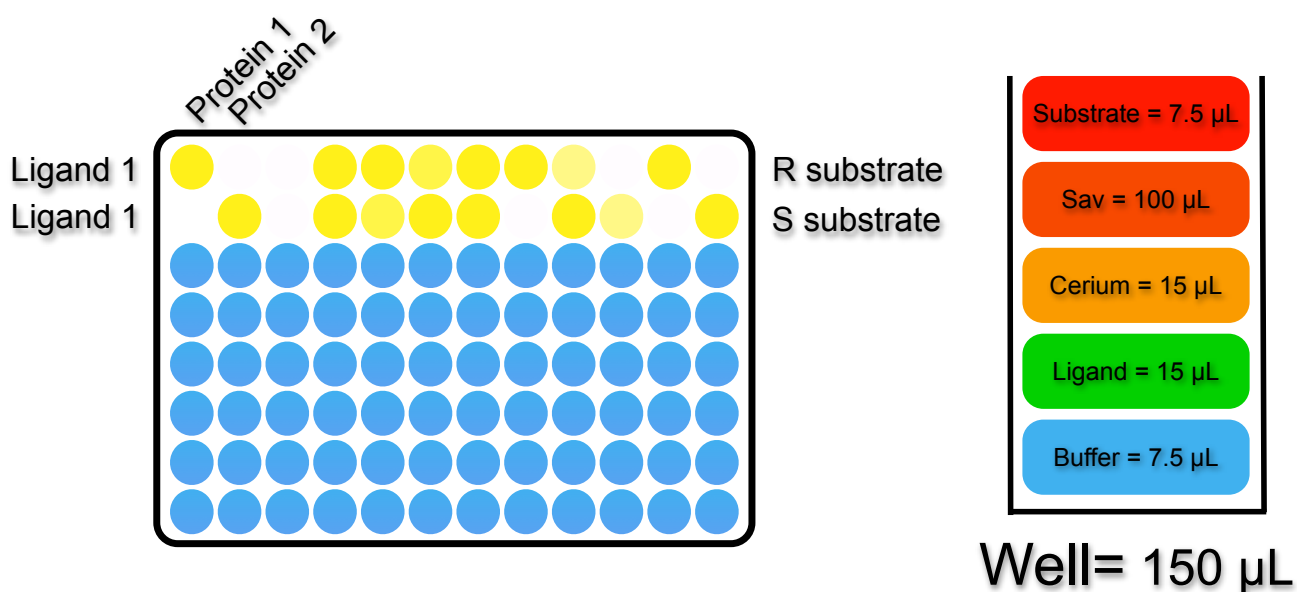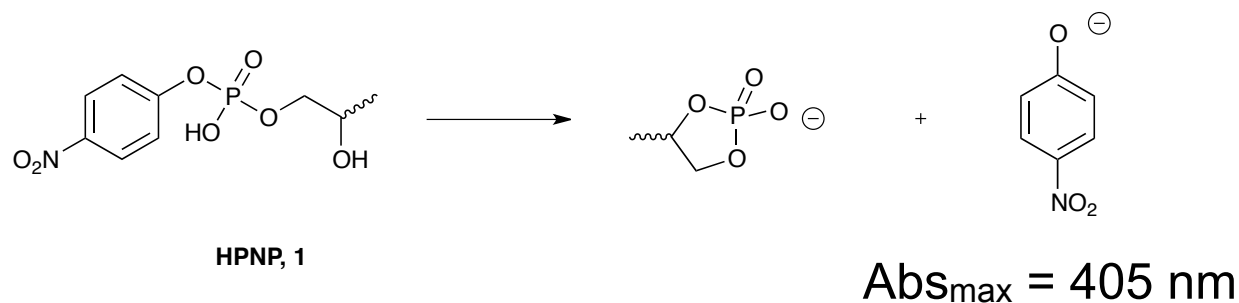
Yellow dots = reaction mixtures

Blue dots = empty wells

Figure 19 Schematic representation of the catalytic setup (Selectivity is given by the Estimated *E*, ratio of the initial slopes for each enantiomer).

7.3 Summary of initial rates

Values given in [mmole·h^{-1}], NR : not determined

Entry	Protein	Enantiomer	Biot-2-IDA	Biot-3-IDA	Biot-HXTA	Biot-4m-HXTA	Biot-4p-HXTA	Biot-phen-HXTA
1	–	(R)-HPNP	2.00E-08	1.83E-08	2.92E-08	3.82E-08	2.68E-08	3.97E-08
2	–	(S)-HPNP	1.30E-08	6.28E-09	0.00E+00	3.03E-08	6.46E-09	4.23E-08
3	S112A	(R)-HPNP	2.89E-09	1.05E-08	6.67E-08	1.03E-07	1.49E-10	6.11E-08
4	S112A	(S)-HPNP	4.39E-09	3.83E-10	7.07E-08	3.21E-08	7.25E-09	1.13E-07
5	S112G	(R)-HPNP	8.18E-10	3.30E-09	1.11E-08	4.08E-09	1.77E-09	1.01E-07
6	S112G	(S)-HPNP	1.05E-08	2.63E-08	7.03E-09	9.31E-09	3.95E-09	1.72E-07
7	S112V	(R)-HPNP	3.75E-09	5.53E-09	3.29E-09	1.32E-08	9.37E-09	1.50E-07
8	S112V	(S)-HPNP	1.04E-09	2.64E-10	3.81E-09	1.65E-08	5.87E-09	7.22E-08
9	S112H	(R)-HPNP	1.05E-08	4.63E-08	4.51E-08	1.09E-10	2.42E-09	1.33E-07
10	S112H	(S)-HPNP	1.22E-08	NR	1.24E-08	NR	3.89E-09	1.47E-07
11	S112N	(R)-HPNP	4.13E-10	8.20E-08	9.51E-09	1.51E-08	2.33E-08	7.19E-08
12	S112N	(S)-HPNP	1.09E-08	6.71E-09	5.93E-08	0.00E+00	0.00E+00	5.52E-08
13	S112D	(R)-HPNP	NR	1.83E-07	2.89E-08	9.44E-08	1.54E-09	1.72E-07
14	S112D	(S)-HPNP	3.15E-08	1.55E-08	1.83E-07	9.17E-08	7.84E-09	0.00E+00
15	S112K	(R)-HPNP	2.35E-09	9.82E-09	3.56E-08	1.86E-08	1.40E-08	9.53E-08
16	S112K	(S)-HPNP	2.40E-09	2.40E-09	8.38E-08	1.05E-07	4.81E-09	1.84E-07
17	S112T	(R)-HPNP	1.17E-09	4.17E-08	2.17E-09	2.65E-08	1.97E-09	1.33E-07
18	S112T	(S)-HPNP	1.77E-08	0.00E+00	1.24E-08	1.11E-07	7.17E-09	5.28E-08
19	WT	(R)-HPNP	1.02E-07	8.84E-08	1.69E-07	2.14E-07	1.46E-07	1.69E-07
20	WT	(S)-HPNP	9.62E-08	9.38E-08	1.58E-07	2.13E-07	1.83E-07	1.76E-07
21	K121G	(R)-HPNP	1.10E-07	9.92E-08	1.65E-07	2.09E-07	1.90E-07	2.10E-07
22	K121G	(S)-HPNP	7.90E-08	9.09E-08	1.64E-07	2.16E-07	1.48E-07	2.43E-07
23	K121H	(R)-HPNP	1.08E-07	9.72E-08	1.72E-07	1.43E-07	2.18E-07	1.30E-07
24	K121H	(S)-HPNP	8.06E-08	1.13E-07	9.08E-08	1.94E-07	1.80E-07	1.81E-07
25	K121N	(R)-HPNP	8.33E-08	7.91E-08	1.56E-07	1.71E-07	1.78E-07	1.78E-07
26	K121N	(S)-HPNP	8.19E-08	7.79E-08	1.36E-07	2.09E-07	2.24E-07	1.15E-07
27	K121R	(R)-HPNP	8.78E-08	7.35E-08	1.49E-07	9.58E-08	1.68E-07	1.69E-07
28	K121R	(S)-HPNP	7.59E-08	9.00E-08	1.25E-07	1.86E-07	1.43E-07	1.37E-07
29	K121F	(R)-HPNP	1.25E-07	1.14E-07	1.87E-07	2.00E-07	2.03E-07	2.02E-07
30	K121F	(S)-HPNP	1.22E-07	1.19E-07	1.39E-07	1.21E-07	1.55E-07	8.74E-08
31	K124G	(R)-HPNP	8.16E-08	1.08E-07	9.61E-08	1.80E-07	6.84E-08	8.53E-08
32	K124G	(S)-HPNP	4.37E-08	8.06E-08	4.30E-08	1.16E-07	2.80E-08	7.02E-08
33	K124V	(R)-HPNP	5.08E-08	6.13E-08	4.19E-08	2.08E-08	3.96E-08	2.90E-08
34	K124V	(S)-HPNP	4.04E-08	4.50E-08	2.06E-08	2.38E-08	3.48E-08	NR
35	K124K	(R)-HPNP	7.22E-08	8.16E-08	1.53E-07	1.70E-07	1.70E-07	1.16E-07
36	K124K	(S)-HPNP	7.91E-08	6.32E-08	8.08E-08	1.80E-07	1.42E-07	1.25E-07
37	K124Y	(R)-HPNP	8.20E-08	8.89E-08	1.47E-07	1.96E-07	1.90E-07	1.09E-07
38	K124Y	(S)-HPNP	7.90E-08	9.09E-08	1.64E-07	2.16E-07	1.48E-07	2.43E-07

Duplicates:

Entry	Biotinylated complex	Sav	(R)-HPNP k_{obs}/k_{uncat}	(S)-HPNP k_{obs}/k_{uncat}
1	{(Biot-4*m*-HXTA)Ce$_2$}$^{3+}$	-	8	8
2	{(Biot-4*m*-HXTA)Ce$_2$}$^{3+}$	-	8	8
3	{(Biot-2-IDA)Ce}$^{2+}$	K121G	29	20
4	{(Biot-2-IDA)Ce}$^{2+}$	K121G	25	18
5	{(Biot-2-IDA)Ce}$^{2+}$	K121F	23	24
6	{(Biot-2-IDA)Ce}$^{2+}$	K121F	28	28
7	{(Biot-HXTA)Ce$_2$}$^{3+}$	K121F	44	29
8	{(Biot-HXTA)Ce$_2$}$^{3+}$	K121F	43	32
9	{(Biot-4*m*-HXTA)Ce$_2$}$^{3+}$	L124Y	41	44
10	{(Biot-4*m*-HXTA)Ce$_2$}$^{3+}$	L124Y	45	49
11	{(Biot-phen-HXTA)Ce$_2$}$^{3+}$	WT	35	37
12	{(Biot-phen-HXTA)Ce$_2$}$^{3+}$	WT	38	40
13	{(Biot-phen-HXTA)Ce$_2$}$^{3+}$	K121G	52	60
14	{(Biot-phen-HXTA)Ce$_2$}$^{3+}$	K121G	47	55
15	{(Biot-phen-HXTA)Ce$_2$}$^{3+}$	K121F	52	19
16	{(Biot-phen-HXTA)Ce$_2$}$^{3+}$	K121F	45	20

7.4 Estimated *E* values

As described in[26]

Entry	Protein	Biot-IDA-2	Biot-IDA-3	BiotHXTA	Biot-4*m*-HXTA	Biot-4*p*-HXTA	Biot-phen-HXTA
1	–	1	1	1	1	1	1
2	112A	1.52	27.48	1.06	3.21	48.49	1.85
3	112G	12.85	7.98	1.58	2.28	2.23	1.70
4	112V	3.61	20.96	1.16	1.25	1.60	2.08
5	112H	1.16	>65	3.64	>65	1.61	1.10
6	112N	1.02	1.02	1.15	1.22	1.26	1.54
7	112D	>65	11.82	6.34	1.03	5.11	>65
8	112K	1.02	4.10	2.35	5.65	2.90	1.00
9	112T	15.15	>65	5.69	4.19	3.63	2.53
10	WT	1.06	1.06	1.07	1.00	1.26	1.04
11	121G	1.39	1.09	1.01	1.03	1.28	1.15
12	121H	1.34	1.16	1.90	1.35	1.21	1.39
13	121N	1.02	1.02	1.15	1.22	1.26	1.54
14	121R	1.16	1.22	1.19	1.95	1.18	1.23
15	121F	1.02	1.05	1.34	1.65	1.31	2.31
16	124G	1.87	1.34	2.24	1.55	2.44	1.21
17	124V	1.26	1.36	2.03	1.14	1.14	>65
18	124K	1.10	1.29	1.89	1.06	1.20	1.08
19	124Y	1.04	1.02	1.12	1.10	1.29	2.23

7.5 Turnover number
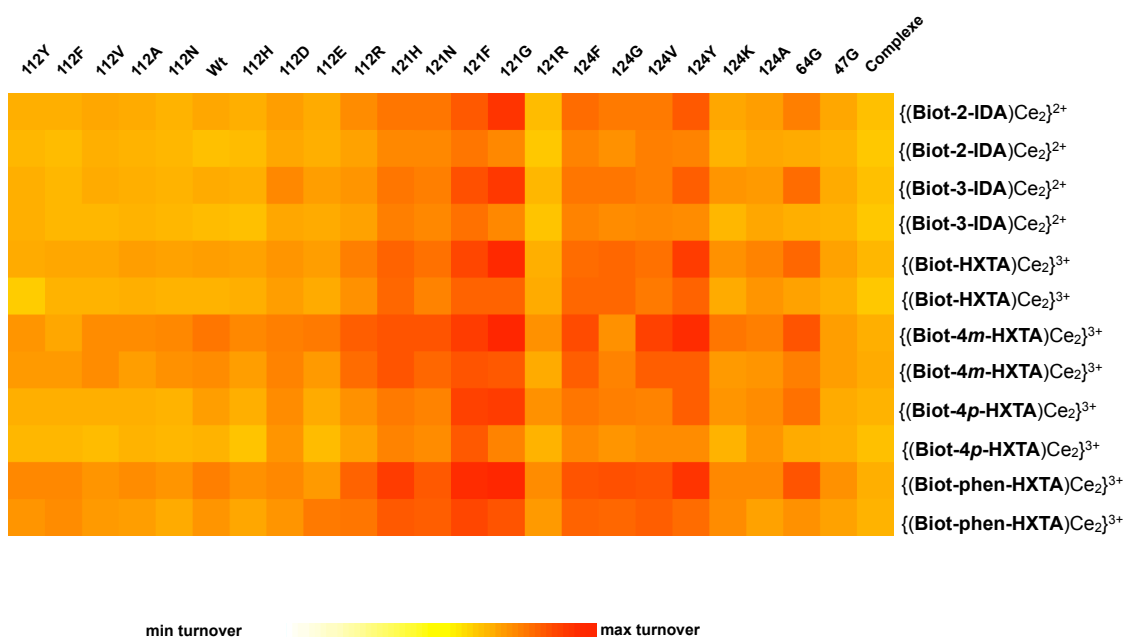
Best conversion results per metalloenzyme

Entry	Metalloenzymes	TON
1	$\{($Biot-2-IDA$)$Ce$\}^{2+} \subset$ K121G	1.64
2	$\{($Biot-3-IDA$)$Ce$\}^{2+} \subset$ K121G	1.61
3	$\{($Biot-HXTA$)$Ce$_2\}^{3+} \subset$ K121G	1.80
4	$\{($Biot-4m-HXTA$)$Ce$_2\}^{3+} \subset$ K121G	1.95
5	$\{($Biot-4p-HXTA$)$Ce$_2\}^{3+} \subset$ K121G	1.55
6	$\{($Biot-phen-HXTA$)$Ce$_2\}^{3+} \subset$ K121G	1.91

7.6 Michaelis-Menten kinetics

The Michaelis-Menten experiment was performed in a 96 well plate and the reactions were monitored with a thermostatted Tecan Safire 2 plate reader. The following solutions were added to each well by means of a 12 channel pipette:

i) **Biot-4*m*-HXTA** (15 μL, 2.4 mM in HEPES (100 mM, pH 7)).

ii) Ceric ammonium nitrate (15 μL, 4.8 mM) in water.

ii) K121G (100 μL, 0.4 mM with 4 active sites in HEPES (100 mM, pH 7)).

iv) The enantiopure **HPNP** substrate (prepared according to the table as a 10-fold concentrated solution, in HEPES (100 mM pH 7)).

v) Buffer (7.5 μLHEPES (100 mM, pH 7)).

The hydrolysis of the substrate was monitored at 37 °C for 4.5 h at 405 nm. The initial rate for each reaction was calculated using the Magellan software.

Results of the Michaelis-Menten kinetics

Entry	Substrate [mM]	Artificial enzyme [mM]	Initial rate (*R*)- **HPNP** [mM s^{-1}]·10^{-7}	Initial rate (*S*)- **HPNP** [mM s^{-1}]·10^{-7}
1	10.000	0.4 mM	7.0455	0.4203
2	10.000	0.4 mM	6.0998	0.3141
3	5.0000	0.4 mM	5.0100	0.1578
4	5.0000	0.4 mM	4.6138	0.0584
5	2.5000	0.4 mM	4.1840	0.7244
6	2.5000	0.4 mM	3.8206	0.7078
7	1.2500	0.4 mM	2.1560	0.7198
8	1.2500	0.4 mM	2.0342	0.4193
9	0.6250	0.4 mM	1.8055	0.4713
10	0.6250	0.4 mM	1.6597	0.3799

11	0.3125	0.4 mM	1.6725	0.3549
12	0.3125	0.4 mM	1.4038	0.0103
13	0.1563	0.4 mM	0.9211	0.6491
14	0.1563	0.4 mM	0.8197	0.5910
15	0.0781	0.4 mM	0.3140	0.2238
16	0.0781	0.4 mM	0.2118	0.1914
17	0.0391	0.4 mM	1.0255	0.1742
18	0.0391	0.4 mM	0.9481	0.1351
19	0.0195	0.4 mM	0.2588	0.3451
20	0.0195	0.4 mM	0.1087	0.3446

Programme:

Michaelis-Menten	(R)-HPNP	(S)-HPNP
Best-fit values		
V_{max}	7.228e-007	3.392e-008
K_M	2.344	0.009141
Std. Error		
V_{max}	4.115e-008	5.077e-009
K_M	0.3504	0.01398

Values given by Prism 5 for mac OS X, Version 5.0, December 21, 2009

8. Bibliography

[1]   a)S. J. Franklin, *Curr. Opin. Chem. Biol.* **2001**, *5*, 201; b)M. Dhanasekaran, S. Negi, Y. Sugiura, *Acc. Chem. Res.* **2006**, *39*, 45; c)S. Info, R. Kovacic, J. Welch, S. Franklin, *J. Am. Chem. Soc.* **2003**; d)J. Sumaoka, W. Chen, Y. Kitamura, T. Tomita, J. Yoshida, *J. Alloys Compd.* **2006**.

[2]   M. E. Branum, A. K. Tipton, S. Zhu, L. Que, *J. Am. Chem. Soc.* **2001**, *123*, 1898.

[3]   a)J. Cowan, *Curr. Opin. Chem. Biol.* **2001**, *5*, 634; b)A. Roigk, R. Hettich, H. Schneider, *Inorg. Chem.* **1998**.

[4]   a)U. Bornscheuer, R. Kazlauskas, *Hydrolases in organic synthesis: regio-and stereoselective biotransformations*, 2nd edition ed., WILEY-VCH Verlag GmBH & Co.kGaA, **2006**; b)M. Creus, T. R. Ward, *Org. Biomol. Chem.* **2007**, *5*, 1835; c)A. Neves, M. Lanznaster, A. Bortoluzzi, R. Peralta, A. Casellato, E. Castellano, P. Herrald, M. Riley, G. Schenk, *J. Am. Chem. Soc.* **2007**, *129*, 7486; d)R. Cox, G. Schenk, N. Mitic, L. Gahan, A. Hengge, *J. Am. Chem. Soc.* **2007**, *129*, 9550; e)M. Du, C. Lamoure, B. Muller, O. Bulgakov, E. Lajeunesse, A. Menez, J. Boulain, *J. Mol. Biol.* **2002**, *316*, 941.

[5]   a)M. Komiyama, N. Takeda, Y. Takahashi, H. Uchida, T. Siiba, T. Kodama, Y. M, *J. Chem. Soc. Perkin Trans.* **1995**, *2*, 269; b)J. Sumaoka, Y. Azuma, M. Komiyama, *Chem. Eur. J.* **1998**, *4*, 205.

[6]   N. E. Dixon, R. J. Geue, J. N. Lambert, S. Moghaddas, P. D. A, A. L. Sargeson, *Chem. Commun.* **1996**, 1287.

[7]   T. Itoh, H. Hisada, T. Sumiya, M. Hosono, Y. Usui, Y. Jujii, *Chem. Commun.* **1997**, 677.

[8]   B. Zhu, D. Q. Zhao, Q.-H. Ni, B.-Q. Huang, Z.-L. Wang, *Inorg. Chem. Commun.* **1999**, *2*, 351.

[9]   C. Liu, S. Yu, D. Li, Z. Liao, X. Sun, H. Xu, *Inorg. Chem.* **2002**, *41*, 913.

[10]   C. Sissi, P. Rossi, F. Felluga, F. Formaggio, M. Palumbo, P. Tecilla, C. Toniolo, P. Scrimin, *J.Am.Chem.Soc.* **2001**, *123*, 3169.

[11]   F. Avenier, F. Hollfelder, *Chem. Eur. J.* **2009**, *15*, 12371.

[12]   F. Avenier, J. B. Domingos, L. D. V. Vliet, F. Hollfelder, *J. Am. Chem. Soc.* **2007**, *129*, 7611.

[13]   a)K. Ito, H. Katada, N. Shigi, M. Komiyama, *Chem. Commun.* **2009**, *21*, 6542; b)H. Katada, H. J. Chen, N. Shigi, M. Komiyama, *Chem. Commun.* **2009**, *10*, 6545.

[14]   F. H. Zelder, A. A. Mokhir, R. Krämer, *Inorg. Chem.* **2003**, *42*, 8618.

[15]   K. D. Copeland, M. P. Fitzsimons, R. P. Houser, J. K. Barton, *Biochemistry* **2002**, *41*, 343.

[16]   a)M. Martin, F. Manea, R. Fiammengo, L. J. Prins, L. Pasquato, P. Scrimin, *J.Am.Chem.Soc.* **2007**, *129*, 6982; b)R. Bonomi, F. Selvestrel, V. Lombardo, C. Sissi, S. Polizzi, F. Mancin, U. Tonellato, P. Scrimin, *J. Am. Chem. Soc.* **2008**, *130*, 15744; c)R. Bonomi, G. Saielli, U. Tonellato, P. Scrimin, F. Mancin, *J. Am. Chem. Soc.* **2009**, *131*, 11278.

[17]   a)A. Nomura, Y. Sugiura, *J.Am.Chem.Soc.* **2004**, *126*, 15374; b)S. Negi, Y. Umeda, S. Masuyama, K. Kano, Y. Sugiura, *Bioorg. Med. Chem. Lett.* **2009**, *19*, 2789.

[18]   R. T. Kovacic, J. T. Welch, S. J. Franklin, *J.Am.Chem.Soc* **2003**, *125*, 6656.

[19]   a)M. Skander, C. Malan, A. Ivanova, T. R. Ward, *Chem. Commun.* **2005**, 4815; b)J. Pierron, C. Malan, M. Creus, J. Gradinaru, I. Hafner, A. Ivanova, A. Sardo, T. R. Ward, *Angew. Chem. Int. Ed.* **2008**, *47*, 701; c)A. Pordea, M. Creus, J. Panek, C. Duboc, D. Mathis, M. Novic, T. R. Ward, *J.Am.Chem.Soc.* **2008**, *130*, 8085.

[20]   M. Komiyama, T. Takarada, in *Metal Ions in Biological Systems, Vol. 40* (Eds.: A. Sigel, H. Sigel), Marcel Dekker, New York, **2003**, pp. 355.

[21]   J. Kankare, A. Karppi, H. Takalo, *Anal. Chim. Acta* **1994**, *295*, 27.

[22]   H. Furutachi, M. Murayama, A. Shiohara, *Chem.Comm.* **2003**, 1900.

[23]   G. M. Morris, R. Huey, W. Lindstrom, M. F. Sanner, R. K. Belew, S. Goodsell, A. J. Olson, *J. Comput. Chem.* **2009**, *30*, 2785.

[24]   M. Skander, N. Humbert, J. Collot, J. Gradinaru, G. Klein, A. Loosli, J. Sauser, A. Zocchi, F. Gilardoni, T. R. Ward, *J. Am. Chem. Soc.* **2004**, *126*, 14411.

[25]   F. Wurm, J. Klos, H. J. Rader, F. Holger, **2009**, *131*, 7954.

[26]   J.-L. Reymond, *Enzyme Assays*, 1 ed., Wiley-VCH, Weinheim, **2005**.
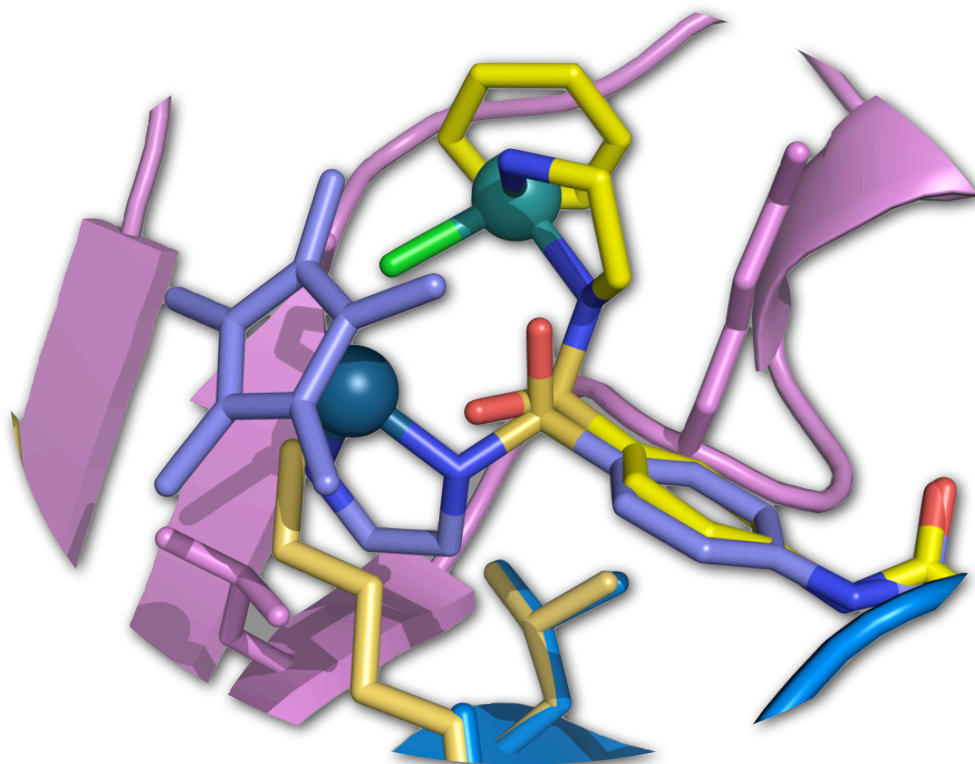
Chapter 3:

Artificial Transfer Hydrogenases for the Enantioselective Reduction of Aryl Ketones and Cyclic Imines

«Le mental intuitif est un don sacré et le mental rationnel est un serviteur fidèle. Nous avons créé une société qui honore le serviteur et a oublié le don»

Albert Einstein

Chapter 3: Artificial transfer hydrogenases for the enantioselective reduction of aryl ketones and cyclic imines

1. Abstract

The first part of the chapter describes the incorporation of biotinylated, "racemic" at metal three-legged d^6-piano stool complexes in streptavidin yielding enantioselective transfer hydrogenation artificial metalloenzymes for the reduction of ketones. In a previous screening step, S112A and S112K were identified, respectively, as the best (*R*) and (*S*)-selective streptavidin mutants for the reduction of acetophenone derivatives.

The X-ray structure analysis of the S112K variant containing the [η^6-(benzene)Ru(**Biot-*p*-L**)] confirmed the prediction that this mutated residue is close to the catalytic site, providing valuable structural insight into the "second coordination sphere" of the complex. The X-ray structure was used to identify two additionnal residues that are likely to influence catalysis: K121 and L124.

To test this hypothesis, a second screening step was carried out in a panel of immobilized double mutants after saturation mutagenesis at positions K121 and L124, conserving the S112K and S112A mutations. The results of this screen for the reduction of ketones confirmed that K121X and L124X mutations can dramatically influence catalysis; further, these experiments showed that a combination of rational design and directed evolution, which was termed "designed evolution", is a powerful means to fine-tune the selectivity of artificial metalloenzymes.

The second part of the chapter describes the incorporation of biotinylated racemic three-legged d^6-piano stool complexes into streptavidin yielding artificial metallohydrogenases for imine reduction. A library of biotinylated complexes was combined with a library of proteins resulting from saturation mutagenesis at position S112. This approach allowed the improvement of conversion and *ee* for the reduction of the drug-precursor 6,7-dimethoxy-1-methyl-3,4-dihydroisoquinoline. The best artificial metalloenzyme with the S112A Sav isoform achieved 100% conversion and an *ee* of up to 93% (*R*). Incorporation of the complex [η^5-(Cp*)Ir(**Biot-*p*-L**)Cl] into the S112A Sav isoform lead to a 3-fold rate acceleration compared to the complex alone.

The X-ray structure of the most selective artificial imine reductase allowed speculations on the reduction mechanism of a drug precursor (Salsolidine). Finally, streptavidin generated insoluble protein polymers cross-linked called CLEAs (Cross Linked Enzymes Aggregates) thus allowing a new protocol for immobilized artificial metalloenzymes for imine reduction.

2. Introduction

2.1 Transfer hydrogenation

Transfer hydrogenation refers to the reduction of an unsaturated molecule using a hydrogen donor other than H$_2$. Transfer hydrogenation (TH) is an alternative to hydrogenation processes and present many advantages: The reaction is easy to implement, takes place under mild conditions and does not use hazardous hydrogen gas.

2.1.1 Ketone reduction

Chiral alcohols are important intermediates in the synthesis of various high value-added chemicals.[1] One of the best routes to obtain such compounds is the asymmetric reduction of

carbonyl compounds. Chemical stereoselective reduction of carbonyl functionalities is a simple transformation but has been a challenge for synthetic chemists. The first example of transfer hydrogenation of carbonyl groups has been described with the Meerwein-Ponndorf-Verley (MPV) reduction discovered in 1925[2] but in the past decade an extensive development of highly active and selective catalysts for the reduction of carbon-heteroatom unsaturated bonds has been described.[3] A major breathrough in asymmetric transfer hydrogenation of carbonyl compounds was achieved with the work of Noyori et al. using d^6 piano-stool ruthenium complexes formed with aminosulfonamide ligands such as Ts-DPEN (*N*-(*p*-toluenesulfonyl)-1,2-diphenylethylenediamine).[4]

2.1.2 Metal complexes

A variety of metal complexes have been used in ATH of carbonyl compounds allowing high conversion and selectivities. Most of them bear bi-, tri-, or tetradentate ligands containing nitrogen, oxygen or phosphorus as coordinating atoms. A selection of some of the best ligands are given in figure 1.[3c, 5] The monotosylated (**1** and **2**) ligand [4, 5b, 6], the 1,2-amino alcohols (**3** and **4**)[3a, 7] and some phosphinoaxazolines derivatives[8] (**5**) give the best conversions and enantioselectivities. In addition, Reetz, recently, described the BINOL-derived disphosphonite ligand (**8**) with very large scope.[9]

Ketone and Imine reduction
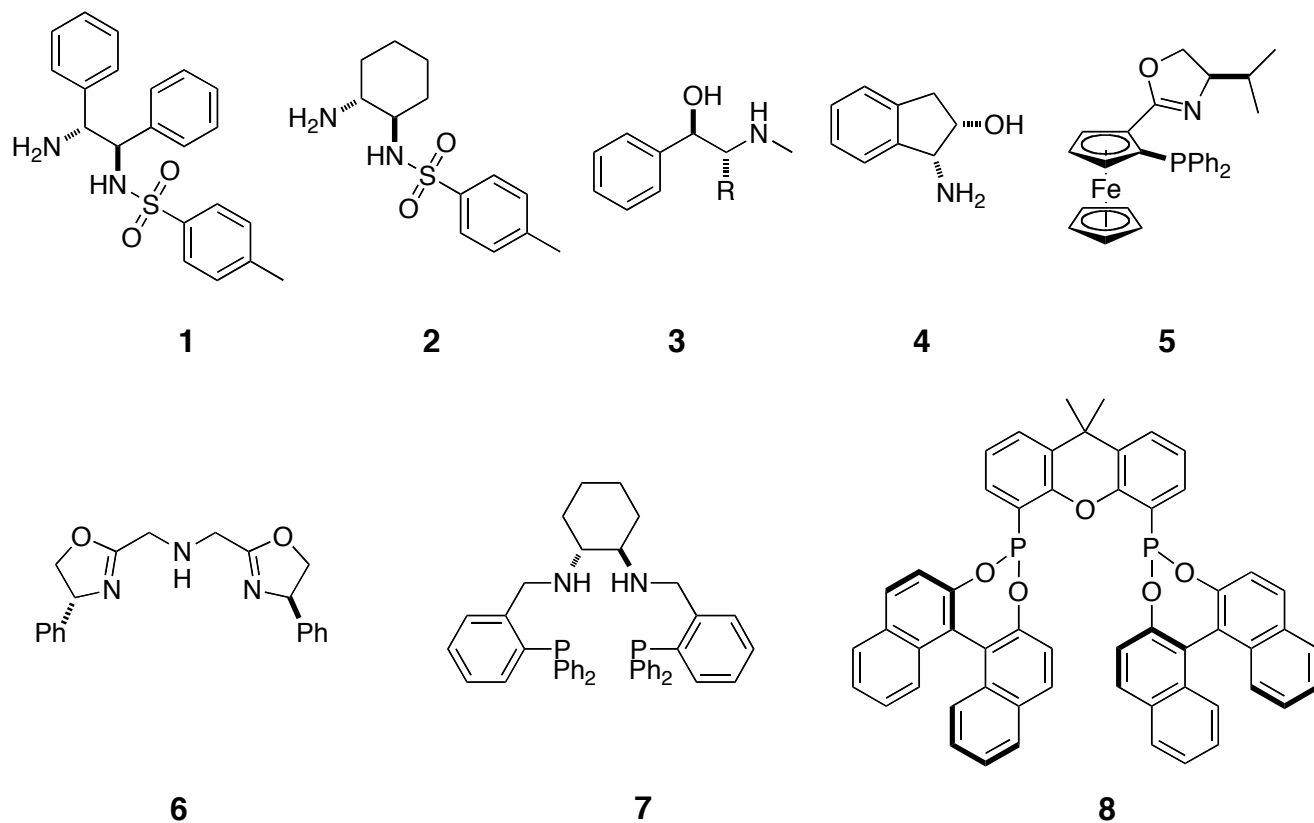
Figure 1 Some of the most effective ligands for the ATH of ketones.

Typical metal fragments associate with the bidentate monotosylated ligands (see figure 1, **1** and **2**) to give half sandwich π-complexes such as Ru-Arene or Ir/Rh-cyclopentadienyl moities possessing an additional ligand, typically a halide (see figure 2).

XH = NHTs, OH
M = Ru, Rh, Ir
n = 6 (Ru), 5 (Rh, Ir)
R = H, alkyl, aryl
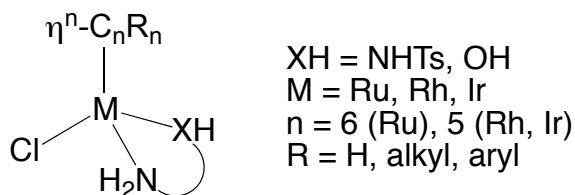
Figure 2 Schematic representation of Ru, Ir or Rh complexes as ATH catalysts precursors.

2.1.3 Hydrogen source

The most common sources of hydrogen for ATH of ketones are isopropanol, azeotropic mixtures of isopronapol with triethylamine, formic acid or formate salts. Isopropanol is the most commonly used solvent and hydrogen donor, as it is cheap and easy to handle. The activation of the catalyst precursor is achieved by addition of a base to the hydrogen donor (e.g. potassium hydroxide).[3a, 10] Isopropanol is oxidized to acetone (a possible substrate for reduction). In consequence, the reduction of ketones in isopropanol is governed by the redox potential of the ketone/alcohol couple. The reversibility of the reaction constitutes a major limitation of the reductions with isopropanol.[3a] To circumvent this problem, formate salts or formic acid triethylamine mixtures have been used in an open system to drive the reaction to completion. The irreversible formation of CO_2 (g) with generation of the metal hydride favours an irreversible reaction.[4] One limitation of the process is the decomposition of the catalyst in contact with high concentrations of formic acid.[3c]

2.1.4 Mechanism

The mechanism of transfer hydrogenation for either imine or ketone reduction is the same and is divided into two broad classes. The first is the MPV reduction by which a metal coordinates both substrate and hydrogen source and hydrogen transfer takes place via a six-membered transition state (see figure 3), the mechanism in called the "direct hydrogen pathway" and is observed when the metal cannot readily form a metal hydride.[11]
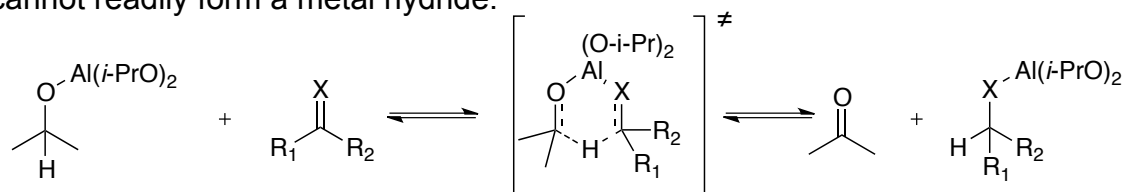
Figure 3 Direct hydrogen pathway, the hydrogen transfer takes place via a six-membered transition state.

In contrast, the second is a "hydridic route" where a metal hydride is involved. Most of the time, metals such as Rh, Ru and Ir favor this mechanism due to their ability to form hydrides. The hydrititic route is further divided in two: the first is a dihydride mechanism and the second one is a monohydride mechanism. The monohydride mechanism contains two different subclasses: the inner sphere without ligand assistance and coordination of the substrate to the metal and the outer sphere with ligand assistance and no coordination of the substrate to the metal. Noyori's Ru(II) Ts-DPEN follows a monohydride mechanism with ligand assistance.[1, 10] (see figure 4)
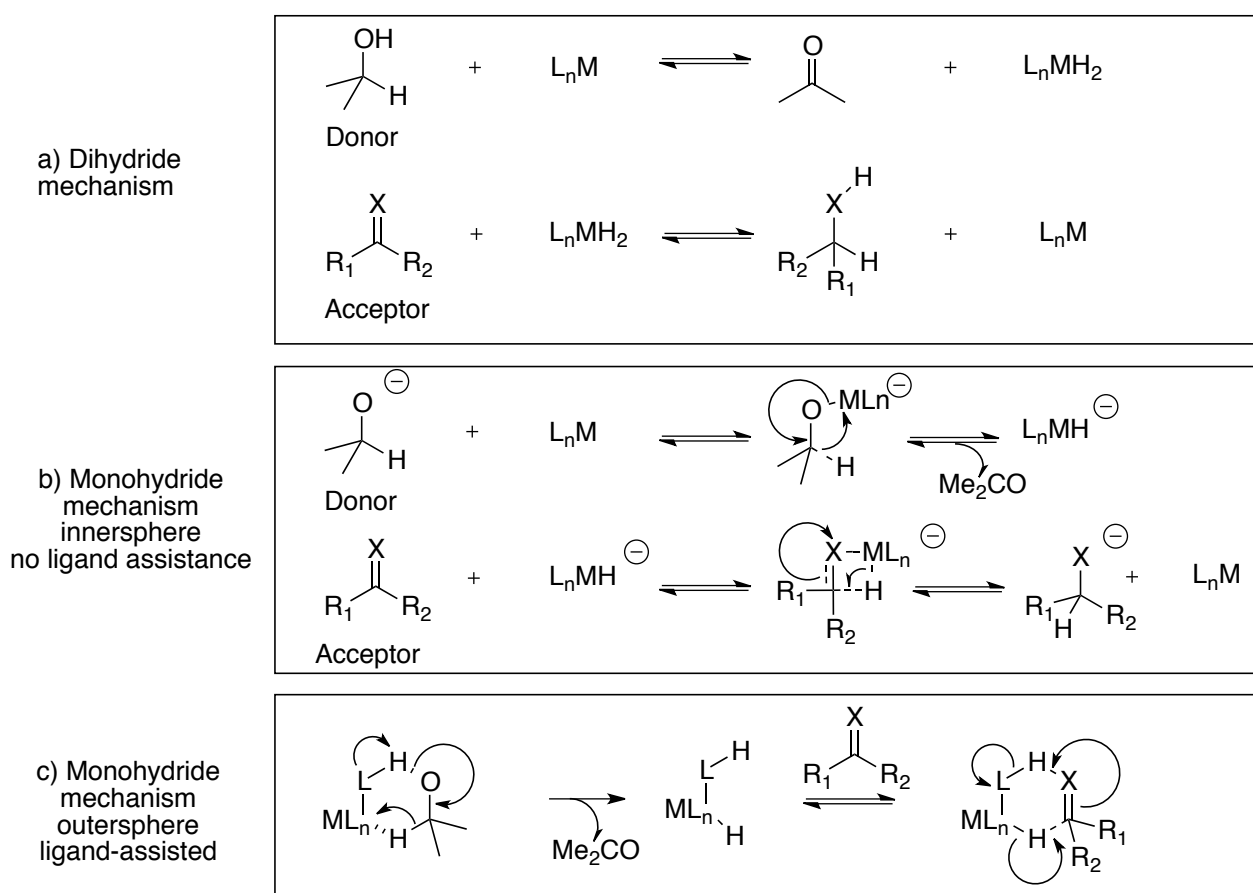
L_n = n ligand(s) coordinated to the metal, L = basic group on the ligand, M = Metal.

Figure 4 Overview of the possible reduction pathways: the dihydride mechanism a) the monohydride mechanism with coordination of the substrate to the metal (inner sphere mechanism)

b) the monohydride mechanism without coordination of the substrate to the metal (outersphere mechanism) c).

The proposed catalytic cycle[11d] for [Ru(p-Cymene)(R,R-TsDPEN)Cl] complex[1, 3a, 12] is depicted in figure 5. The true catalytic species is the 16 e$^-$ Ru complex **B** formed from the catalyst precursor **A** by elimination of HCl in the presence of a base. Deprotonation of the hydrogen donor leads to the 18 e$^-$ Ru-hydride complex **C**. The hydride and the axial NH proton are transferred simultaneously from the 18 e- Ru complex to the substrate via a six membered ring transition state, to regenerate the 16 e- complex **B**.[11d]
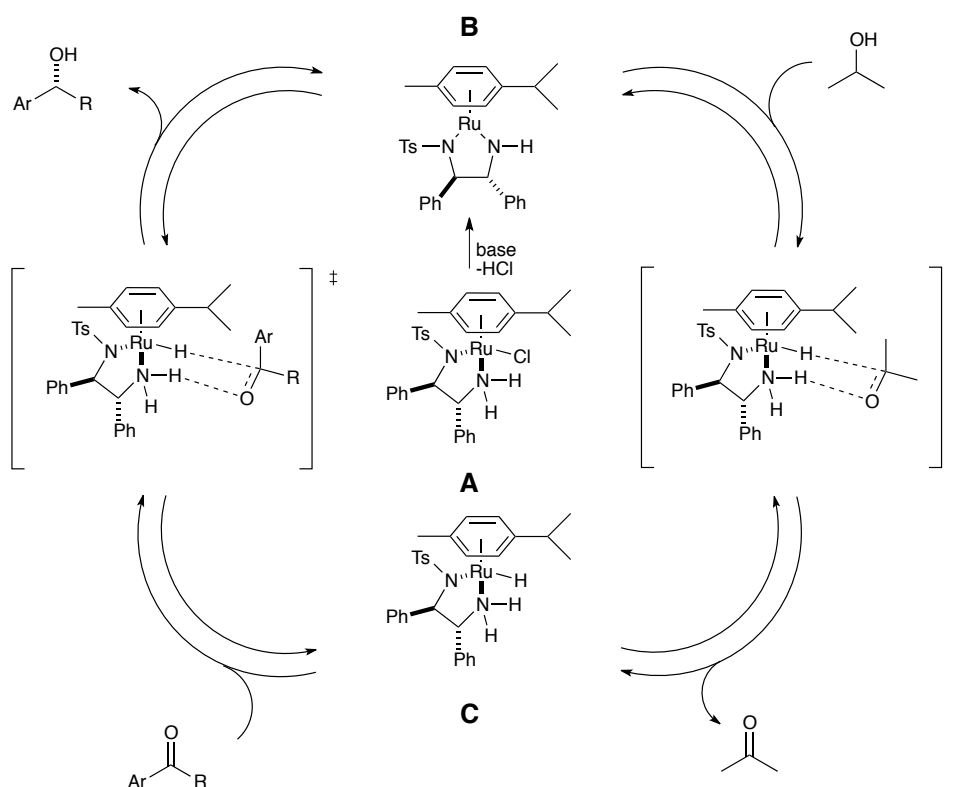
Figure 5 Catalytic cycle for the transfer hydrogenation of on aromatic ketone using the [Ru(p-Cymene)(R,R-TsDPEN)Cl] and isopropanol as the hydrogen donor.[11d]

2.1.5 Enantioselection mechanism

The enantioselectivity of the reaction presented in figure 6 is the result of a combination of steric and electronic factors.[1] From the trigonal planar 16 e$^-$ complex, the hydride species is formed, the chirality at the ruthenium is dictated by the enantiopure ligand to give one major diastereomer of the complex.[3a] The conformation of the five-membered ring formed by the chelating ligand and the ruthenium is defined by the bulky groups on the ligand (Phenyl groups in the case of Ts-DPEN) occupying pseudo-equatorial positions.[3a] The enantiodiscrimination between the two prochiral faces of the ketone is caused by chemical interactions between the capping arene and the aryl group of the ketone.[13] Computational studies have shown that the C-H•••π is contributing to the stabilization of the transition state and is the major factor governing the enantiodiscrimination.[1] In this context, the modulation of the capping arene influence the enandiscrimination process and increased C-H•••π interactions provide better enantiodiscriminations (see figure 6).[3c]
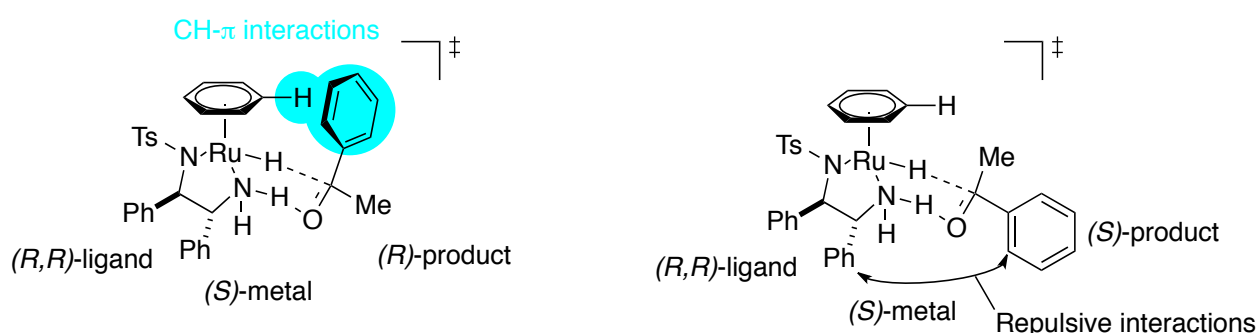
Figure 6 Favored transition state (with C-H•••π interactions) and less favored transition state (without C-H•••π interactions).

2.1.6 Water compatible systems

Recently, aquaeous transfer hydrogenation reactions of ketones were developed.[5b] For this purpose, water-soluble ligands bearing polar or ionic groups (e.g. sulfonic acids) were synthetized and used for aqueous transfer hydrogenation.[14] However, non-modified water-insoluble ligands were more active and enantioselective.[5b] To solve the problem of solubility of both the substrate and the catalyst, surfactants were added to the reaction mixture but in most of the case, the insolubility of the ketone did not affect the reaction rate.[5b] Finally, the reduction rates were considerably faster using HCOONa than the HCOOH/Et$_3$N azeotrope or i-PrOH.[15] In this context, Xiao has showed that both the reaction rate and the enantioselectivity of aqueous transfer hydrogenation reactions critically depend on the pH.[16]

2.1.7 Asymmetric transfer hydrogenation of non aromatic ketones

Aryl alkyl ketones are reduced with excellent enantioselectivities. In contrast, dialkylketones are challenging to reduce due to the absence of the C-H•••π interaction between the capping arene and the aryl group of the substrate.[1, 13] Woggon et al. reported on a Ru(II) Ts-DPEN complex linked to a β-cyclodextrin.[17] This catalytic entity provides a hydrophobic cavity for aliphatic substrates. Tethered ligand-arene Ru complexes were also described for the selective reduction of cyclohexyl methyl ketone.[18] Ru phosphino-oxazolides were developed as an alternative for the reduction of dialkylketones.[8b, 19]

2.2. Imine reduction

Enantiopure amines represent an important class of compounds as they find wide use in industry (pharmaceutical, agrochemical and flavor).[20] In this context, enzymatic, homogeneous catalysis and chemoenzymatic approaches offer complementary means for the preparation of such targets.[21] Artificial metalloenzymes complete these approaches and have received increasing attention in the past years. The Ward group has previously reported artificial metalloenzymes for ketone reduction via transfer hydrogenation inspired by Noyori and coworkers but not for cyclic imines.[22]

2.2.1 Transfer hydrogenation (TH) and asymmetric Transfer Hydrogenation (ATH) of imines in organic solvents

In 1987, it was reported that $Ru_3(CO)_{12}$ was able to catalyze the transfer hydrogenation (TH) of benzylideanilines in isopropanol. The isolated active catalyst was a trimetallic hydride.[23] A Few years later, in 1992, racemic imine reduction via $[RuCl_2(PPh_3)]$[24] was reported by Bäckvall. X-ray analysis of the catalyst demonstrated a metal hydride complex and mechanistic studies showed that a monohydride mechanism without ligand-assistance was operative (see figure 4). Many catalysts were described to be efficient for the TH of imines and a good example is given by the highly effective Shvo diruthenium catalyst studied by Casey and Bäckvall (**9**).[11a, 25] The asymmetric transfer hydrogenation (ATH) of imines under very mild conditions (room temperature and no need of hydrogen gas) via the Ru(II) Ts-DPEN[26] (**10**) was reported by Noyori and coworkers in 1996 (see figure 7). An azeotropic mixture of formic acid, triethylamine were usually used as H_2 source.

a)   b)

9   **10**
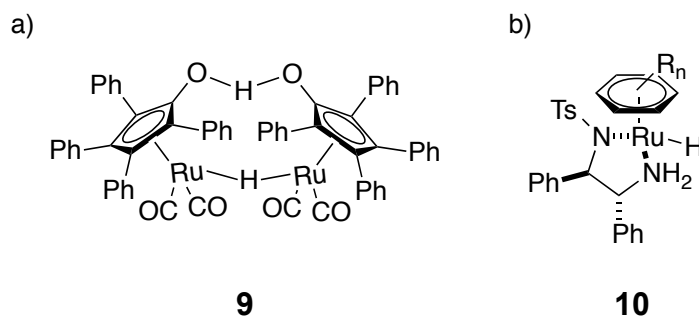
Figure 7 Some efficient catalysts for TH and ATH of imines. The Shvo catalyst dissociates in solution thereby forming the catalytically active mononuclear species a) Noyori's Ru(II) Ts-DPEN, an active catalyst working via a ligand-assisted monohydride mechanism b).

Ru(II) Ts-DPEN also allowed the reduction of cyclic imines bearing an alkyl and a benzyl groups providing very effective and general routes for the asymmetric synthesis of isoquinoline alkaloids and direct access to natural products. In contrast, imines bearing two aryl on the imine carbon are reduced with lower enantioselectivity.[11c]

2.2.2 Asymmetric transfer hydrogenation of imines in water

Some studies have achieved the ATH of imines in water, for example, Xiao et al. have shown that Ru(II) Ts-DPEN bearing an SO_3H is an active water soluble catalyst.[15] Wu et al, using the same catalytic system were able to reduce cyclic imines and iminiums in water.[28] A surfactant (CTAB = cetyl trimethylammonium bromide) and sodium formate as a hydrogen source were used to improve the *ee*. In the same spirit, Süss-Fink et al. where able to apply cationic arene ruthenium complexes containing chiral sulfonated diamine ligands for ketone and imine reduction in water.[29] Some other recent developments allowed immobilization of active complexes for ATH of imines in water. The system is based on a polymer-immoblized Ru(II) TsDPEN and has the advantage of recyclability while giving high *ee*.[30]

Major achievements were obtained by Xiao et al. on ATH of imines in water. He first performed the reduction of cyclic imines with a Cp* Rh(III) Ts-DPEN catalyst giving excellent yields and *ee*.[31] The nature of the catalyst conterion played a major role in conversion; SbF_6^- had the biggest influence on the reaction allowing full conversion of the substrate. He later performed ATH of quinolines using pH regulation. Excellent *ees* and conversions were obtained especially for the Cp* Rh(III) Ts-DPEN complexes.[32]

Finally, Pihko et al. reported high enantioselectivities for the preparation of tetrahydroisoquinolines and β-carboline alkaloids using Ru(II) Ts-DPEN in water.[33] The anion in this context played a determinant role in conversion of substrates. Moreover, lanthanide salts such as $La(OTf)_3$ or surfactants such as CTAB improved the conversion of insoluble deactivated substrates.

It is interesting to mention that, many studies were achieved in the ATH of imines but the mechanism of the reaction is still a matter of debate.

2.2.3 Imine reduction mechanism with Ru(II) Ts-DPEN

Noyori et al. proposed a widely accepted mechanism for the transfer hydrogenation of ketones with Ru(II) Ts-DPEN as catalyst. In contrast, the mechanism of imine reduction is less well understood. Generally, cyclic imines are reduced with high enantioselectivity and the rate of the reaction is usually higher than that of ketone reduction by asymmetric transfer hydrogenation catalysts based on Ts-DPEN. The mechanism of imine reduction has been discussed and different modes of reduction have been proposed.[34]

A C-H•••π interaction plays a key role in the mechanism of enantioselective ketone reduction but imine reduction seems to proceed via a different mechanism. Bäckvall[26b] has shown that only protonated imines are reduced by isolated hydride intermediates. In contrast, Blackmond's

investigations on imine reduction with a Rh(III) catalyst suggested that a deprotonated imine is the true substrate (not the corresponding iminium).[35]

The mechanism of ketone reduction cannot be simply superimposed to that of imine reduction as shown by the opposite sense of asymmetric induction observed using Noyori's Ru(II) Ts-DPEN complex.[34] Within this context, Wills proposed two alternative mechanisms.[34] The first is the reduction of the imine via a six-membered transition state oriented such that the relative positions of alkyl and aryl groups are inverted compared to the proposed transition state in Noyori's mechanism (see figure 8). The second one is a reduction through an ionic mechanism where the imine
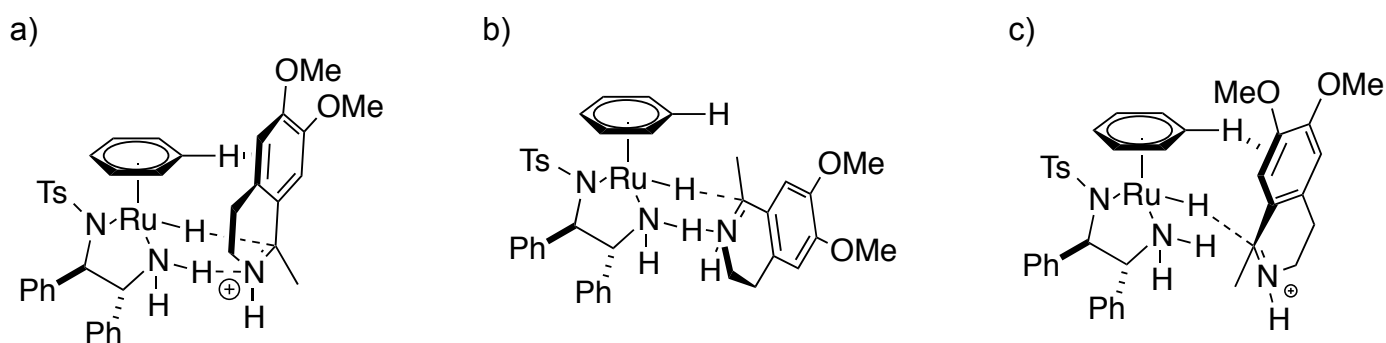
Figure 8 Proposed transition states for imine reduction using Noyori's (*R,R*)-TsDPEN catalyst (*R*)-product predicted by Noyori's mechanism: Produces incorrect product enantiomer (*S*) a)(*S*)-product predicted by Wills' mechanism: Produces correct product enantiomer (Wills' proposed mecanism) b) (*S*)-product predicted by Wills' mechanism: Produces correct product enantiomer (Wills' proposed mecanism) c)

forms an iminium cation without the involvement of a six-membered transition state. It allows the formation of C-H••• π interactions and delivers the correct enantiomer. However, Wills' investigations of these mechanisms with Ru(II) *N*-alkylated Ts-DPEN ligands for ketone and imine reduction didn't give a definitive description of the mechanism of imine reduction.

2.2.4 Artificial transfer hydrogenases

Letondor et al.[22] reported, on artificial transfer hydrogenases for the reduction of prochiral ketones. The hybrid catalysts were created by combination of various biotinylated metal d^6 piano stool complexes. In particular, the [η^6-(benzene)Ru(**Biot-*p*-L**)Cl] and [η^6-(*p*-cymene)Ru(**Biot-*p*-L**)Cl] complexes were combined with a library of Sav isoforms generated by saturation mutagenesis at position S112. They provided good (*S*)-selective respectively (*R*)-selective catalysts. Later on, to get insight into artificial transfer hydrogenases, efforts were invested to crystallize the most promising combination of biotinylated d^6 piano stool into Sav isoforms. A crystal structure of the [η^6-(benzene)Ru(**Biot-*p*-L**)Cl] ⊂ S112K Sav (In collaboration with Dr. Marc Creus, Isolde Letrong and Prof. Ronald Stenkamp from University of Washington). The refined structure (1.58 A resolution, PDB code 2QCB) revealed the spatial organization of the active site of the (*S*)-selective metalloenzyme. It is important to mention that the occupancy of the ruthenium inside streptavidin is 20% due probably to:

- Conformational flexibility inside the protein

- Ruthenium decomplexation during co-crystallization

- Steric clashes (in the case of simultaneous occupation of the two adjacent binding sites by the ruthenium complex). Furthermore, the metal is located near a subunit-subunit interface and stands close to the neighboring biotinylated complex (The Ru, Ru distance is about 4.44 Å). In this context, incorporation of the bulky biotinylated complex doesn't generate a structural

reorganization of the protein. Compared to the Sav WT, a root mean square (RMS) 0.276 Å for the 121 $C\alpha$ atoms was computed (see figure 9). Interestingly, only the (S)-enantiomer of the biotinylated complex [η^6-(benzene)Ru(**Biot-*p*-L**)Cl] was localized in the crystal structure. In homogeneous systems, the (S)-Ru configuration is known to generate the (S)-reduction product of acetophenone derivatives. Most interestingly, the [η^6-(benzene)Ru(**Biot-*p*-L**)Cl] was the most (S)-selective hybrid catalyst identified in previous studies in our group. It renders possible the enantioselective discrimination by the protein for one of the two enantiomers of the complex given by second coordination sphere interactions. The structure also demonstrated that, S112 position lies close to the Ru atom (in accordance with the docked structure[22b]). Additional short contacts between the biotinylated catalysts [η^6-(benzene)Ru(**Biot-*p*-L**)Cl] can be identified:

- Residues of the L 7,8 (110-124) of both Sav monomer A and B

- G48 (part of the loop 3,4) of the monomer A

- H87 (part of the loop 5,6) of the monomer A

Position 121 is of particular interest since it may interact with the trajectory of the incoming substrate (monomer A) or with capping arene (monomer B). Further investigation on the crystal structure demonstrated that position 124 may interact with the SO_2 moiety of the ligand thus influencing the position of the biotinylated complex inside the pocket.

Even if the structure provides important knowledge about the position of the biotinylated complex into Sav, it does not provide any information about the reaction mechanism. As a consequence, evolution of the artificial metalloenzyme cannot be based only on rational redesign. It thus required mutagenesis and screening experiments to further optimize the artificial enzyme. In order to generate highly (R) and (S)-selective artificial metalloenzymes, the most selective biotinylated complexes were combined with a designed evolution strategy. Design evolution relied on

saturation mutagenesis at selected close-lying positions identified by X-ray cristallography (see figure 9).
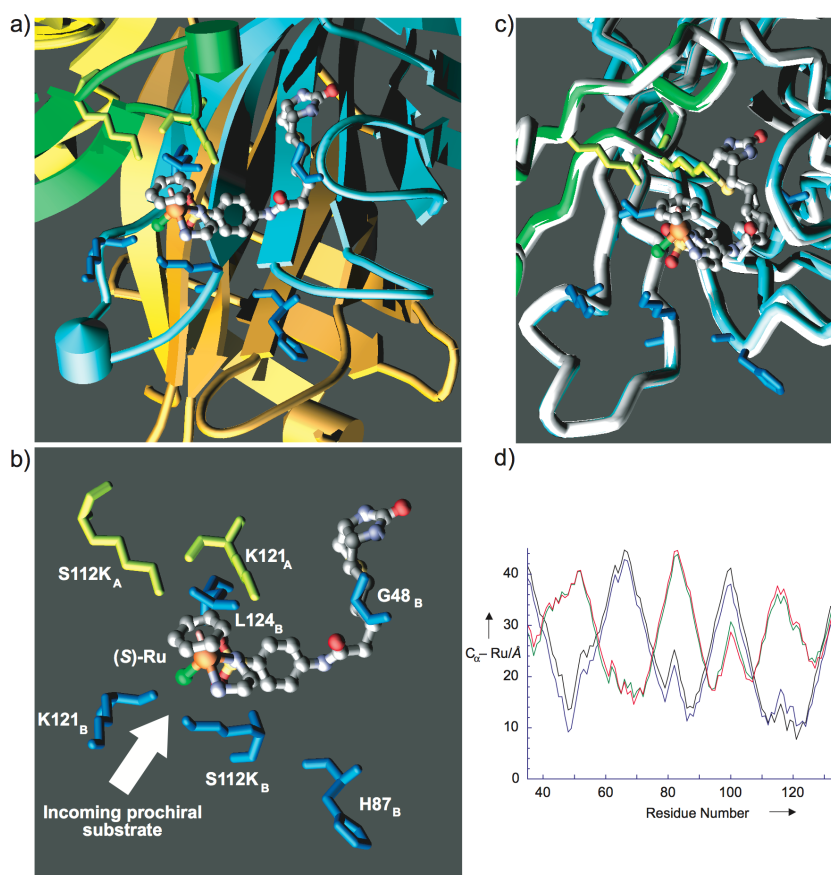
Figure 9 X-ray crystal structure of [η^6-(benzene)Ru(**Biot-*p*-L**)Cl] $\subset$ S112K Sav. Close-up view (only monomer B (blue) occupied by the biotinylated catalyst (ball-and-stick representation); monomers A (green), C (orange), and D (yellow)) a) Highlight of amino acid side-chain residues displaying short contacts with Ru. The absolute configuration at ruthenium is (*S*) b) Superimposition of the structure of [η^6-(benzene)Ru(**Biot-*p*-L**)Cl] $\subset$ S112K Sav with the structure of biotin $\subset$ core streptavidin (PDB reference code 1STP, only monomers A and B displayed for clarity; biotin: white stick, core streptavidin: white tube) c) Ru C$_\alpha$ distances extracted from the X-ray structure of [η^6-(benzene)Ru(**Biot-*p*-L**)Cl] $\subset$ S112K Sav; monomers: A black, B blue, C green, and

D red d).

For this second round of optimisation, the enantioselective reduction of dialkylketones was selected. Dialkylketone substrates are challenging since they don't exhibit the critical C-H•••π interaction with the complex. In natural enzymes (e.g. ADHs), the second coordination sphere plays a critical role in the enantiodiscrimination of such substrates. It was reasoned that with this artificial system, controlling the second coordination sphere around the catalyst may allow exquisite enantiodiscrimination even for challenging substrates. Saturation mutagenesis at 112 did not suffice to produce high levels of selectivity for the reduction of dialkyl ketones. Identification of residues close to the metal center was of particular interest for two reasons: the first one is an interaction with the metal center and the second one is an interaction with the incoming substrate. It this context, K121 and L124 positions were selected for saturation mutagenesis. K121 may steer the delivery of the substrate while may L124 alter the position of the complex in the binding pocket. Since good enantioselectivity was provided by the [η^6-(p-cymene)Ru(**Biot-*p*-L**)Cl] ⊂ S112A towards the (*R*)-enantiomer and [η^6-(benzene)Ru(**Biot-*p*-L**)Cl] ⊂ S112K towards the (*S)*-product, saturation mutagenesis was performed at the position 121 and 124 keeping the position S112A and S112K thus generating a library of double mutants. A total of 114 Sav mutants were produced (K121X, L124X, S112A-K121X, S112K-K121X and S112K-K121X, S112K-K124X) and tested with complexes [η^6-(*p*-cymene)Ru(**Biot-*p*-L**)Cl] and [η^6-(benzene)Ru(**Biot-*p*-L**)Cl]). The activated *p*-bromoacetophenone and the challenging 4-phenyl-2-butanone were chosen as model aromatic, and aliphatic substrates respectively (see figure 9). The acceleration of the screening process was achived by immobilization of artificial metallotransferase. Hence, the implemented library allowed extending the concept of artificial metallotransferase for the reduction of prochiral cyclic imines.

3. Ketone reduction: results and discussion

3.1 Extraction-Immobilization Protocol: Quick Screening Strategy

To accelerate the optimization process, a quick screening protocol was implemented. The first round of screening for the chemogenetic optimization required the use of milligram quantities (3-4 mg per catalytic experiment) of the twenty purified Sav mutants to perform the catalytic experiments. Since the production and purification of Sav in our laboratory lasts nearly three weeks for the production of one mutant (including purification and lyophilisation), an alternative technique for testing the 114 new Sav mutants was necessary.

3.2 Catalysis with Streptavidin-Containing Crude Cell Extracts

In order to generate a fast screening, a screen method was implemented on cell crude extracts produced in small volume culture of E.coli bacteria (50 ml) giving approximatively 1 mg of protein (determined by titration using B_4F). The cell extracts were treated with DNAase and extracted in 1.5 ml of water to recover the protein tested in catalysis. The quantification of streptavidin in extracts demonstrates that the concentration of the protein is three times lower than the concentration of the protein in optimal catalysis conditions. This lead to lower conversions compared to standard conditions. The crude extracts were tested in catalysis. However no conversion and *ee* was observed (see table 1). A variety of cell debris are still present (DNA, Lipids, Proteins, Sugars, Salts) all of these components may inhibit the catalysis by interaction with the metal center. These results suggest that, in contrast to enzyme optimization via evolutionary techniques– where screening can be performed on colonies or crude cell extracts –, the presence of an exogenous set of molecules inhibit the artificial metalloenzymes. Indeed, to the best of our knowledge, all experiments in the area of artificial metalloenzymes have thus far been performed with homogeneous purified proteins. This long purification step is the bottleneck for artificial

metalloenzyme optimization.

Table 1 Comparison of the results obtained with purified S112Y Sav crude cell extracts containing S112Y Sav for the reduction of acetophenone using [η^6-(p-cymene)Ru(**Biot-p-L**)Cl].

Entry	Protein	Sav [μM]	Conv. (%)	ee (%)
1	pure	251	95	90 (*R*)
2	pure	100	59	60 (*R*)
3	Cell extract	100	0	-
4	Pure + cell extract	100	0	-

3.3 Immobilisation process

To resolve the problem of protein purification, an immobilization protocol was implemented (in collaboration with Dr. Anca Pordea) of Sav using iminobiotin sepharose and biotin sepharose (commercially available, see figure 10 and 12). Since biotin or imino-biotin has a high affinity for streptavidin, it was speculated that immobilisation of Sav directly from the crude cell extracts could be possible. In this context, iminobiotin sepharose allows the release of Sav after purification by adjusting the pH. When biotin-sepharose is used, one binding site is sacrificed for immobilisation thus leaving three free binding sites to incorporate the biotinylated piano stool complex and to perform catalysis (see figure 12). Comparison of the two immobilisation techniques showed that both methods can be used for rapid purification of Sav but with some loss of conversion and enantioselectivity (see table 2). Futhermore some disadvantages are apparent for the immobilization techniques. First the affinity of Sav for imino-biotin is lower than the affinity for biotin, it is especially problematic for low protein concentration in some cell crude extracts. Secondly, for iminobiotin sepharose immobilisation, the pH must be adjusted for the catalysis (form pH=2.9 to 6.25) increasing the total volume of the catalysis and generating lower *ee* and conversion. In contrast, immobilization on biotin-sepharose appeared to be a more robust system

and was selected for further use for the screening of the 114 Sav mutants (see figure 10 and 11). Guanidinium chloride (1 M solution) and the HCOONa/B(OH)$_3$ mixture (the hydrogen source for catalysis) were used as washing solutions for the first and the second washing steps, respectively.

Table 2 Comparison of the iminobiotin- and biotin-sepharose extraction and purification techniques of streptavidin from crude cell extracts. The catalysis were performed using [η^6-(p-cymene)Ru(**Biot-p-L**)Cl] $\subset$ P64G Sav for the reduction of p-methylacetophenone. The washing steps in the case of biotin-sepharose immobilization were realized using H$_2$O / DMF = 50 / 1.

Entry	Purification technique	Protein	Conv(%)	ee (%)
1	-	pure	92	94 (R)
2	biotin	pure	92	93 (R)
3	iminobiotin	pure	90	87 (R)
4	biotin	Cell extract	76	73 (R)
5	iminobiotin	Cell extract	57	82 (R)

The immobilization protocol on biotin-sepharose was further tested with various Sav isoforms and compared with non-immobilized streptavidin (see table 3).

Table 3 Comparison of the results obtained for the transfer hydrogenation of *p*-bromoacetophenone (**11**) using biotin-sepharose immobilized- and purified homogeneous artificial metalloenzymes [η^6-(arene)Ru(**Biot-*p*-L**)Cl] Sav.

Entry	η^6-(arene)	Sav isoforms	Pure non-immobilized Sav		Immobilized Sav (from cellular extract)	
			Conv (%)	*ee* (%)	Conv (%)	*ee* (%)
1	*p*-cymene	Wt Sav	93	87 (*R*)	81	65 (*R*)
2	benzene	Wt Sav	43	57 (*S*)	31	39 (*S*)
3	*p*-cymene	S112A Sav	78	87 (*R*)	57	64 (*R*)
4	benzene	S112KSav	25	44 (*S*)	21	38 (*S*)

Although the purification and immobilization process with biotin sepharose leads to a noticeable erosion of the ee and the conversion, the immobilization protocol of biotin-sepharose was used to speed up the catalytic rounds thus allowing valuable trends for the catalytic runs. The protocol was extensively used to perform round of designed evolution (see figure 10 and 11).

a) Immobilisation on iminobiotin-sepharose
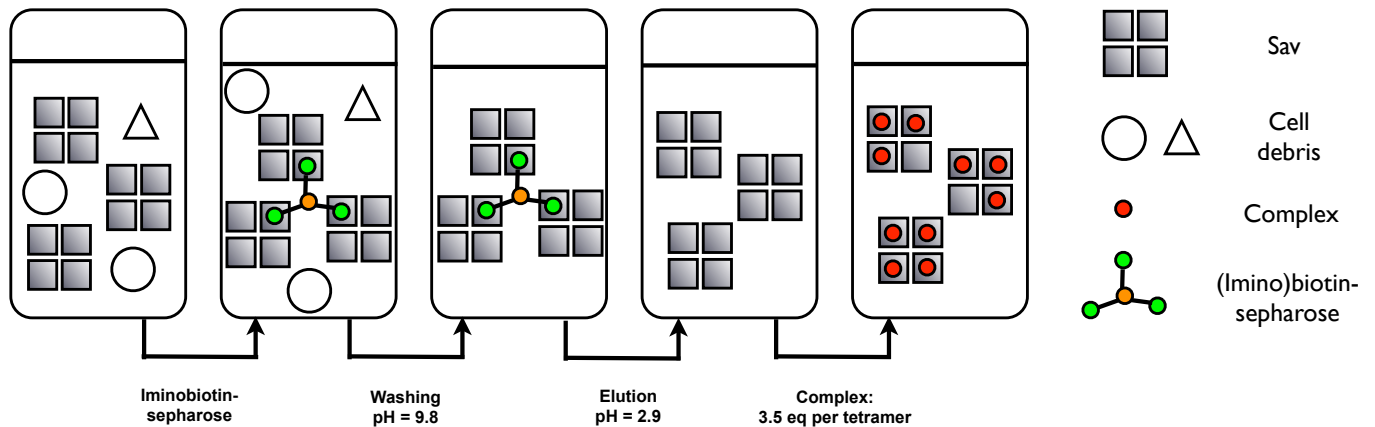
b) Immobilisation on biotin-sepharose
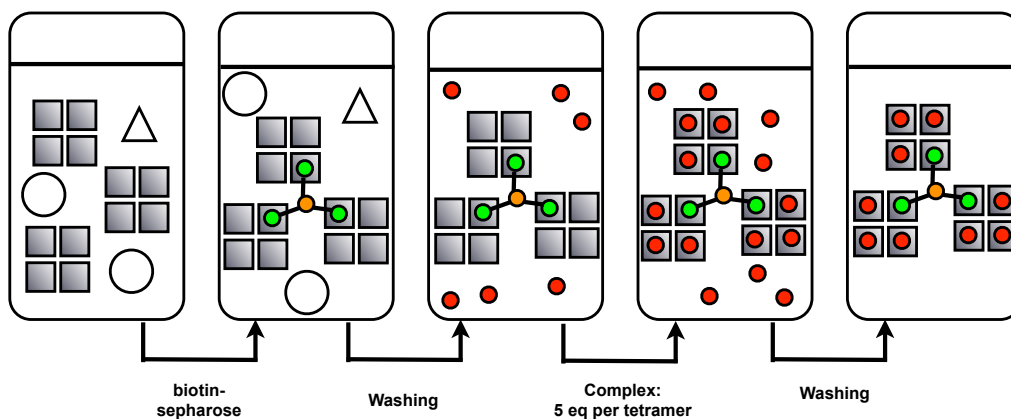
Figure 10 Rapid techniques for the extraction and purification of streptavidin from crude cell extracts. Immobilization on iminobiotin-sepharose, followed by washing (pH = 9.8) and elution (pH = 2.9) steps affords pure Sav a) Using biotin-sepharose affords the immobilized artificial metalloenzyme after several washing cycles b)

Step 1: Culture

Step 8: Analysis

Step 2: Centrifugation

Step 7: HPLC

Step 3:Extraction

Step 6: Catalysis

Step 4: Quantification

Step 5: Fishing
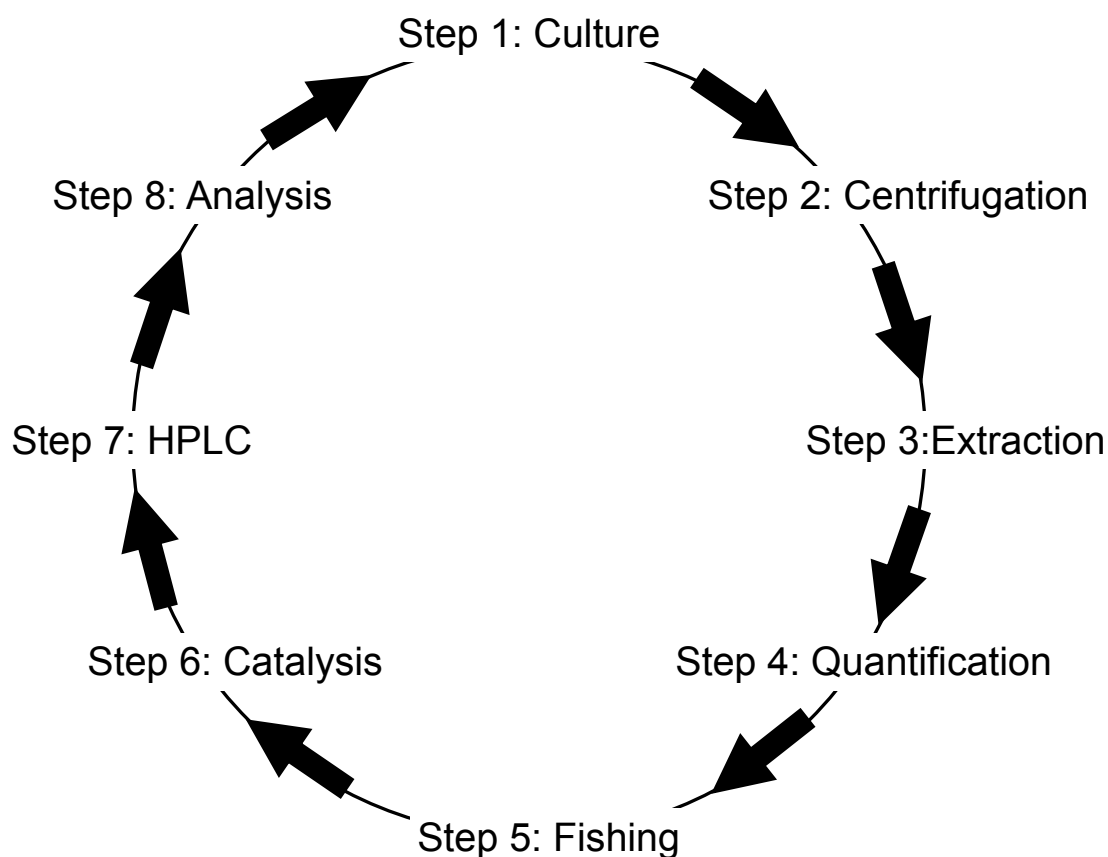
Figure 11 Catalysis process with immobilization

Step 1: Cell culture of E.Coli (50 ml) producing Sav isoforms

Step 2: Centrifugation of the bacteria and freezing of the pellet

Step 3: Extraction of the protein in water (total volume of 1.5 ml)

Step 4: Quantification of the crude extracts containing Sav (B_4F titration)

Step 5: Fishing of the protein with biotin-sepharose

Step 6: Catalysis with immobilized Sav

Step 7: HPLC analysis of the catalysis

Step 8: Analysis of the results

a)

b)

11

12
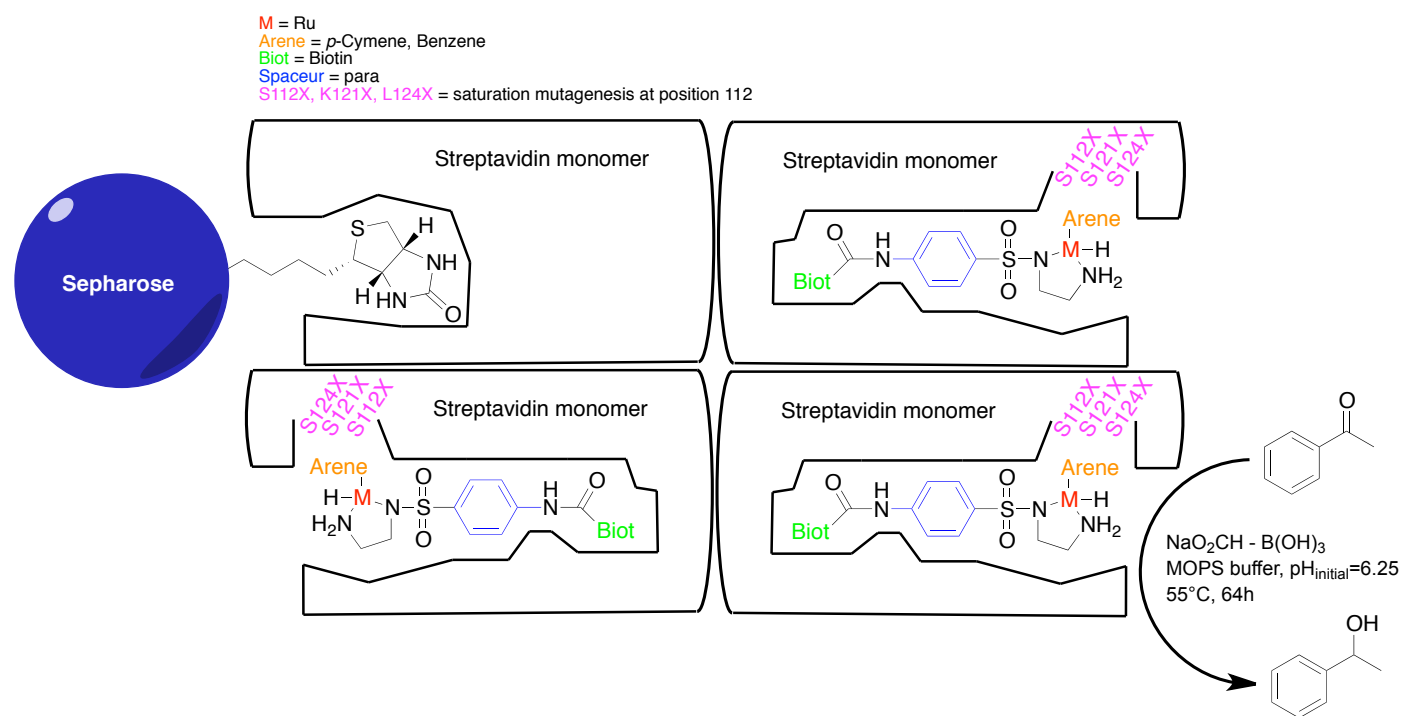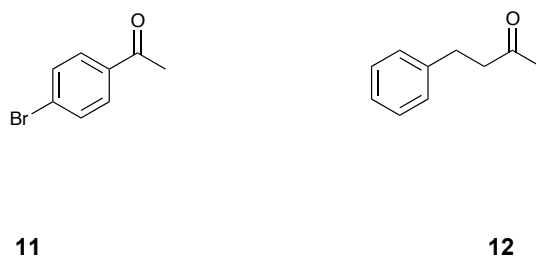
Figure 12 Schematic representation of the immobilized artificial metalloenzyme for transfert hydrogenation reactions a) Substrates used for transfer hydrogenation of ketones b)

3.4 Screening and Trends of the Immobilized Artificial Metalloenzymes

Catalytic experiments of the screening were performed in collaboration with Dr. Anca Pordea using the immobilization strategy described previously. Semi-quantitative trends were obtained out of the experiments for both the reduction of 4-phenyl-2-butanone and for *p*-Bromoacetophenone (see figure 12 and 13). The enantioselective trends revealed in a fingerprint display where cherry color codes for the (*S*)-product while green codes for (*R*)-product. Two substrates are depicted in one square for comparison. The fingerprint allows rapid comparison between each combination of mutants and complexes thus allowing qualitative analysis of trends.
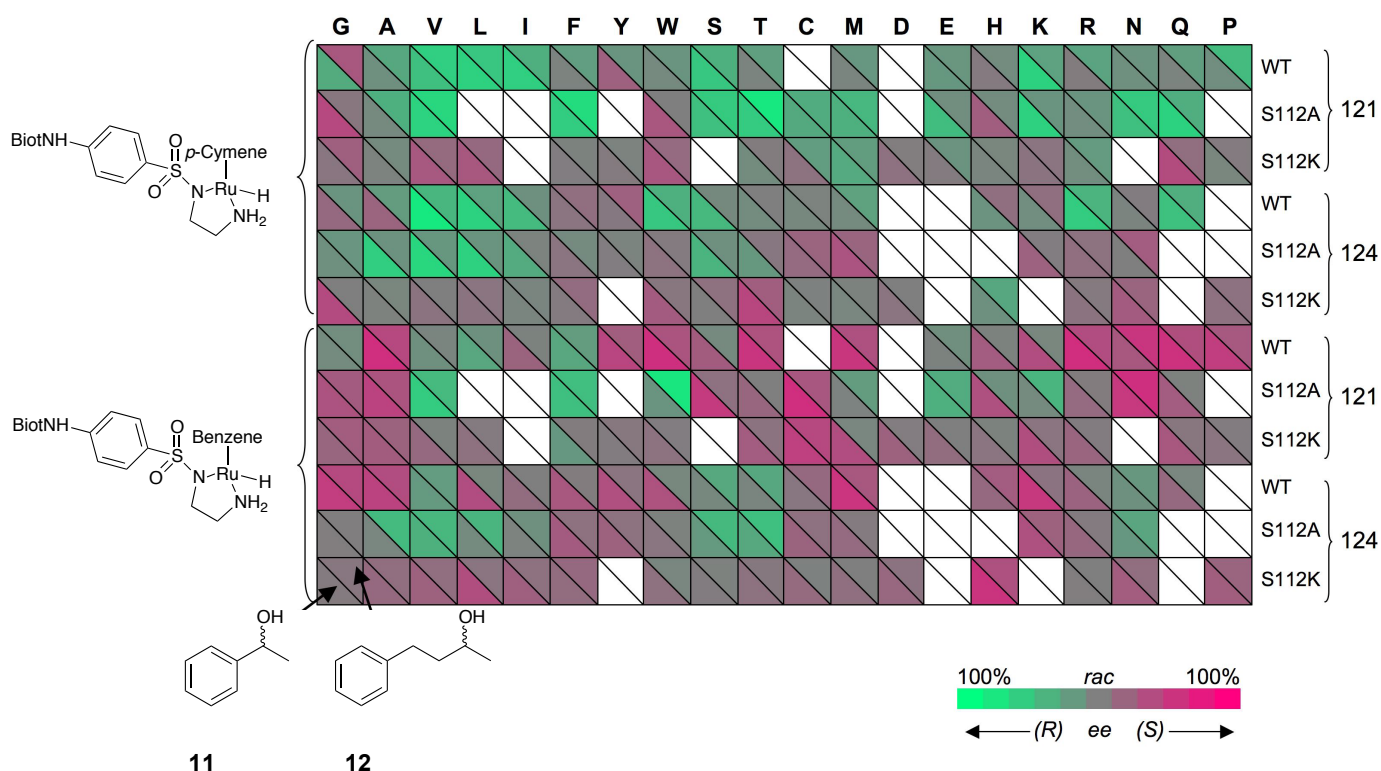
Figure 13 Fingerprint of the results obtained for the ketone reduction catalysez by artificial metalloenzymes.

3.5 Substrate: aromatic *vs.* dialkyl ketone

In general, the two substrates behave similarly in terms of enantioselectivity. It is noteworthy that the enantioselectivity obtained for the dialkyl product is greater or opposite to the *ee* of the aromatic product for more than half of the artificial metalloenzymes, reaching a Δee (difference in enantioselectivity) of up to 64% (Figure 13 and table 4, entries 1 and 2). This suggests that protein-substrate interactions, reminiscent of keto-reductases, are intimately involved in the enantioselection mechanism, as the classical C-H•••π interaction cannot be invoked for dialkyl substrate (**12**). In most of the experiments, the activated *p*-bromoacetophenone (**11**) affords much better conversions than the aliphatic substrate (**12**). The challenging dialkyl ketone gives comparable (*R*)-selectivity to the acetophenone derivative (**11**), albeit using different biotinylated catalyst ⊂ protein combinations (*ee*'s up to 83 % (*R*) for (**11**) and 82% (*R*) for (**12**) (see table 4, entries 3 and 4). In contrast, with some rare exceptions (Table 4, entry 5), only modest (*S*)-selectivities are obtained with substrate (**12**) (see figure 14).

Table 4 Selected results for the designed evolution of the reduction of ketones (**11**) and (**12**) in the presence of biotin-sepharose-immobilized artificial metalloenzymes [η^6-(arene)Ru(**Biot-*p*-L**)Cl] ⊂ Sav mutant. Entry η^6-(arene) Sav isoform Substrate Conv. (%) *ee* (%).

Entry	η^6-(arene)	Sav isoform	Substrate	Conv. (%)	*ee* (%)
1	benzene	S112A-K121W	**11**	89	16 (*R*)
2	benzene	S112A-K121W	**12**	86	80 (*R*)
3	*p*-cymene	L124V	**11**	90	83 (*R*)
4	*p*-cymene	S112A-K121T	**12**	84	82 (*R*)
5	benzene	S112A-K121N	**12**	95	62 (*S*)
6	*p*-cymene	S112A-K121N	**12**	81	58 (*R*)
7	benzene	S112A-K121N	**11**	99	55 (*S*)
8	*p*-cymene	S112A-K121N	**11**	63	50 (*R*)
9	*p*-cymene	S112A-K121F	**12**	96	73 (*R*)
10	*p*-cymene	S112A-K121V	**12**	92	68 (*R*)

11	p-cymene	S112A-K121V	**12**	73	66 (R)
12	benzene	S112A-K121C	**12**	63	63 (S)
13	benzene	S112K-L124H	**12**	64	59 (S)
14	benzene	K121R	**12**	96	64 (S)

3.6 Capping arene: *p*-cymene versus benzene

In general the two substrates behave similarly in enantioselectivity trends. It is interesting also to mention that good (R)-enantioselectivities are given by the p-cymene complex while (S)-selectivities are obtained by the benzene even if less impressive, respecting the trend observed in previous studies.[22c] S112A-K121N illustrate at best the opposite enantioselectivity tendency. Interestingly, some deviations are apparent from the (S) trend given by the benzene complex and are most often observed with the position S112A. For example with: $[\eta^6\text{-(benzene)Ru}(\textbf{Biot-}\textit{p}\textbf{-L})\text{Cl}]$ ⊂ S112A-K121W Sav with 80 (R). (Table 4, entry 2)

3.7 Nature of the S112X residues: WT, S112A, S112K

Some of the best (R)- and (S)-selectivities for both the aromatic and the aliphatic substrates are obtained with catalyst variants bearing the S112A mutation (Table 4, entries 4-5 and 9-12). Overall, the double mutants are less selective when incorporating S112K mutation, suggesting that a small side chain (alanine or serine) at position 112 may increase the influence of beneficial K121X or L124X mutations. The best S112K double mutant is $[\eta^6\text{-}(\textit{p}\text{-cymene})\text{Ru}(\textbf{Biot-}\textit{p}\textbf{-L})\text{Cl}]$ ⊂ S112K -124H Sav which affords 59% *ee* (S) for the reduction of substrate (**12**) (Table 4, entry 13). Thus, within this round of designed evolution, the S112K mutation can be regarded as an evolutionary dead-end.
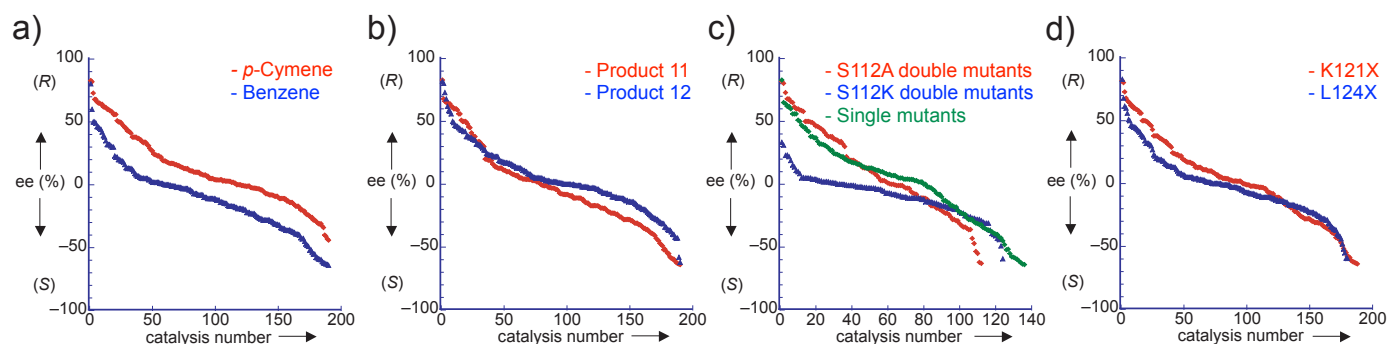
Figure 14 Enantioselectivity trends of the immobilized artificial transfer hydrogenases. The results are arranged from the highest to the lowest *ee* value, according to: a) the nature of the capping arene: *p*-cymene or benzene b) the nature of the substrate c) the nature of the S112X residue: S112A, S112K and S112 d) the position of the site of mutation: K121X and L124X.

3.8 Evalutation of homogeneous purified Sav Isoforms on representative substrates

The best results using the immobilized hybrid catalysts were subsequently reproduced using the purified Sav mutant in a homogeneous phase. An increase in *ee* and conversion could be observed in almost all cases (Table 5, entries 1-7). An interesting behaviour could be seen in the case of some proteins bearing mutations in position 121, which afforded opposite enantioselectivities when the pure protein was used instead of the immobilized form. The most striking examples are the Sav mutants bearing the K121G mutation (Table 5, entries 8-9), which inverted the enantioselectivity in combination with $[\eta^6$-(*p*-cymene)Ru(**Biot-*p*-L**)Cl]. It is tempting to speculate that the presence of the sepharose perturbed the spatial arrangement of the bulky $[\eta^6$-(*p*-cymene)Ru(**Biot-*p*-L**)Cl] within these mutants.

Table 5 Selected results for the optimization of the reduction of ketones (**11**) and (**12**) in the presence of immobilized- and purified artificial metalloenzymes [η^6-(arene)Ru(**Biot-*p*-L**)Cl] Ì Sav mutant.

Entry	η^6-(arene)	Sav isoform	substrate	Immobilized Sav (from cell extract)	Pure non-immobilized Sav
1	*p*-cymene	L124V	**11**	83 (90)	91 (96)
2	benzene	S112A-K121N	**11**	-55 (99)	-75 (98)
3	benzene	S112K-L124H	**11**	-59 (64)	-65 (94)
4	benzene	K121R	**11**	-64 (96)	-68 (95)
5	*p*-cymene	S112A-K121T	**12**	82 (84)	88 (99)
6	benzene	S112A-K121W	**12**	80 (86)	84 (99)
7	benzene	S112A-K121N	**12**	-62 (95)	-72 (100)
8	*p*-cymene	S112A-K121G	**11**	-43 (97)	38 (66)
9	*p*-cymene	K121G	**12**	-31 (73)	23 (20)
10	*p*-cymene	S112K-K121C	**11**	-11 (91)	41 (68)

The reconstructed evolutionary path of the best (*R*)- and (*S*)-selective hybrid catalysts for the reduction of 4-phenyl-2-butanone (**12**) is depicted in figure 15. It is interesting to note that the most selective artificial enzymes identified for the dialkyl ketone substrate ([η^6-(*p*-cymene)Ru(**Biot-*p*-L**)Cl] ⊂ S112A-K121T Sav and ([η^6-(benzene)Ru(**Biot-*p*-L**)Cl] ⊂ S112A-K121N Sav) are reached by an evolutionary path involving a combination of two poorly adapted mutations that would not normally be selected individually. Screening for enantioselectivity likely optimizes second coordination sphere interactions between substrate and protein, exerting an evolutionary pressure toward substrate specialization.
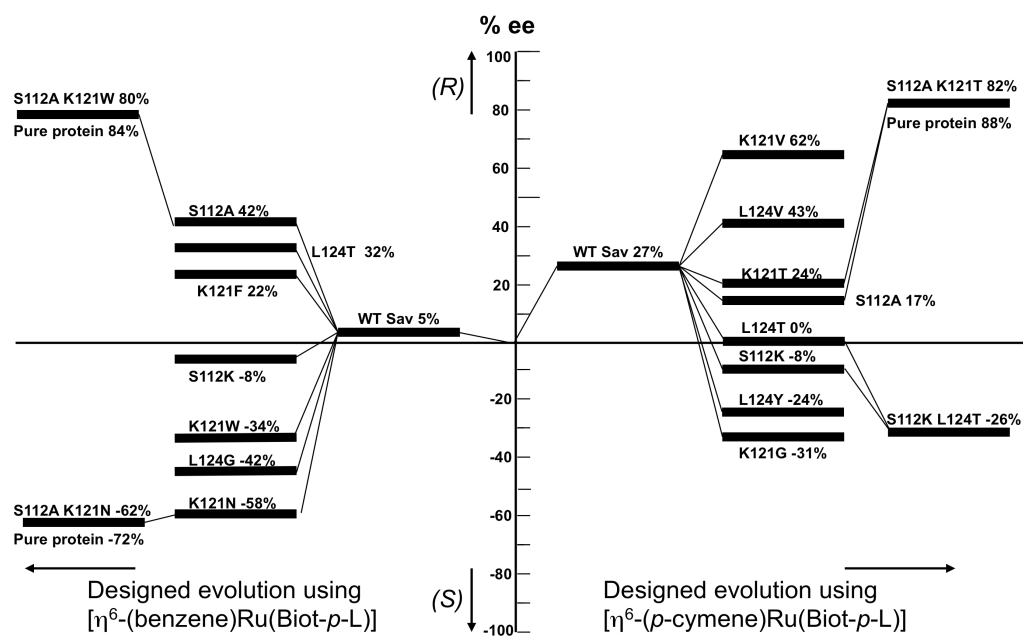
Figure 15 Reconstructed evolutionary path of the best (*R*)- and (*S*)-selective immobilized hybrid catalysts for the reduction of 4-phenyl-2-butanone (**12**).

4. Ketone reduction: conclusion

In summary, identification of (*R*)- and (*S*)-selective artificial metalloenzymes by a chemogenetic optimization procedure and the information provided by the structural characterization of [η^6-(benzene)Ru(**Biot-*p*-L**)Cl] $\subset$ S112K Sav has allowed us to implement a designed evolution protocol for the optimization of artificial transfer hydrogenases. The method is based on the combination between rational and combinatorial modifications, *i.e.* the mutation sites were identified from the X-ray structure and the most efficient residues were selected after screening of the enzyme variants obtained by saturation mutagenesis. A straightforward screening step, performed on crude cellular extracts, allowed the identification of [η^6-(*p*-cymene)Ru(**Biot-*p*-L**)Cl] $\subset$ S112A-K121T Sav for the enantioselective reduction of dialkyl ketones. While a single point mutation was sufficient to generate selective catalysts for the aromatic ketones (>90% *ee*), double mutants obtained by the designed evolution protocol were required to identify best hybrid catalysts for the reduction of dialkyl substrates.

5. Imine reduction: results and discussion

5.1 Screening Strategy

In our previous study on artificial metalloenzymes for the hydrogenation of ketones, it was established that chemical optimization brings more diversity than the genetic counterpart.[22c] To reduce the number of screening experiments, a representational search strategy was applied to optimize conversion and selectivity of the artificial metalloenzymes (see figure 16). In a first screening round, all 18 catalysts precursors were evaluated in combination with one streptavidin isoform (WT) (see table 6). For the second round, the most promising biotinylated catalysts were screened with 19 streptavidin isoforms derived from saturation mutagenesis at position S112 (see figure 17). Finally, the best catalyst ⊂ protein combinations (hybrid catalyst) were optimized with regard to reaction conditions (pH, Temp, Conc,...).

Concept
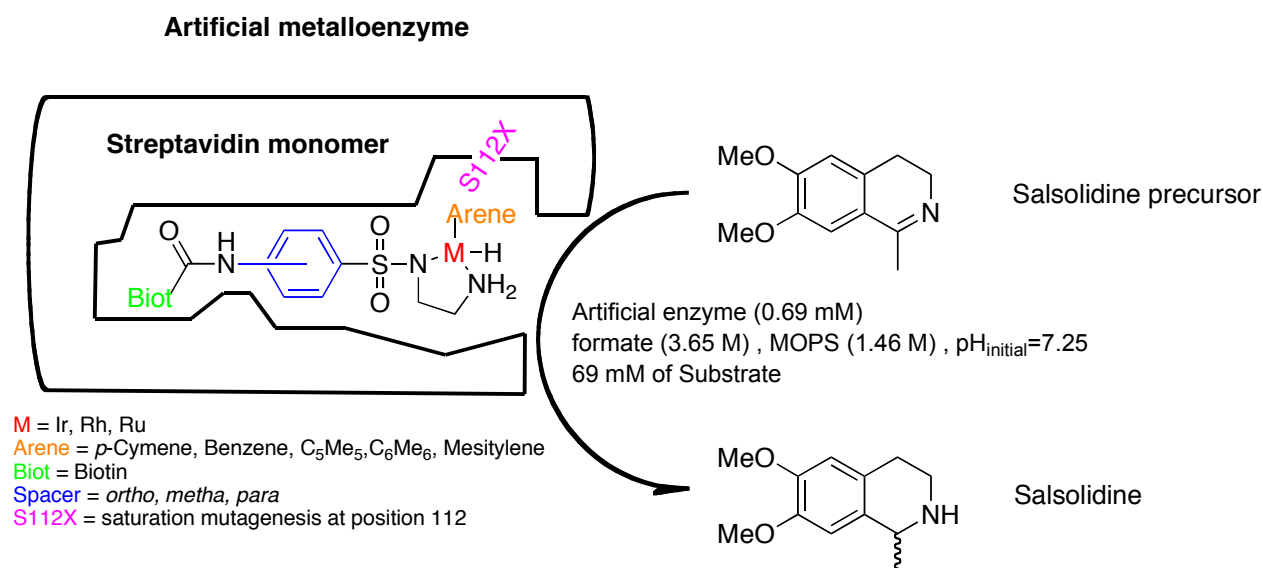
Figure 16 Schematic representation of the artificial metalloenzyme bearing a biotinylated d^6 piano stool complex for the reduction of the salsolidine precursor. The host protein (streptavidin, black) displays a high affinity for the anchor (biotin, green); introduction of a spacer (blue) and variation of

the metal (red) and the η^n-bonded arene (orange) allows one to chemically optimize the activity and the selectivity of the catalyst. Saturation mutagenesis (magenta) allows genetic optimization of the host protein.

5.2 Chemical diversity

Chemical diversity is provided using three different biotinylated ligands (*ortho*, *meta* or *para* position of the biotin anchor), 5 different capping arenes and the metal (Ru, Rh, Ir). For the first optimization step, the catalysts precursors were screened in the presence of WT Sav. The results of the screening experiments are summarized in table 6 for each substrate-protein-ligand combination (experiments were performed in collaboration with Annette Mutschler and Karoline Kersten).

Table 6 Complexes optimization for salsolidine production.

Entry	Complexes	Loading (%)	Protein	Conversion (%)	*ee* (%)
1	$[\eta^5$-(Cp*)Ir(**Biot-o-L**)Cl]	1	WT	21	31 (*S*)
2	$[\eta^5$-(Cp*)Rh(**Biot-o-L**)Cl]	1	WT	98	10 (*S*)
3	$[\eta^6$-(*p*-cymene)Ru(**Biot-o-L**)Cl]	1	WT	63	8 (*S*)
4	$[\eta^6$-(mesitylene)Ru(**Biot-o-L**)Cl]	1	WT	99	3 (*S*)
5	$[\eta^6$-(benzene)Ru(**Biot-m-L**)Cl]	1	WT	19	0 (*R*)
6	$[\eta^6$-(C$_6$Me$_6$)Ru(**Biot-m-L**)Cl]	1	WT	19	0 (*R*)
7	$[\eta^5$-(Cp*)Rh(**Biot-m-L**)Cl]	1	WT	61	2 (*R*)
8	$[\eta^6$-(benzene)Ru(**Biot-o-L**)Cl]	1	WT	29	3 (*R*)
9	$[\eta^6$-(C$_6$Me$_6$)Ru(**Biot-o-L**)Cl]	1	WT	29	3 (*R*)
10	$[\eta^5$-(Cp*)Ir(**Biot-m-L**)Cl]	1	WT	100	4 (*R*)
11	$[\eta^6$-(mesitylene)Ru(**Biot-m-L**)Cl]	1	WT	49	5 (*R*)
12	$[\eta^6$-(*p*-cymeme)Ru(**Biot-m-L**)Cl]	1	WT	53	11 (*R*)
13	$[\eta^6$-(mesitylene)Ru(**Biot-p-L**)Cl]	1	WT	76	12 (*R*)
14	$[\eta^6$-(cymene)Ru(**Biot-p-L**)Cl]	1	WT	81	18 (*R*)
15	$[\eta^6$-(benzene)Ru(**Biot-p-L**)Cl]	1	WT	30	23 (*R*)
16	$[\eta^6$-(C$_6$Me$_6$)Ru(**Biot-p-L**)Cl]	1	WT	77	36 (*R*)
17	$[\eta^5$-(Cp*)Ir(**Biot-p-L**)Cl]	1	WT	98	36 (*R*)
18	$[\eta^5$-(Cp*)Rh(**Biot-p-L**)Cl]	1	WT	97	69 (*R*)

Catalysis conditions: $[\eta^5\text{-}(Cp^*)Ir(\textbf{Biot-}\textit{\textbf{p}}\textbf{-L})Cl] \subset$ Sav (0.69 mM) , Sodium formate (3.65 M) , MOPS (1.46 M), $pH_{initial}$ = 7.25, Salsolidine precusor (69 mM), 55°C, 5 h.

Of a library of 18 complexes tested, it appeared that the orientation of the spacer and the capping arene played an important role in both the conversion and enantioselectivity (Table 6). Futhermore, iridium and rhodium in conjugation with Cp* gave the best enantioselectivities ((*R)* and (*S)*, (table 6, entries 1 and 18) with the **Biot-*p*-L** ligand (*R*) respectively the **Biot-*o*-L** (*S*).

5.3 Genetic diversity

Improvements of the *ee* and conversion for the reduction of salsolidine precursor were achieved. Table 7 summarizes the best catalytic results obtained for 19 Sav variants at position S112X (S112P not included due difficult production of the protein). The best *ee* in favor of the (*R)*-enantiomer was obtained with S112A allowing 85% (*R*) *ee* and complete conversion (Table 7, entry 1 and figure 17). This mutant was therefore selected for further investigations. In contrast, the best *ee* in favor of the (*S)*-enantiomer was obtained with S112K affording 57% (*S*) *ee* and 83% conversion (Table 7, entry 19)

Table 7 Catalysis optimization through saturation mutagenesis at the S112 position

Entry	Complexes	Loading (%)	Protein	Conversion (%)	*ee* (%)
1	$[\eta^5\text{-}(Cp^*)Ir(\textbf{Biot-}\textit{\textbf{p}}\textbf{-L})Cl]$	1	S112A Sav	100	85 (*R*)
2	$[\eta^5\text{-}(Cp^*)Ir(\textbf{Biot-}\textit{\textbf{p}}\textbf{-L})Cl]$	1	S112G Sav	100	60 (*R*)
3	$[\eta^5\text{-}(Cp^*)Ir(\textbf{Biot-}\textit{\textbf{p}}\textbf{-L})Cl]$	1	WT Sav	100	57 (*R*)
4	$[\eta^5\text{-}(Cp^*)Ir(\textbf{Biot-}\textit{\textbf{p}}\textbf{-L})Cl]$	1	S112Y Sav	100	50 (*R*)
5	$[\eta^5\text{-}(Cp^*)Ir(\textbf{Biot-}\textit{\textbf{p}}\textbf{-L})Cl]$	1	S112T Sav	15	46 (*R*)
6	$[\eta^5\text{-}(Cp^*)Ir(\textbf{Biot-}\textit{\textbf{p}}\textbf{-L})Cl]$	1	S112F Sav	100	37 (*R*)
7	$[\eta^5\text{-}(Cp^*)Ir(\textbf{Biot-}\textit{\textbf{p}}\textbf{-L})Cl]$	1	S112D Sav	100	29 (*R*)
8	$[\eta^5\text{-}(Cp^*)Ir(\textbf{Biot-}\textit{\textbf{p}}\textbf{-L})Cl]$	1	S112C Sav	75	20 (*R*)
9	$[\eta^5\text{-}(Cp^*)Ir(\textbf{Biot-}\textit{\textbf{p}}\textbf{-L})Cl]$	1	S112N Sav	87	19 (*R*)
10	$[\eta^5\text{-}(Cp^*)Ir(\textbf{Biot-}\textit{\textbf{p}}\textbf{-L})Cl]$	1	S112V Sav	100	19 (*R*)
11	$[\eta^5\text{-}(Cp^*)Ir(\textbf{Biot-}\textit{\textbf{p}}\textbf{-L})Cl]$	1	S112L Sav	91	15 (*R*)
12	$[\eta^5\text{-}(Cp^*)Ir(\textbf{Biot-}\textit{\textbf{p}}\textbf{-L})Cl]$	1	S112H Sav	13	9 (*R*)

13	$[\eta^5$-(Cp*)Ir(**Biot-_p_-L**)Cl]	1	S112W Sav	100	7 (_R_)
14	$[\eta^5$-(Cp*)Ir(**Biot-_p_-L**)Cl]	1	S112E Sav	80	5 (_R_)
15	$[\eta^5$-(Cp*)Ir(**Biot-_p_-L**)Cl]	1	S112I Sav	75	5 (_S_)
16	$[\eta^5$-(Cp*)Ir(**Biot-_p_-L**)Cl]	1	S112Q Sav	47	16 (_S_)
17	$[\eta^5$-(Cp*)Ir(**Biot-_p_-L**)Cl]	1	S112R Sav	100	19 (_S_)
18	$[\eta^5$-(Cp*)Ir(**Biot-_p_-L**)Cl]	1	S112M Sav	26	19 (_S_)
19	$[\eta^5$-(Cp*)Ir(**Biot-_p_-L**)Cl]	1	S112K Sav	83	57 (_S_)

Catalysis conditions: $[\eta^5$-(Cp*)Ir(**Biot-_p_-L**)Cl] $\subset$ Sav (0.69 mM, metal complex) , Sodium formate (3.65 M) , MOPS (1.46 M), $pH_{initial}$ = 7.25, Salsolidine precursor (69 mM), 55 °C, 1 h.
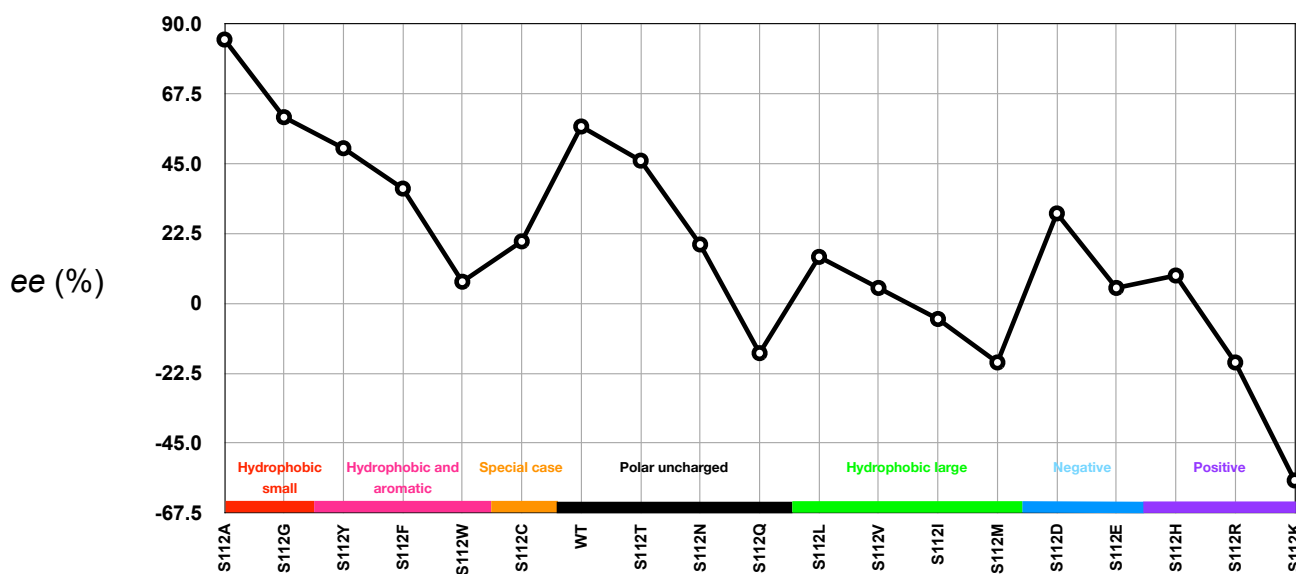
Figure 17 Enantiomeric excess and conversion as a function of the Sav isoform used in catalysis.

Referring to table 7, the only clear trend that can be observed is the following:

- The small hydrophobic residues gave the best enantioselectivities and conversions towards the (R)-product and in particular the [η^5-(Cp*)Ir(**Biot-p-L**)Cl $\subset$ S112A] (Table 7, entry 1). Assuming that the ligand is the most important factor in determining ee, then a small (or absent) side-chain may allow best placement of the metal, without steric hindrance.

- Aromatic residues gave good enantioselectivities and good conversion highlighted by the [η^5-(Cp*)Ir(**Biot-p-L**)Cl] $\subset$ S112Y (Table 7, entry 4).

- Negatively charged residues gave poor enantioselectivities but excellent conversions. (Table 7, entry 7 and 14)

- Positively charged aminoacids gave the best enantioselectivities and conversion in favor of the (S)-product. In particular the [η^5-(Cp*)Ir(**Biot-p-L**)Cl] $\subset$ S112K (Table 7, entry 19).

5.4 Loading optimisation

In order to study the catalyst performance, the loading of the catalyst was varied by increasing the concentration of the salsolidine precursor. This allowed determining the TON of the artificial metalloenzyme at a fixed concentration (0.69 mM) of the catalyst precursor. Despite loss of enantioselectivity at lower loadings, the complex showed an excellent activity up to 1000 turnovers (Table 8, entry 5).

Table 8 Loading optimization.

Entry	Complexes	Loading (%)	Protein	Temp. (°C)	Time (h)	Conversion (%)	ee
1	[η^5-(Cp*)Ir(**Biot-p-L**)Cl]	1	S112A	25	5	100	92 (R)
2	[η^5-(Cp*)Ir(**Biot-p-L**)Cl]	1	S112A	55	1	100	83 (R)
3	[η^5-(Cp*)Ir(**Biot-p-L**)Cl]	0.10	S112A	25	6	63	92 (R)
4	[η^5-(Cp*)Ir(**Biot-p-L**)Cl]	0.10	S112A	25	26	99	91 (R)
5	[η^5-(Cp*)Ir(**Biot-p-L**)Cl]	0.10	S112A	55	120	100	82 (R)

Catalysis conditions: [η^5-(Cp*)Ir(**Biot-p-L**)Cl] $\subset$ Sav (0.69 mM, metal complex), formate (3.65 M), MOPS (1.46 M), $pH_{initial}$ = 7.25, Salsolidine precursor (69 mM, 1% loading), (690 mM, 0.1 % loading), (6900 mM, 0.01% loading), 25 °C.

5.5 Temperature optimisation

As shown previously (Table 8, entries 1 and 2), temperature played a major role in the outcome of the catalysis. In order to determine the best *ee*, the catalysis temperature was decreased from 55°C to 0°C.

Table 9 Temperature optimization using the S112A mutant.

Entry	Complexes	Loading (%)	Protein	Temp. (°C)	Time (h)	Conversion (%)	ee
1	[η^5-(Cp*)Ir(**Biot-p-L**)Cl]	1	S112A	55	1	100	85 (R)
2	[η^5-(Cp*)Ir(**Biot-p-L**)Cl]	1	S112A	25	5	90	87 (R)
3	[η^5-(Cp*)Ir(**Biot-p-L**)Cl]	1	S112A	25	1	100	89 (R)
4	[η^5-(Cp*)Ir(**Biot-p-L**)Cl]	1	S112A	4	5	100	92 (R)
5	[η^5-(Cp*)Ir(**Biot-p-L**)Cl]	1	S112A	0	5	42	93 (R)

Catalysis conditions: [η^5-(Cp*)Ir(**Biot-p-L**)Cl] $\subset$ Sav (0.69 mM, metal complex) , Sodium formate (3.65 M) , MOPS (1.46 M), $pH_{initial}$ = 7.25, Salsolidine precursor (69 mM).

The enantioselectivity increased from 85 % (*R*) up to 93 % (*R*) going from 55 °C to 0 °C thus demonstrating that temperature has a significant influence on the enantioselectivity of the reaction (Table 9, entries 4 and 5).

5.6 Michaelis-Menten kinetics

In order to assess the kinetic behaviour of imine reduction, Michaelis-Menten saturation kinetics was measured and the substrate concentration versus initial rate was plotted.(see figure 18).

Table 10 Kinetic parameters.

Entry		k_{cat} (h^{-1})	K_m (mM)	V_{max} (mM h^{-1})	k_{cat}/K_m (h^{-1}mM)
1	$[\eta^5$-(Cp*)Ir(**Biot-*p*-L**)Cl]	64.2	0.18	15.6	356
2	$[\eta^5$-(Cp*)Ir(**Biot-*p*-L**)Cl] $\subset$				294
	S112A	138.2	0.47	40.8	

a)

b)
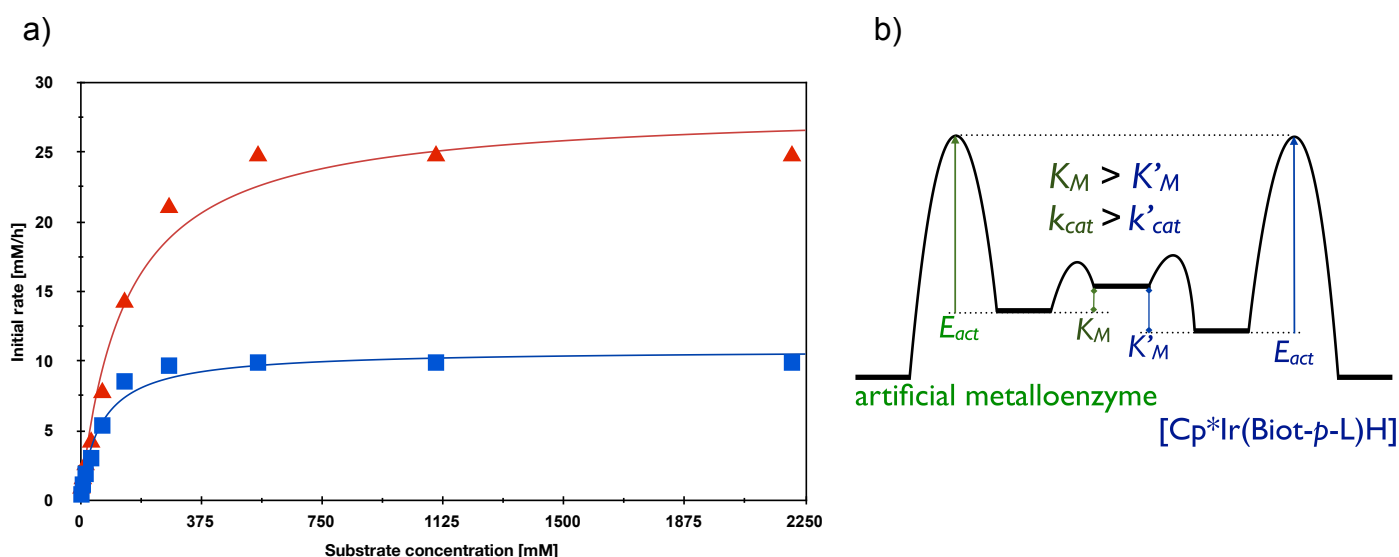
Figure 18 Saturation kinetics plot for the ATH catalyzed by [Cp*Ir(**Biot-*p*-L**)Cl] (square) and [Cp*Ir(**Biot-*p*-L**)Cl] $\subset$ S112A Sav (triangles). The solid lines correspond to the Michaelis-Menten fit using the K_M and k_{cat} displayed above a) simplified model to rationalize the correlation between K_M and k_{cat} b)

The imine reduction using the $[\eta^5\text{-}(Cp^*)Ir(\textbf{Biot-}\textit{p}\textbf{-L})Cl]$ anchored to S112A streptavidin showed a k_{cat} of 138.2 h^{-1} (see table 10). This is 2.71 times faster than the free complex (k_{cat} = 64.2 h^{-1}). The K_M of the artificial metalloenzyme (K_M = 0.47 mM) is higher than that for the complex alone (K_M = 0.18 mM). This correlation may be rationalized by assuming that the decrease in affinity raises the energy of the enzyme·substrate intermediate, which in turn leads to a decrease in the activation barrier, (see figure 18 b). Compared to other artificial metalloenzymes formed using biotin-streptavidin technology, this system is the fastest and the most efficient to date (see table 11).

Table 11 Michaelis-Menten comparison of the imine reductase with a hydrogenase.

Entry	System		k_{cat} (h^{-1})	K_M (mM)	V_{max} (mM h^{-1})	k_{cat}/K_m (h^{-1} mM)	*Ref.*
1	Imine reductase	Complex alone	64.2	0.18	15.6	356	This work
2	Imine reductase	Complex ⊂ protein	138.2	0.47	40.8	294	This work
3	Hydrogenase	Complex alone	180	7.38	10.38	24.39	Ref.[37]
4	Hydrogenase	Complex ⊂ protein	269	3.18	15.24	84.59	Ref.[37]

5.7 Immobilisation of the catalyst

In order to immobilize the artificial enzymes two approaches were used. The first is immobilization via iminobiotin-sepharose previously developped for transfer hydrogenation reactions of ketones[22c], giving the opportunity to use cell extracts containing streptavidin isoforms.

The second approach was to use cross linked streptavidin. Glutaraldehyde, polyethylene imine (PEI) or activated dextrans were used as cross linking-agents. The resulting cross-linked enzyme aggregates called CLEAs (see figure 19) were developed by Sheldon et al.[36] This allowed

formation of insoluble protein polymers in catalytic conditions but that conserved the binding properties for B₄F (Biotin-4-fluoresceine) and therefore for the biotinylated complex. Table 12 summarizes the catalytic results obtained with CLEAs in same experimental conditions as those used for the non-immobilized catalysts.
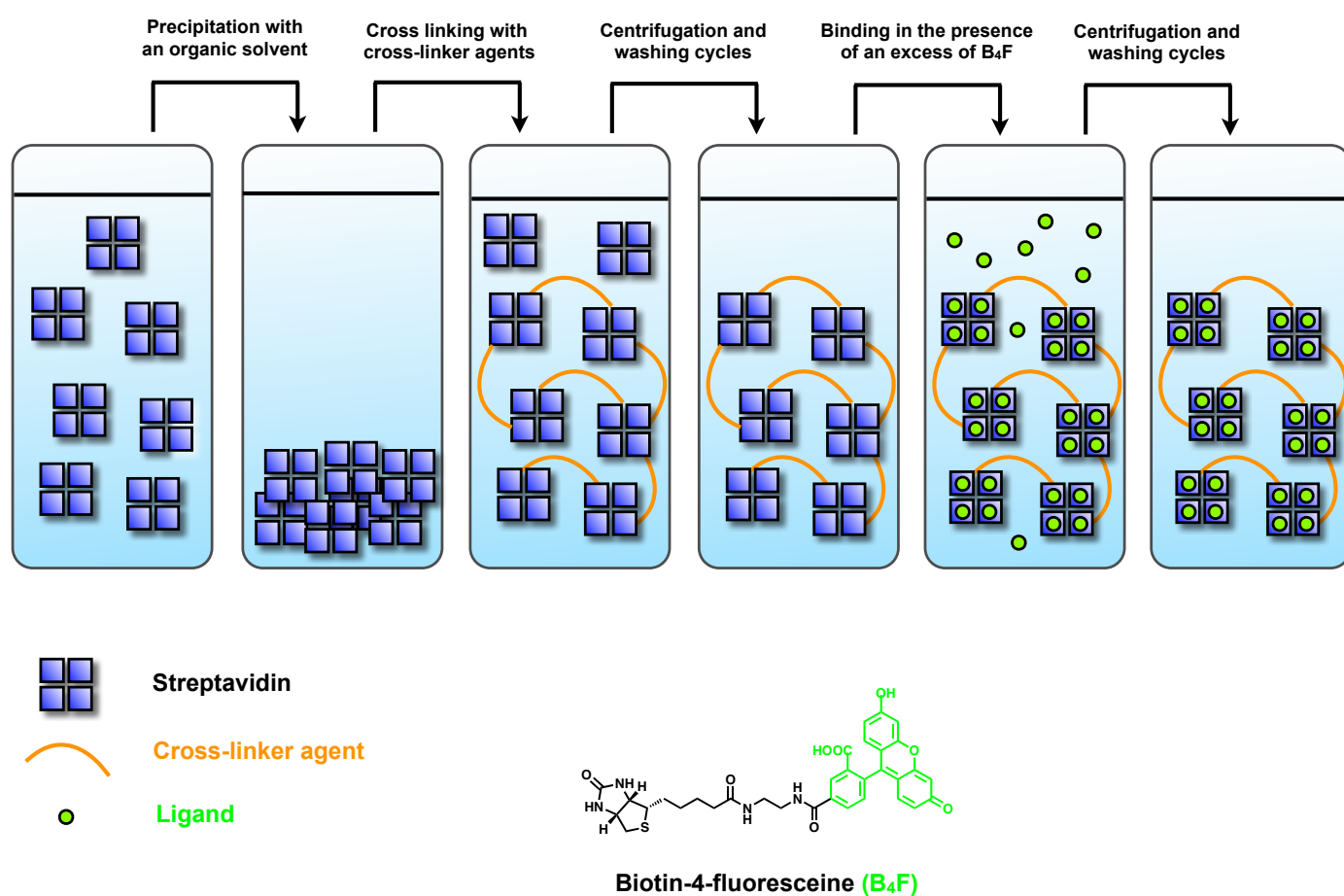
Figure 19 Schematic representation of the CLEAs formation with cross-linker agents.

Table 12 Selected results for transfer hydrogenation of imines using CLEA immobilized artificial metalloenzymes.

Entry	Complexes	Loading (%)	Protein	Conversion (%)	*ee*
1	$[\eta^5\text{-}(Cp^*)Ir(\textbf{Biot-}\textit{p}\textbf{-L})Cl]$	1	S112A Cleas Glu	87	49 (*R*)
2	$[\eta^5\text{-}(Cp^*)Ir(\textbf{Biot-}\textit{p}\textbf{-L})Cl]$	1	S112A Cleas PEI	100	18 (*R*)
3	$[\eta^5\text{-}(Cp^*)Ir(\textbf{Biot-}\textit{p}\textbf{-L})Cl]$	1	S112A Cleas Dex	72	43 (*R*)

4	$[\eta^5\text{-(Cp*)Ir}(\textbf{Biot-}\textit{p}\textbf{-L})Cl]$	1	Wt Cleas Glu	93	39 (R)
5	$[\eta^5\text{-(Cp*)Ir}(\textbf{Biot-}\textit{p}\textbf{-L})Cl]$	1	Wt Cleas PEI	97	22 (R)
6	$[\eta^5\text{-(Cp*)Ir}(\textbf{Biot-}\textit{p}\textbf{-L})Cl]$	1	Wt Cleas Dex	72	34 (R)
7	$[\eta^5\text{-(Cp*)Ir}(\textbf{Biot-}\textit{p}\textbf{-L})Cl]$	1	S112A immobilized	74	14 (R)
8	$[\eta^5\text{-(Cp*)Ir}(\textbf{Biot-}\textit{p}\textbf{-L})Cl]$	1	S112A	100	93 (R)

Catalysis conditions: $[\eta^5\text{-(cp*)Ir}(\textbf{Biot-}\textit{p}\textbf{-L})Cl] \subset$ Sav (0.69 mM, metal complex) , Sodium formate (3.65 M) , MOPS (1.46 M), $pH_{initial}$=7.25, Salsolidine precursor (69 mM), 25 °C, 5 h. Glu = Glutaraldehyde, PEI = Polyethylene imines, Dex = Dextrans, Immobilised = immobilized with biotin-sepharose.

From the table 12, it appeared that the best system for immobilization of S112A is based on glutaraldehyde as a cross-linker agent (Table 12, entry 1). However, the *ee* is lower than for the non-immobilized enzyme (Table 12 entry 8). Polyethylene imine cross-linkers were, in contrast, less efficient (Table 12, entry.2). Furthermore, immobilized streptavidin on iminobiotin sepharose was least efficient (Table 12, entry 7).

5.8 CLEAs gels

To determine the size and the binding capacity of the CLEAs, SDS-PAGE analysis were performed. The SDS-page in figure 20 shows the migration of the cross-linked streptavidin. S112A Sav cross-linked with glutaraldehyde didn't migrate through the stacking gel. This may be due to the size of the CLEAs or to the low solubility of the polymer. The same trend was observed with the PEI cross-linker. In contrast, the S112A isoform cross-linked with activated dextrans demonstrates migration abilities into the SDS-page. This could be explained by lower cross-linking, allowing migration throught the acrylamide gel. Moreover, the gel shows a plethora of bands suggesting different populations of polymers with different sizes. In this context, it is interesting to mention that the polymer formed with activated dextrans is more a gel-like than an insoluble

precipitate as in the case of S112A Sav cross-linked with glutaraldehyde. The same trend was observed with the WT streptavidin except that the PEI cross-linked streptavidin presented similar pattern of bands as for the activated dextrans with S112A. Finally, the ability to detect the CLEAs using B_4F showed that the polymer binds this modified biotin and suggest that biotinylated complexes do bind to the polymer.
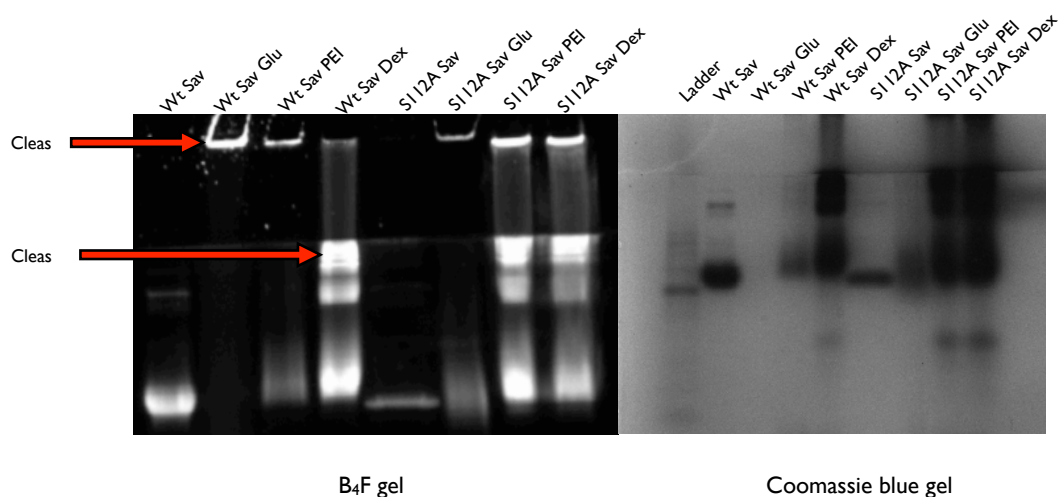
Figure 20 SDS-page of the Cross-linked Streptavidin with Glutaraldehyde, PEI or Dex

5.9 Crystal structure of the $[\eta^5$-(Cp*)Ir(Biot-*p*-L)Cl] $\subset$ S112A

In order to get insight into artificial transfer hydrogenase, efforts were invested to crystallize the most promising combination for the reduction of imines which consist of the $[\eta^5$-(Cp*)Ir(**Biot-*p*-L**)Cl] $\subset$ S112A (see figure 21). Crystals of the $[\eta^5$-(Cp*)Ir(**Biot-*p*-L**)Cl] $\subset$ S112A were obtained (Crystal structure determined by Tillmann Heinisch in collaboration with Prof. Tilman Schirmer, Biozentrum). The refined structure (1.9 Å resolution) allowed the identification of the environment of surrounding the active site of the artificial metalloenzyme. The occupancy of the $[\eta^5$-(Cp*)Ir(**Biot-*p*-L**)Cl] into streptavidin S112A Sav isoform was of 50% with soaking methods compared to the $[\eta^6$-(benzene)Ru(**Biot-*p*-L**)Cl] into S112K Sav isoform (20% occupancy, 1.58 Å

resolution, PDB code 2QCB) with cocrystallization. Comparing the structure of the $[\eta^5$-(Cp*)Ir(**Biot-p-L**)Cl] $\subset$ S112A with $[\eta^6$-(benzene)Ru(**Biot-p-L**)Cl] $\subset$ S112K[22c] allows some interesting observations: The absolute configuration of the metal in the biotinylated complex is conserved in the two structures and is (*S*). The spatial organization markedly differs, a rotation of 150° around the S-N axes allows superimposition of the two different complexes. In this context, the position of the $[\eta^6$-(benzene)Ru(**Biot-p-L**)Cl] $\subset$ S112K it not really perturbed by the mutation. In contrary, the position 121 is close to the $[\eta^6$-(benzene)Ru(**Biot-p-L**)Cl] $\subset$ S112K while not to the $[\eta^5$-(Cp*)Ir(**Biot-p-L**)Cl] $\subset$ S112A. It demonstrates that positions 112, 121 and 124 are closest one to the metal center, depending on the nature of the complex, each one would have their own effect on the position of the metal center in the protein. Furthermore, the position of the sulfonamide is not changed for each complexes suggesting that only a rotation around the S-N bond is required to adapt the position of the complexes into the protein.

Ketone and Imine reduction
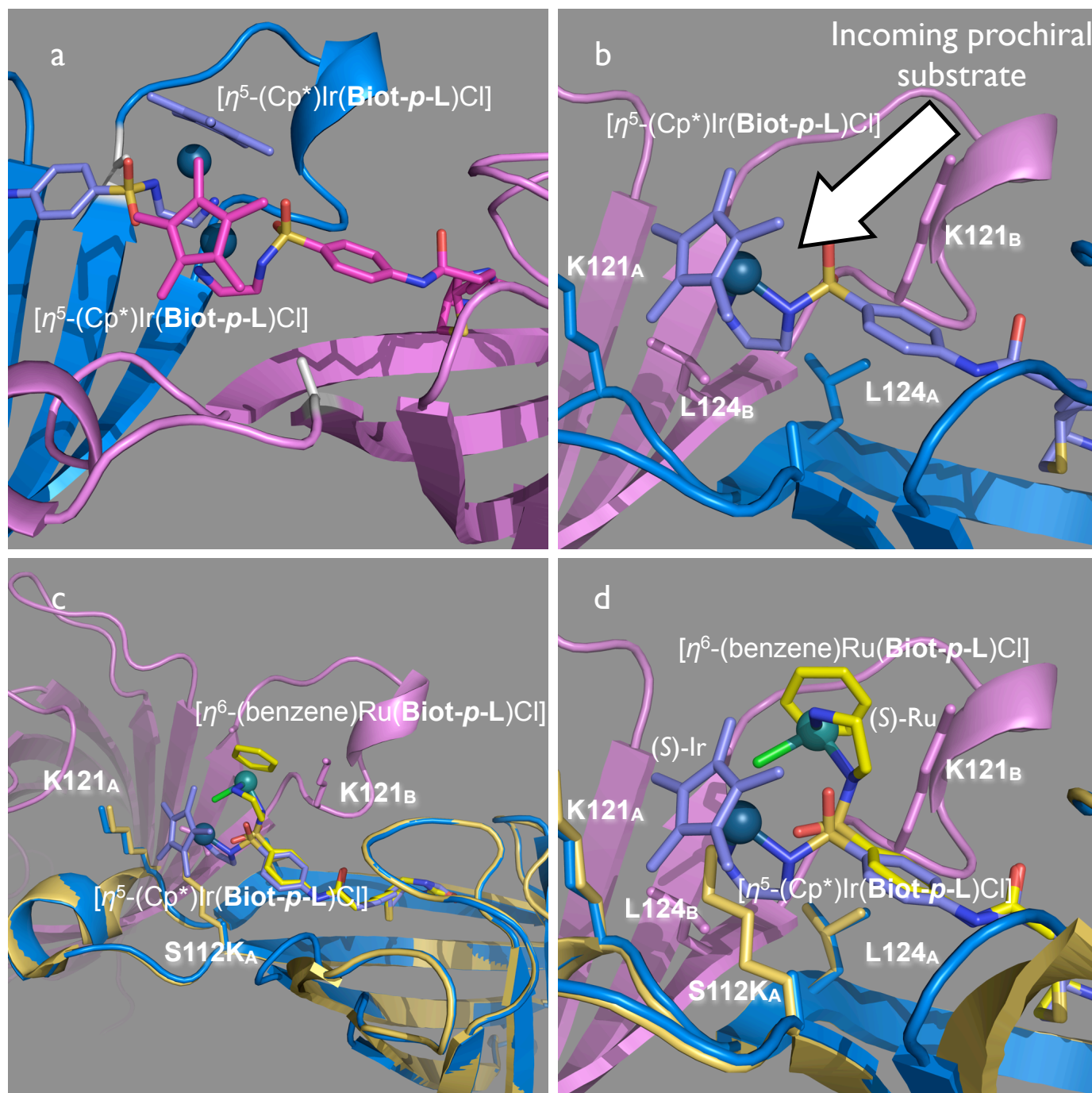
Figure 21 Crystal structure of the $[\eta^5\text{-(Cp*)Ir}(\textbf{Biot-}\textbf{\textit{p}-L})\text{Cl}] \subset \text{S112A}$. Figure of two adjacent monomers of streptavidin bearing each one an $[\eta^5\text{-(cp*)Ir}(\textbf{Biot-}\textbf{\textit{p}-L})\text{Cl}]$ a) View of one complex bound to streptavidin with close lying residues highlighted (A is for the monomer A, B is for the monomer B) b)

Superposition of two crystal structures, the first one for ketone reduction bearing an $[\eta^5$-(benzene)Ru(**Biot-*p*-L**)Cl] $\subset$ S112K and the second one bearing a $[\eta^5$-(Cp*)Ir(**Biot-*p*-L**)Cl] $\subset$ S112A c) Close-up view of the two superimposed structures with close lying aminoacids d)

6. Imine reduction: mechanistic discussion

Comparison of Noyori's Ru(II) Ts-DPEN catalyst with $[\eta^5$-(Cp*)Ir(**Biot-*p*-L**)Cl] biotinylated complex (see figure 22), suggests that the chirality at the metal in the protein may be determinant for the enantioselection mechanism. For both the Ru(II) Ts-DPEN and the biotinylated piano stool with the same configuration at the metal, the chirality of the product should be maintained if C-H•••π interactions occur (see figure 22).

By extension, for the reduction of imines, the (*R*)-product should be produced with a six-membered transition state via a C-H•••π interactions. In fact, for the imine reduction with Noyori's system, the opposite enantiomer is produced suggesting that another mechanism is involved (see introduction).[11d] This contrast with $(\eta^5$-(Cp*)Ir(**Biot-*p*-L**)Cl $\subset$ S112A which generates the (*R*)-product both for ketone and imine reduction.

The crystal structure depicted in the previous paragraph demonstrated that only one of the two enantiomers (the *S* one) of the biotinylated complex (bearing a chloride) is preferred by the protein during the crystallization process. In this context, it is speculated that Sav selects one of the two enantiomers of the complex. If the chloride is replaced by a hydride to generate the active catalyst, it would mean that the preferred active complex is (*R*). In this situation the substrate can be presented in four different orientations (see figure 22) to the metal generating four different possible mechanisms for the reduction. Two of them are non-concerted mechanisms and two of

them are non C-H••π mechanisms (Figure 22). Since the (R) product is generated with the S112A hybrid catalyst (η^5-(Cp*)Ir(**Biot-_p_-L**)Cl $\subset$ S112A) it could be could argued that only two mechanisms are possible. The first one is a mechanism with a C-H••π interaction but non-concerted and the second one is a non C-H••π mechanism but concerted. It is interesting to mention that these possibilities are in agreement with the alternative mechanism proposed by Wills for the imine reduction by Ru(II) Ts-DPEN.
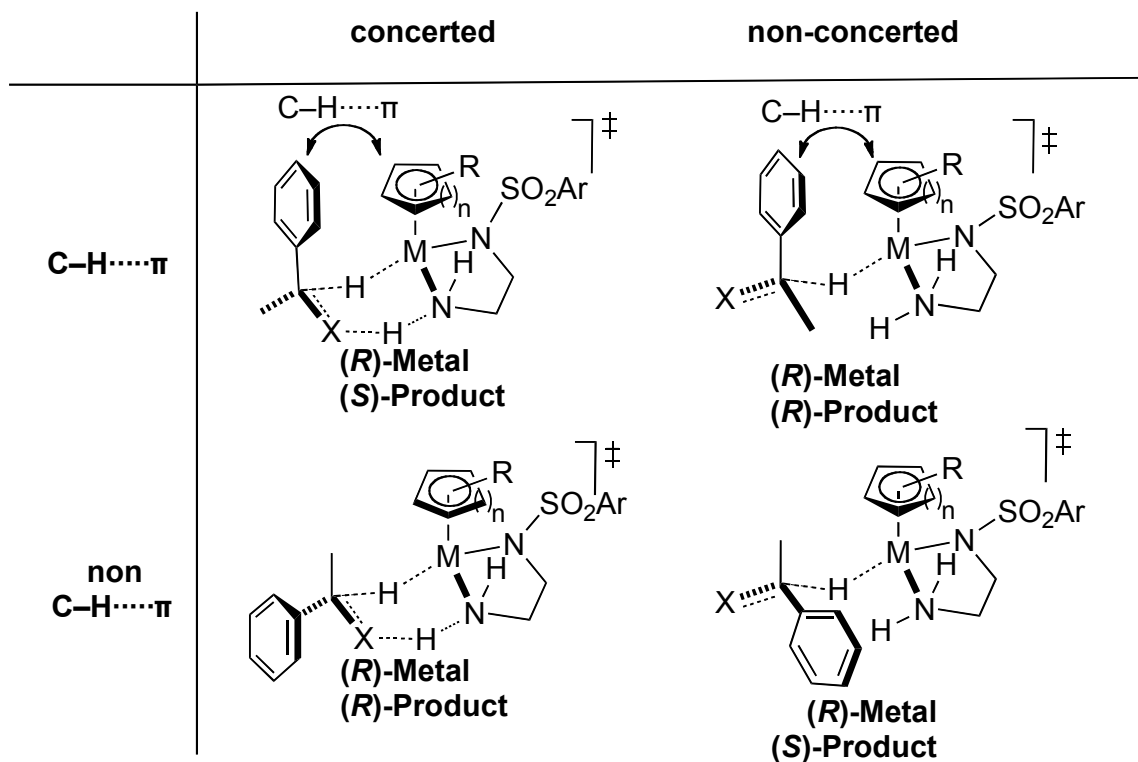
Figure 22 Four different possible transition states for ketone and imine reduction.

The replacement of the S112A with S112K affords the (S) product. It suggest a concerted mechanism with C-H•••π interaction or a non-concerted without C-H•••π interactions (see figure 22).

7. Imine reduction: conclusion

In conclusion, the first highly efficient artificial metalloenzyme, based on biotin-avidin technology, for the ATH of cyclic imines (salsolidine) in water was created. The conjugation of the biotinylated catalyst with streptavidin showed an acceleration of the reaction when compared to the free complex, as well as Michaelis-Menten kinetics, thus efficiently mimicking natural enzymes. Positional scanning[22b] was highly efficient for the improvement of artificial imine reductases reaching *ee* up to 93% with 100% conversion. A new protocol for the immobilization of these artificial metalloenzymes, based on the formation of streptavidin polymers called CLEAs (cross-linked enzymes aggregates) was implemented and suggested the potential for future practical applications. Finally, the crystal structure of this new imine reductase and its comparison with a ketone reductase provided valuable insights on catalytic results and on possible mechanisms for ATH of cyclic imines.

8. Experimental part

8.1 Ketone reduction

8.1.1 Catalysis : standard conditions

All experiments were carried out using standard Schlenk techniques, with thoroughly degassed solutions (nitrogen-flushed).

8.1.2 Description of the catalytic runs

Boric Acid - Sodium Formate Mixture. Boric acid (2.10 g, 34 mmol) and sodium formate (2.72 g, 40 mmol) were dissolved in water (40 ml). The pH was adjusted to 6.25 with NaOH pellets and the solution was thoroughly degassed. The concentration of the final stock-solution was: $[B(OH)_3]$ = 0.85M, [HCOONa] = 1M.

d-Biotin – Sepharose : The beads of biotin – sepharose (2350 µl wet beads; Affiland, Belgium) were washed with water and then resuspended in water in a total volume of 4000 µl. The binding capacity of the beads was 40 mg of avidin per ml of wet beads.

General Procedure for the Transfer Hydrogenation with Immobilized Protein. To a solution of cell extract containing the streptavidin (0.15 µmol) was added the suspension of biotin – sepharose (215 µl containing 125 µl wet beads; the solution contained a two-fold excess of protein with respect to the beads). The resulting suspension was vigorously stirred at room temperature for 60 min. The beads containing the immobilized protein (0.075 µmol) were centrifuged in 1.5 ml eppendorf tubes and washed three times with 400 µl of a 1M guanidinium chloride solution and one time with 400 µl of water, then resuspended in degassed water in a total volume of 750 µl. The suspension was thoroughly degassed (nitrogen flushed). The degassed immobilized protein (337 µl suspension, 0.0337 µmol) was mixed in an eppendorf tube with the precursor complex $[\eta^6$-
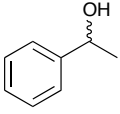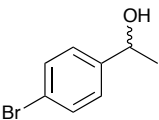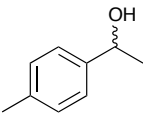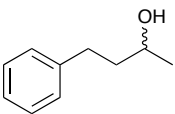
(arene)RuCl(**Biot–*p*-L**)] (4.27 µL of a 0.0395 M stock-solution in DMF, 0.169 µmol Ru) and shaked at room temperature for 10 min. The beads were centrifuged in 1.5 ml eppendorf tubes, washed three times with 200 µL boric acid - formate mixture, one time with 200 µL water and then resuspended in degassed water in a total volume of 340 µL. The boric acid - formate mixture (405 µl) and the MOPS buffer (135 µL of a 1M stock-solution, pH adjusted to 6.25) were added. The resulting suspension was divided in two different test tubes (400 µL per test tube, containing 0.015 µmol protein, 0.045 µmol Ru, 180 µmol HCOONa) and the corresponding substrate (para-bromoacetophenone (**11**) or 4- phenyl-2-butanone (**12**), 4.5 µmol) was added to each tube.

The test tubes were placed in a magnetically-stirred multireactor, purged several times with nitrogen and heated at 55°C for 64 hours. After completion, the reaction mixture was extracted with Et_2O (4 × 0.5 mL) and dried over Na_2SO_4. The organic solution was filtered through a short silicagel plug that was thoroughly washed with Et_2O, concentrated and subjected to HPLC analysis.

Catalysis with purified protein: The lyophilized streptavidin was dissolved in mQ (100 µM solution). The solution was thoroughly degassed (nitrogen flushed). The degassed protein (150 µL solution, 0.015 µmol) was mixed in a test tube with the precursor complex [η^6-(arene)RuCl(**Biot–*p*-L**)] (1.27 µL of a 0.0395 M stock- solution in DMF, 0.05 µmol Ru) and stirred at room temperature for 10 min. The boric acid - formate mixture (200 µL) and the MOPS buffer (67 µL of a 1M stock-solution, pH adjusted to 6.25) were added and the corresponding substrate was added to each tube. The test tubes were placed in a magnetically stirred multireactor, purged several times with nitrogen and heated at 55 °C for 64 hours. After completion, the reaction mixture was extracted with Et_2O (4 × 0.5 mL) and dried over Na_2SO_4. The organic solution was filtered through a short silicagel plug that was thoroughly washed with Et_2O, concentrated and subjected to HPLC analysis.

8.1.3 HPLC analysis

Table 13 HPLC conditions, retention times and absolut configurations for the reduction products.[a]

Alcohol	Column	Conditions	t_1	t_2	Detection
	OD-H	Hexane / i-PrOH 95 / 5 flow 0.7 mL / min	17.8 (R)	22.7 (S)	215 nm
	OD-H	Hexane / i-PrOH 95 / 5 flow 0.7 mL / min	11.6 (S)	12.9 (R)	225 nm
	(S,S)-ULMO	Hexane / DME 100 / 1.5 Flow 1 mL / min	16.6 (R)	19.5 (S)	215 nm
	OD-H	Hexane / i-PrOH 95 / 5 Flow 0.7 mL / min	13.9[b] (R)	20.6[b] (S)	215 nm

[a] The absolute configuration was assigned by comparison with published results.

[b] The absolute configuration was asseigned by comparison with enantiopure sample.

8.2 Imine reduction

8.2.1 Catalysis: standard conditions

All experiments were carried out using standard Schlenk techniques, with thoroughly degassed solutions (nitrogen-flushed).

8.2.2 Preparation of stock solutions

Formate, 4.0 M / MOPS, 1.6 M: 3.4 g of sodium formate and 4.20 g of MOPS were dissolved in 12.5 mL of Milli-Q water and the pH was adjusted to 7.25, using solid NaOH. Metal complex, 0.0395 M: $[\eta^6$-(arene)Ru(**Biot-*p*-L**)Cl] resp. $[\eta^5$-(Cp*)M(**Biot-*p*-L**)Cl] were dissolved in degassed DMF and kept under nitrogen at 4°C prior to use. Substrate, 1.0 M: 6,7-dimethoxy-1-methyl-3,4-dihydroisoquinoline was dissolved in degassed Milli-Q water.

8.2.3 General Procedure for Asymmetric Transfer Hydrogenation (ATH)

Streptavidin was directly weighed into the reaction tubes*, (0.206 mM tetramer concentration) having been calculated 1.2 equivalents of as binding sites with respect to the quantity of metal complex used in catalysis. The tubes were carefully flushed with nitrogen and 200 µL of degassed formate/MOPS stock solution was added. The mixture was stirred for 5-10 min until the protein was completely dissolved. 3.8 µL of precursor complex stock solution was added and again the reaction mixture was stirred for 10 min. Finally, 15 µL of substrate stock solution was added. The test tube was placed in a magnetically stirred multireactor, purged several times with nitrogen and heated to the appropriated temperature and time. *Alternatively, the appropriate quantity of Streptavidin was dissolved in formate/MOPS stock solution and degassed. Both methods produced the same results.

Table 14 Conditions used per reaction tube.

Entry	Stock solution	Concentration of stock [M]	Volume applied [µL]	Concentration in assay [mM]
1	HCOONa	4.0	200	3650
2	MOPS	1.6		1460
3	Streptavidin	-	-	0.206 (tetrameric)
4	Metal complex	0.0395	3.8	0.69
5	Substrate	1	15	69

For higher catalyst loadings, the concentration of the catalyst was kept constant and substrate concentration was increased 10 times (0.1%) and 100 times for (0.01%). To test the effect of Lanthanum triflate (La(OTf)$_3$), a 1 to 1 mixture of the substrate with the salt was prepared in degassed water before adding it to the reaction. Preparation of complexes and immobilization of the protein was set up according to literature descriptions.[22b, 22c, 37]

8.2.4 Sample workup

After completion, 500 µL of Milli-Q water was added to the reaction mixture, and the pH was adjusted to approximatively 12, adding a 20 % NaOH solution. The reaction mixture was extracted with 4 x 1 mL of CH$_2$Cl$_2$, dried over Na$_2$SO$_4$, concentrated and subjected to HPLC analysis.

8.2.5 Analytical data

The conversion and the *ee* of the reduction products were determined by chiral HPLC, using a Chiracel OD-H column (5 µm, 250 x 4.6 mm, Daicel Chemical Industries, Tokyo). A hexane/isopropanol/diethylamine (90/10/0.1) mixture was used as eluent with a flow of 1mL / min. The retention times for the amines and the imine are (UV-detection at 280 nm):

(R)-6,7-dimethoxy-1-methyl-1,2,3,4-tetrahydroisoquinoline, t = 15.8 min

(S)-6,7-dimethoxy-1-methyl-1,2,3,4-tetrahydroisoquinoline, t = 13.6 min

6,7-dimethoxy-1-methyl-3,4-dihydroisoquinoline, t = 9.2 min

The absolute configurations of the enantiomers were assigned by comparison with the commercial reference substance *(S)*-6,7-dimethoxy-1-methyl-1,2,3,4-tetrahydroisoquinoline. To determine the conversion, a response factor was determined, taking into account the different UV responses for the imine and the amine. Therefore, 2.30 mg of commercial 6,7-dimethoxy-1-methyl-3,4-dihydroisoquinoline imine substrate (solution 1) and 2.20 mg of commercial *(S)*-6,7-dimethoxy-1-methyl-1,2,3,4-tetrahydroisoquinoline ((*S*)-Salsolidine, solution 2) were dissolved in 3 mL of CH_2Cl_2 each. Different molar ratios of imine and amine were prepared and subjected to HPLC analysis. The ratio of the peak areas imine/amine was plotted against the molar ratio imine/amine. The slope of the regression line indicated the response factor.

Table 15 Conditions used per reaction tube

Entry	Solution 1 [μL]	Solution 2 [μL]
1	900	100
2	700	300
3	500	500
4	300	700
5	100	900

Linear regression of the points gave the following equation:

$$\frac{A_1}{A_2} = 3.6\frac{S}{P} \qquad \text{where} \qquad \frac{S}{P} = \frac{A_2 \cdot 3.6}{A_1}$$

A_1 = HPLC area of the substrate

A_2 = HPLC area of the product (*R*+*S* enantiomer)

S/P = substrate/product (corrected conversion)

8.2.4 Michaelis Menten experiments[37]

Michaelis-Menten experiments were performed using the same catalysis procedure described above. Substrate concentration was varied keeping constant the complex concentration (0.69 mM). The conversion was determined after 20 minutes of reaction using HPLC as described previously.

Table 16 Conditions used per reaction tube.

Entry	Substrate concentration [mM]	Ratio substrate/complex
1	4.31	6.25
2	8.62	12.5
3	17.25	25
4	34.50	50
5	69	100
6	138	200
7	276	400
8	552	800
9	1104	1600
10	2208	3200

The observed initial rate is described as:

$$v = \frac{\left([substrate]_0 \bullet conversion\right)}{t}$$

Calculated from the Michaelis-Menten equation:

$$v = \frac{V_{max}[S]}{K_m + [S]}$$

The fitting of the conversions obtained with a Michaelis-Menten equation was done using a fitting program: GraphPad Prism version 5.02 for Windows, GraphPad Software, San Diego California USA, www.graphpad.com.

The following kinetic parameters were obtained:

Table 17 Kinetic parameters for artificial imine reductase.

Michaelis-Menten	$[\eta^5\text{-(Cp*)Ir(}\mathbf{Biot\text{-}p\text{-}L})\text{Cl}]$	$[\eta^5\text{-(Cp*)Ir(}\mathbf{Biot\text{-}p\text{-}L})\text{Cl}] \subset \text{S112A}$
Best-fit values		
Vmax	0.1814	0.4720
Km	64.22	138.2
Std. Error		
Vmax	0.007429	0.02177
Km	11.05	23.24
95% Confidence Intervals		
Vmax	0.1643 to 0.1985	0.4218 to 0.5222
Km	38.73 to 89.70	84.63 to 191.8
Goodness of Fit		
Degrees of Freedom	8	8
R²	0.9759	0.9811
Absolute Sum of Squares	0.0009774	0.005085
Sy.x	0.01105	0.02521
Constraints		
Km	Km > 0.0	Km > 0.0
Number of points		
Analyzed	10	10

k_{cat} values were are calculated using the following equation:

$$V_{max} = k_{cat} \bullet [E]_0$$

Entry	System	k_{cat}
1	$[\eta^5\text{-(Cp*)M(}\mathbf{Biot\text{-}p\text{-}L})\text{Cl}]$	15.6 h^{-1}
2	$[\eta^5\text{-(Cp*)M(}\mathbf{Biot\text{-}p\text{-}L})\text{Cl}] \subset \text{S112A}$	40.8 h^{-1}

8.1.5 Gels

Analysis of the Sav proteins polymers (CLEAs) was performed by SDS-PAGE prepared as follows:

Table 18 Preparation of the SDS-Page.

Entry	SDS loading gel (12%)	SDS stacking gel (5%)
1	5 mL of dd H_2O	3.4 mL of dd H_2O
2	6 mL of 30% acrylamide	1 mL of 30% acrylamide
3	3.8 mL of Tris pH=8.8	1.5 mL of Tris pH=6.8
4	75 μL of 20% SDS	30 μL of 20% SDS
5	100 μL of 15% APS	40 μL of 15% APS
6	6 μL of TEMED	6 μL of TEMED

Samples were loaded on a gel as follows:

Entry	Protein
1	BenchMark Ladder (Invitrogen)
2	S112A (2 μL)
3	S11A Glu CLEAs
4	S11A PEI CLEAs
5	S11A Dex CLEAs
6	Wt
7	Wt Glu CLEAs
8	Wt PEI CLEAs
9	Wt Dex CLEAs

Each sample contains a 6X loading buffer (6 μL) and biotin-4-fluorescein (2 μL) to reveal the Sav protein on the gel. Gels were analysed using a Biorad camera system.

8.2.6 Cleas[38]

To form CLEAs, the following protocol is used :

1) 100 mg of Sav S112A and Sav Wt are dissolved in 3 ml of H_2O mQ

2) 7 ml of dimethoxyethane are added until precipitation

3) The reaction tubes are stirred on ice

4) Polyethylene imine (PEI) (250 μL of a solution 25%), glutaraldehyde (250 μL of a solution 25%) or activated dextrans (250 μL of a solution 25%) are added to the solutions at 4°C.

5) $NaBH_4$ was added to the reaction at rt and stirred 1h (2 fold excess compared to the concentration of cross-linker)

6) The reactions are stirred 16h

7) Insoluble polymers are centrifuged and lyophilized

9. Bibliography

[1]   R. Noyori, T. Okhuma, *Angew. Chem. Int. Ed.* **2001**, *40*.
[2]   a)H. Meerwein, R. Schmidt, *Justus Liebigs Ann. Chem.* **1925**, *444*, 221; b)A. Verley, *Bull. Soc. Chim. Fr.* **1925**, *37*, 537; c)W. Ponndorf, *Angew. Chem. Int. Ed.* **1926**, *39*, 138.
[3]   a)K.-J. Haack, S. Hashiguchi, A. Fujii, T. Ikariya, R. Noyori, *Angew. Chem. Int. Ed.* **1997**, *36*, 285; b)M. J. Palmer, M. Wills, *Tetrahedron: Asymmetry* **1999**, *10*, 2045; c)S. Gladiali, E. Alberico, *Chem. Soc. Rev.* **2006**, *35*, 226.
[4]   S. Hashiguchi, A. Fujii, J. Takehara, T. Ikariya, R. Noyori, *J. Am. Chem. Soc.* **1995**, *117*, 7562.
[5]   a)H. U. Blaser, C. Malan, B. Pugin, F. Spindler, H. Steiner, M. Studer, *Adv. Synth. Catal.* **2003**, *345*, 103; b)X. Wu, J. Xiao, *Chem. Commun.* **2007**, 2449.
[6]   K. Puentener, L. Schwink, P. Knochel, *Tetrahedron Lett.* **1996**, *37*, 8165.
[7]   a)K. Everaere, A. Mortreux, J.-F. Carpentier, *Adv. Synth. Catal.* **2003**, *345*, 67; b)M. Palmer, T. Walsgrove, M. Wills, *J. Org. Chem.* **1997**, *62*.
[8]   a)T. Sammakia, E. L. Stangeland, *J. Org. Chem.* **1997**, *62*, 6104; b)Y. Nishibayashi, I. Takei, S. Uemura, M. Hidai, *Organometallics* **1999**, *18*, 2291.
[9]   M. T. Reetz, X. Li, *J. Am. Chem. Soc.* **2006**, *128*, 1044.
[10]   M. Yamakawa, H. Ito, R. Noyori, *J. Am. Chem. Soc.* **2000**, *122*, 1466.
[11]   a)Samec Joseph S. M., Bäckvall Jan E., Andersonn Pher G., Brandt Peter, *Chem. Soc. Rev.* **2006**, *35*, 237; b)S. E. Clapham, A. Hadzovic, R. H. Morris, *J. Coord. Chem.* **2004**, *248*, 2201; c)T. Ikariya, K. Murata, R. Noyori, *Org. Biomol. Chem.* **2006**, *4*, 393; d)P. Andersson, I. M. Munslow, *Modern Reduction Methods*, Wiley-VCH Verlag GmbH & Co. KGaA, **2007**.
[12]   R. Noyori, S. Hashiguchi, *Acc. Chem. Res.* **1997**, *30*, 97.
[13]   R. Noyori, M. Yamakawa, S. Hashiguchi, *J. Org. Chem.* **2001**, *66*, 7931.
[14]   C. Bubert, J. Blacker, S. M. Brown, J. Crosby, S. ZFitzjohn, J. P. Muxworthy, T. Thorpe, J. M. J. Williams, *Tetrahedron Lett.* **2001**, *42*, 4037.
[15]   X. Wu, X. Li, W. Hems, W. Hems, F. King, J. Xiao, *Org. Biomol. Chem.* **2004**, *2*, 1818.
[16]   a)X. Wu, X. Li, F. King, J. Xiao, *Angew. Chem. Int. Ed.* **2005**, *44*, 3407; b)S. Ogo, T. Abur, Y. Watanabe, *Organometallics* **2002**, *21*, 2964.
[17]   A. Schlatter, M. K. Kundu, W. D. Woggon, *Angew. Chem. Int. Ed.* **2004**, *43*, 6731.
[18]   A. M. Hayes, D. J. Morris, G. J. Clarkson, M. Wills, *J. Am. Chem. Soc.* **2005**, *127*, 7318.
[19]   a)T. Langer, G. Helmchen, *Tetrahedron Lett.* **1996**, *37*, 1381; b)Y. Jiang, Q. Jiang, G. Zhu, X. Zhang, *Tetrahedron Lett.* **1997**, *38*, 215.
[20]   M. Höhne, T. Bornscheuer, *ChemCatChem* **2009**, *1*, 42.
[21]   a)N. J. Turner, *Nat. Chem. Biol.* **2009**, *5*, 567; b)R. Carr, M. Alexeeva, M. J. Dawson, V. Gotor-Fernández, C. E. Humphrey, N. J. Turner, *ChemBioChem* **2005**, *6*, 637; c)J. Paetzold, J. E. Bäckvall, *J. Am. Chem. Soc.* **2005**, *127*, 17620; d)E. N. Jacobsen, A. Pfaltz, H. Yamamoto, *Comprehensive Asymmetric Catalysis*, Springer, **2004**.
[22]   a)C. Letondor, N. Humbert, T. Ward, *Proc. Natl. Acad. Sci. U.S.A.* **2005**; b)C. Letondor, A. Pordea, N. Humbert, A. Ivanova, S. Mazurek, M. Novic, T. Ward, *J. Am. Chem. Soc.* **2006**, *128*, 8320; c)M. Creus, A. Pordea, T. Rossel, A. Sardo, C. Letondor, A. Ivanova, I. Letrong, R. E. Stenkamp, T. R. Ward, *Angew. Chem. Int. Ed.* **2008**, *47*, 1400.
[23]   A. Basu, S. Bhaduri, K. Sharma, P. G. Jones, *Chem. Commun.* **1987**, 1126.
[24]   E. Mizushima, M. Yamaguchi, T. Yamagishi, *J. Mol. Catal. A: Chem.* **1999**, *148*, 69.
[25]   a)Samec Joseph S. M., J. E. Bäckvall, *Chem. Eur. J.* **2002**, *8*, 2955; b)A. H. Ell, J. B. Johnson, I. J. E. Bäckval, *Chem. Commun.* **2003**, 1652; c)C. P. Casey, J. B. Johnson, *J. Am. Chem. Soc.* **2005**, *127*, 1883.
[26]   a)N. Uematsu, A. Jujii, S. Hashiguchi, T. Ikariya, R. Noyori, *J. Am. Chem. Soc.* **1996**, *118*, 4946; b)J. B. A. Berg, J. S. M. Samec, J.-E. B. ckvall, *Chem. Commun.* **2006**, 2771.
[27]   Lindstöm U.M., Andersson F., *Angew.Chem. Int. Ed.* **2006**, *118*, 562.
[28]   J. W. F. Wang, Y. Ma, X. Cui, L. Cun, J. Zhu, J. Deng, B. BYu, *Chem. Commun.* **2006**, 1766.
[29]   J. Canivet, G. Süss-Fink, *Green Chem.* **2007**, *9*, 391.
[30]   N. Haraguchi, K. Tsuru, Y. Arakawa, S. Itsuno, *Org. Biomol. Chem.* **2008**, *7*, 69.
[31]   L. Chaoqu, X. Jianliang, *J. Am. Chem. Soc.* **2008**, *130*, 13208.
[32]   C. Wang, C. Li, X. Wu, A. Pettman, X. Jianliang, *Angew. Chem. Int. Ed.* **2009**, *48*, 6524.
[33]   L. Evanno, J. Rormala, M. P. Petri, *Chem. Eur. J.* **2009**, *15*, 12963.
[34]   J. E. D. Martins, G. J. Clarkson, M. Wills, *Org. Lett.* **2008**, *11*, 848.
[35]   D. G. Blackmond, M. Ropic, M. Stefinovic, *Org. Process Res. Dev.* **2006**, *10*, 457.
[36]   Cao Linqiu, Van Langen Luuk, Sheldon Roger A, *Curr. Opin. Biotechnol.* **2003**, *14*, 387.
[37]   U. E. Rusbandi, L. Cheikh, M. Skander, A. Ivanova, M. Creus, N. Humbert, T. R. Ward, *Adv. Synth. Catal.* **2007**, *349*, 1923.
[38]   R. A. Sheldon, *Biochem. Soc. Trans.* **2007**, *35*, 1583.
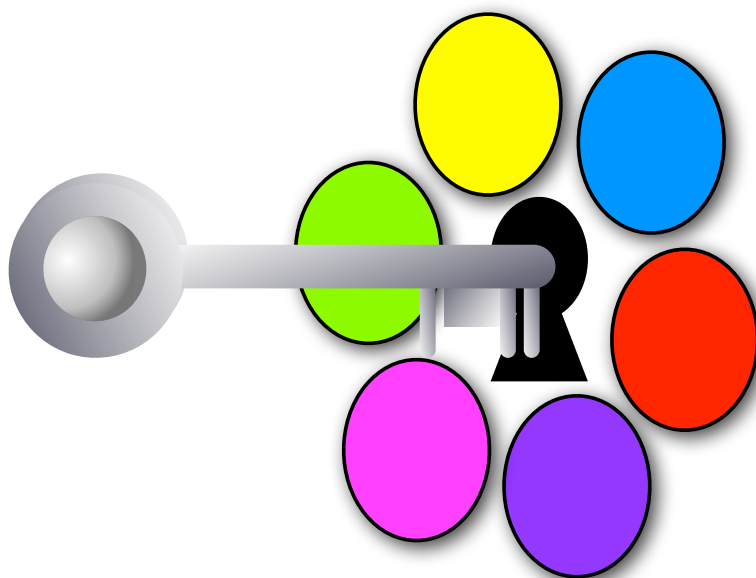
Chapter 4:

General Conclusion and Perspectives

«La grandeur des actions humaines se mesure à l'inspiration qui les fait naître»

Louis Pasteur

Chapter 4: General conclusion and perspectives

Natural enzymes are divided in six different classes according to the chemical transformation they catalyze (see figure 1). By extension artificial metalloenzymes were extensively studied in order to mimick and understand these chemical transformations classes found in natural enzymes. In the six classes, no example of artificial metallohydrolases based on supramolecular anchoring was described in litterature.
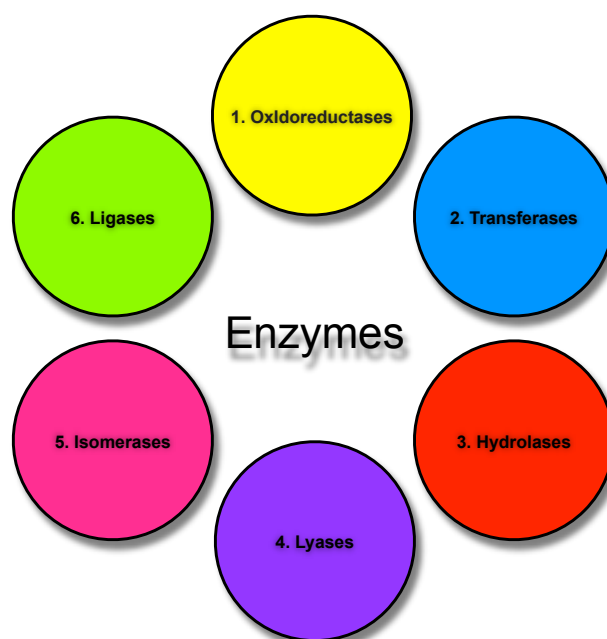
Figure 1 Six enzymes classes'

This thesis focused on two different classes of artificial metalloenzymes: phosphate transferases (hydrolases, EC 3) and transfer hydrogenases (oxidoreductases, EC 1).

The first part of the chapter presented the first example of a selective artificial hydrolase (EC 3) based on biotin-streptavidin. The introduction of biotinylated Ce(IV) complexes afforded an artificial metallohydrolase. The substrate of choice was a chiral phosphodiester mimicking RNA. The chemogenetic optimisation allowed to identify the best hybrid catalysts for the transformation thus

mimicking alkaline phosphatase or purple acid phosphatase. The second coordination sphere arround the artificial metalloenzyme allowed improvements of the activity and selectivity. Hence, the high throughput screening methods based on colorimetric assays have proven their efficiency for the identification of best hybrid catalysts.

The second part of this thesis dealt with artificial transfer hydrogenases (EC 1). The best (*R*) and (*S*)-selective streptavidin-based artificial transfer hydrogenases were described in our laboratory for the enantioselective reduction of acetophenone derivatives. The X-ray structure of the best (*S*)-selective hybrid catalyst was the starting point of a directed evolution protocol that allowed to futher optimize the reduction of dialkylketones (see figure 2). The choice of the chemical fragment in the fisrt screening round have proven efficiency to ameliorate the activity and the selectivity towards challenging substrates. Several interactions are involved in the enantioselection mechanism. Rounds of mutagenesis at selected positions allowed fine-tuning the environnement around the organometallic catalyst to improve interactions with the substrate. These specialized enzymes were obtained with a modest screening effort and based on a protein immobilisation protocol performed on cellular crude extracts. The concept of artificial transfer hydrogenase was extended to the reduction of cyclic imines using saturation mutagenesis at position 112. Some variants of the produced library of artificial metalloenzymes showed high activity and selectivity toward the reduction of a salsolidine precursor. The crystal structure of the first artificial imine reductase allowed speculations on the mechanism of both reduction of aryl ketones and cyclic imines.
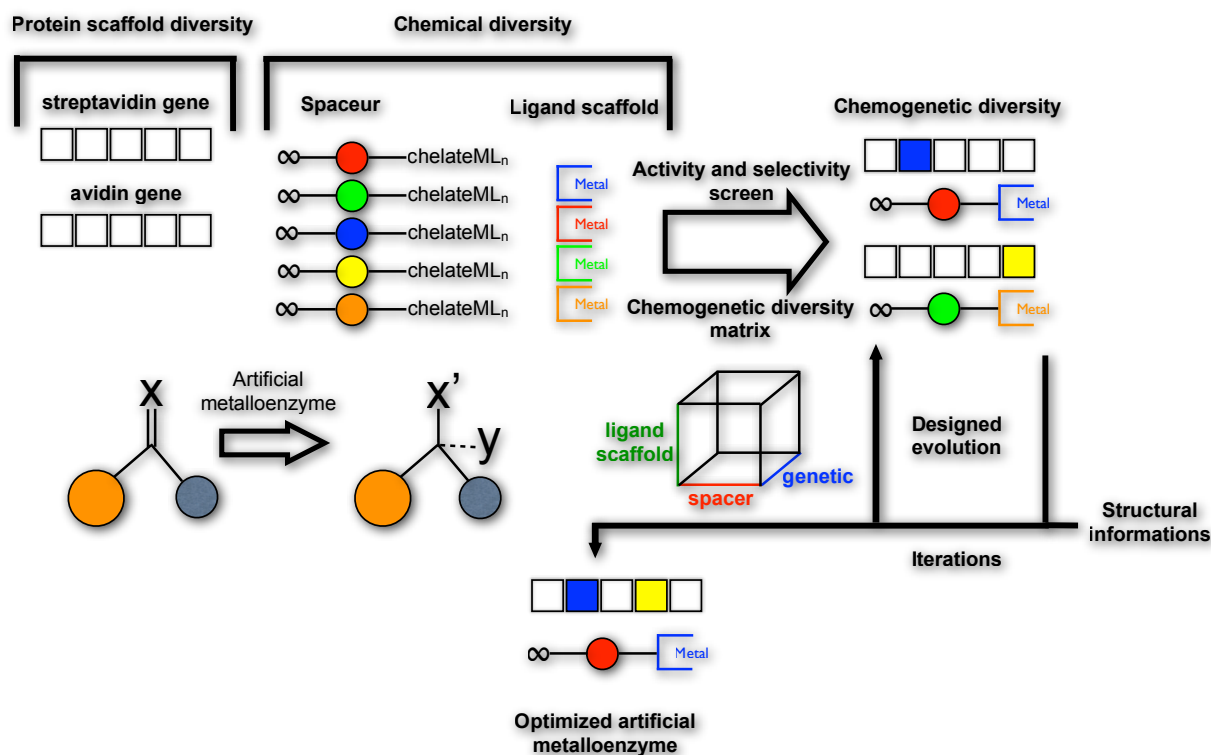
Figure 2 Designed evolution protocol

Artificial metalloenzymes enzymes currently suffer from low activity (few turnovers) and high cost of production. The challenge remains in the developpement of highly active hybrid catalysts. Therefore, the efficient optimisation of artificial metalloenzymes needs a robust high troughput screening method e.g. based on colorimetric assays. For the moment, the hybrid catalysts are produced with pure protein or immobilized proteins. The challenge therefore remains in the identification of a robust system that can be evolved on cellular crude extracts. This would accelerate the process of "designed evolution" and would therefore allow a quick identification of highly active and selective hybrid catalysts for a given reaction opening new routes for the effective synthesis of enantiopure chemicals.

General Conclusion and Perspectives

Annex

<div style="text-align: right">

Annex:

</div>

Annex

Annex

Part 1: Artificial phospholipases

9.1 Introduction

The interest in new phospholipids and phospholipid analogs stems from their potential use as biodegradable surfactants, carriers of drugs or genes or as biologically active compounds in medicine and agriculture. However, the synthesis of these substances is difficult by chemical means since control of regio- and stereoselectivity must be ensured.[1]

Four types of phospholipases (A,B,C,D) which hydrolyze phospholipids with different regioselectivities, have been identified.[1] The cleavage sites for phosphatidyl choline are depicted in figure 1. The physiological role of phospholipases is believed to be the degradation of phospholipid components of cell membranes and the digestion of phospholipid-containing fats in food. They ensure regulation of membrane vesicule trafficking, cytosqueletal reorganisation, cell proliferation and survival signalling.[2] Dysfunctions of phospholipases are known to generate inflammations and phagocytosis, diabetes, neuronal and cardiac stimulation, oncogenesis and metastasis.[2-3]

PLA = Phospholipase A (A$_1$ + A$_2$)
PLC = Phospholipase C
PLD = Phospholipase D

Annex
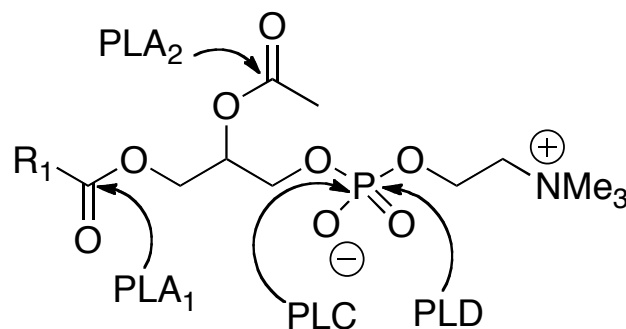
Figure 1 Reaction site of each class of phospholipases. Phospholipase B is a combinaition of both PLA$_1$ and PLA$_2$ activities.

Most of the time, insoluble phospholipids form bilayers, micelles or liposomes in water[4] (see figure 2). Natural enzymes have adapted the environment of the active site to favour interactions of the amino acids around the catalytic center with the charged part of the phospholipids.[3] It leads to close contact between the enzyme and the substrate favouring the reaction.[5]

liposome   micelle   bilayer sheet
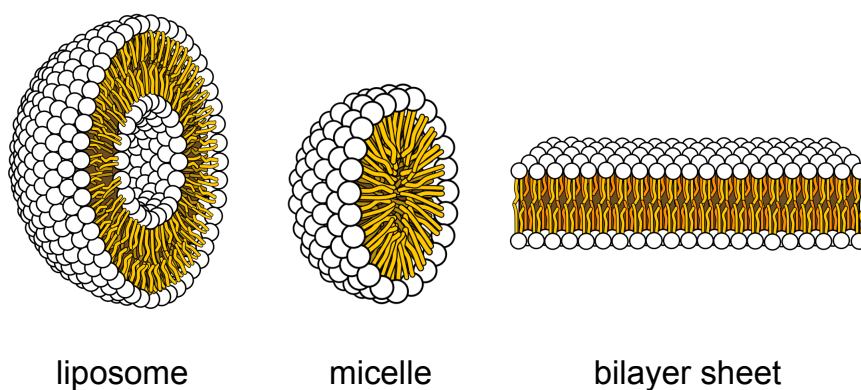
Figure 2 Three possible layouts of phospholipids

Classical phospholipase D (PLD) is a phosphodiesterase that catalyzes the hydrolysis of phosphatidylcholine, the most abundant membrane phospholipid, to form the free base (choline) and phosphatidic acid. Of the four classes, phospholipase D is the only phosphodiesterase that catalyzes the hydrolysis of a non-water miscible to substrate to generate a phospholipid and an alcohol. Futhermore, phospholipase D is the most commonly used phospholipase in organic syntheses. Hydrolysis with PLD leads to phosphatidic acids, but in the presence of suitable alcohols, *e.g.* ethanolamine, glycerol, serine, PLD also catalyzes an efficient head group exchange. These reactions are usually performed in a biphasic mixture in order to ensure high enzymatic activity.[1]

Annex

Phosphodiesterases activities of natural enzymes are widely discussed in literature and many examples cite purple acid phosphatase and alkaline phosphatase for the hydrolysis of phosphodiesters.[6] Trying to mimic these enzymes has also been investigated with a large variety of artificial systems containing an active site bearing Lewis acids (Mg(II), Mn(II), Ce(IV), Zn(II), Cu(II), Fe(III)).[7] However, all of these systems use a soluble substrate. To our knowledge, no artificial phospholipases for non-miscible substrates has been described in literature to date.

Based on the biotin-streptavidin technology previously reported by Whitesides et al.[8], artificial phospholipases are presented herein. The idea was to incorporate the catalyst inside a pocket using supramolecular anchoring via the biotin-(strept)avidin couple. Increasing kinetic parameters of the catalyst and generation of enantioselective discrimination towards non-miscible to water substrates was expected. The biotinylated complex of choice was a dinuclear cerium based catalyst described by Que et al.[9] The catalyst is known to have a good hydrolytic acceleration rate towards the substrate bisnitrophenylphosphate (BNPP) and is also capable of cleaving double stranded DNA (ds-DNA).[10]

Previous reports in our group showed that incorporation of biotinylated complexes into streptavidin leads to active and enantioselective artificial metalloenzymes for various reactions.[11] Both chemical diversity of the ligand scaffold and genetic diversity, for fine tuning, were exploited with success.[11e]

Annex

Herein, it is shown that artificial phospholipases (see figure 3) based on biotin-streptavidin technology can be chemo-genetically optimized to improve characteristics such as selectivity and conversion towards phospholipids.

9.2 Results and discussion

To generate diversity, both chemical and genetic optimization strategies were combined. Combining *m* streptavidin isoforms with *n* biotinylated catalyst precursors yields a two-dimensional diversity matrix of *n,m* combinations. A screening method was established in 96 well plates by following the nitrophenolate absorbance at 405 nm (hydrolysis of the substrate). A total of six complexes were formed *in situ* in the plate by mixing the ligand dissolved in HEPES, 100 mM pH=8 and cerium ammonium nitrate (CAN). After 15 minutes of incubation at 37 °C, streptavidin isoforms (8 per plate) in HEPES buffer solution were directly added in separate wells to the complexes and incubated for 15 minutes at 37 °C to form the hybrid catalyst. Both enantiomers of the substrate were added prior reading in the spectrometer (37 °C). A total of 276 possibilities were screened. After 3 h reaction, a workup protocol was established in order to dissolve the suspensions. DMSO was added to each well and mixed. Plates were centrifuged at 4400 rpm during 10 minutes and a carbonate buffer at pH = 9 was added to enhance the intensity of the yellow colour. The conversion was determined by measuring the absorbance at 405 nm. Previous work showed that 3 positions in loop 7,8 of streptavidin S112, K121, L124 were close to the biotinylated complex and that these may influence both conversion and enantioselectivity of the catalyst.

Based on these observations, representative mutations at these three positions were selected including: aromatic, polar, non-polar and charged amino acids residues. The conversions were determined after 3 hours (end-point assay).

Annex

Concept
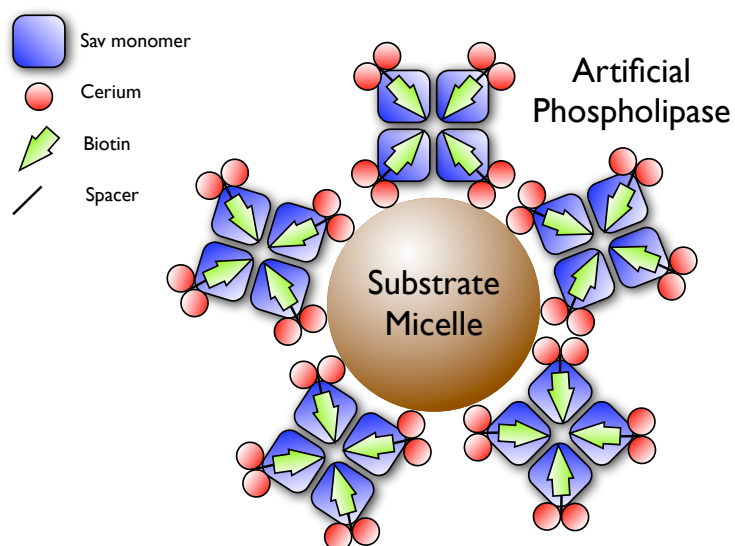
Figure 3 Schematic representation of the artificial phospholipase based on the biotin-streptavidin technology. The anionic substrate forms micelles in water which interact with the cationic artificial metalloenzyme

Annex

9.2.1 Substrates

Three amphiphylic substrates were synthesised in enantiopure form according to the literature. All of the substrates were insoluble in water thus forming micelles (see figure 4).
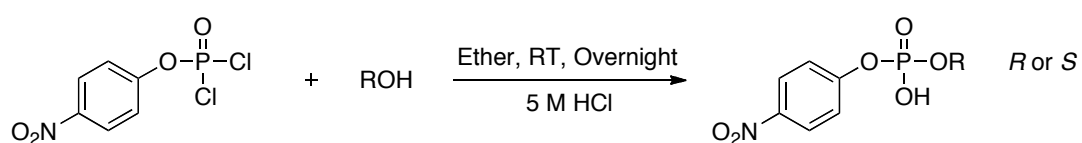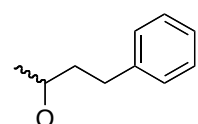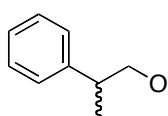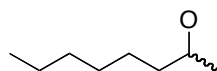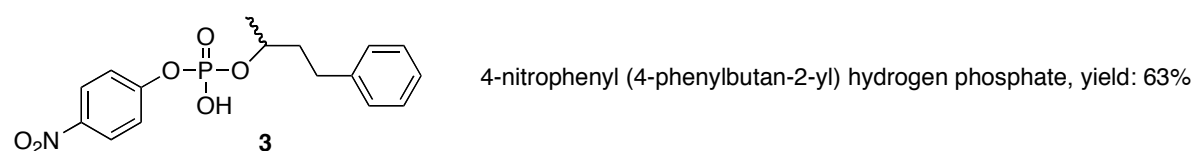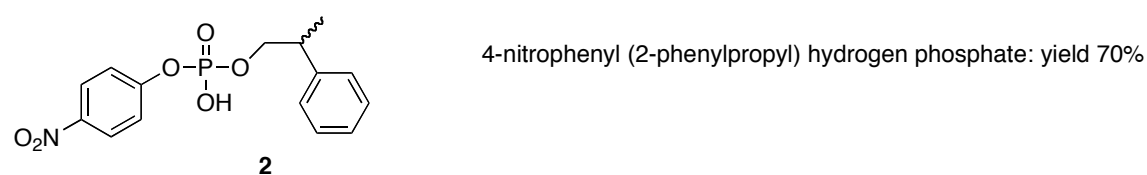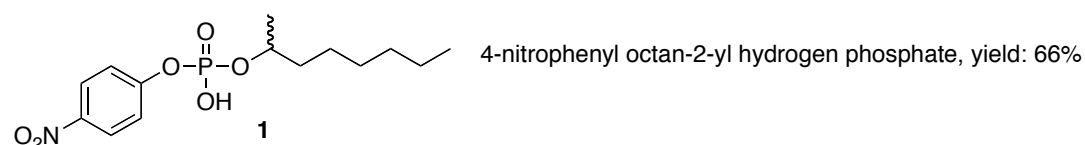
Figure 4 Synthesis of enantiopure phosphodiesters.

7.2.2 Genetic Diversity

The mutant library presented in chapter 2 for HPNP hydrolysis was used for this study.

Annex

9.2.3 Chemical Diversity

A total of three biotinylated cerium complexes; {(**Biot-HXTA**)Ce$_2$}$^{3+}$, {(**Biot-2-IDA**)Ce}$^{2+}$, {(**Biot-3-IDA**)Ce}$^{2+}$, were prepared *in situ* by reaction of the appropriate ligand dissolved in HEPES buffer (100 mM, pH=8) with cerium ammonium nitrate (CAN). For the first optimization step, the three catalysts precursors were screened in the presence of WT Sav. The substrate was dissolved in acetonitrile and added to the reaction wells prior to reading. The results of the conversion (TON) are summarized using a fingerprint display for each substrate-protein-ligand combination. The conversion is color-coded from white (no conversion) to red (best conversion). The display shows the best combination of complex/mutant/substrate under the screening conditions (see figure 5)

Interesting features are apparent from figure 5:

Turnover number (see figure 5):

i)   The dinuclear cerium complexes presented a higher hydrolytic activity against the phosphodiester substrates compared to the mononuclear complexes, especially for substrate 1 and 2.

ii)   Of all the mutants tested, only mutations at positions K121R & K121N increased the TON, while mutations at positions 112 and 124 showed almost no improvement.

Of all the complexes used, {(**Biot-HXTA**)Ce$_2$}$^{3+}$ gave the best conversions for the hydrolysis of the substrate probably due to the cooperativity between the two metals. It is especially true for substrate (**1**) that presents a non-aromatic side chain. The increased activity observed for this substrate, in combination with S112R or S112N (Table.1, entry 1 and 2) could be due to a higher accessibility of the substrate to the active site.

Annex

Enantioselectivity (see figure 6):

    i)   Both chemical and genetic diversity can lead to an increase in the enantioselectivity.

    ii)   The IDA ligand gaves better estimated E values than the HXTA scaffold.

    iii)   The best estimated E values of the catalytic runs is 13.15 for {(**Biot-2-IDA**)Ce}$^{2+}$ ⊂ 112F.

    iv)   Most of the mutants that lead to enantioselectivity are aromatic or negatively charged amino acid.

{(**Biot-2-IDA**)Ce}$^{2+}$ and {(**Biot-HXTA**)Ce$_2$}$^{3+}$ were more efficient at discriminating enantiomers of substrate **1** (see table.2). Aromatic residues with the mentioned complexes improve enantiodiscrimination. In addition, some of the mutants with the same complex yielded the opposite enantiomer for the hydrolysis and best examples are given for substrate **3** (Table 2, entry 1 compared 10). Interestingly, aromatic residues gave best enantiodiscriminations while best activities were obtained with non-aromatic substrates.
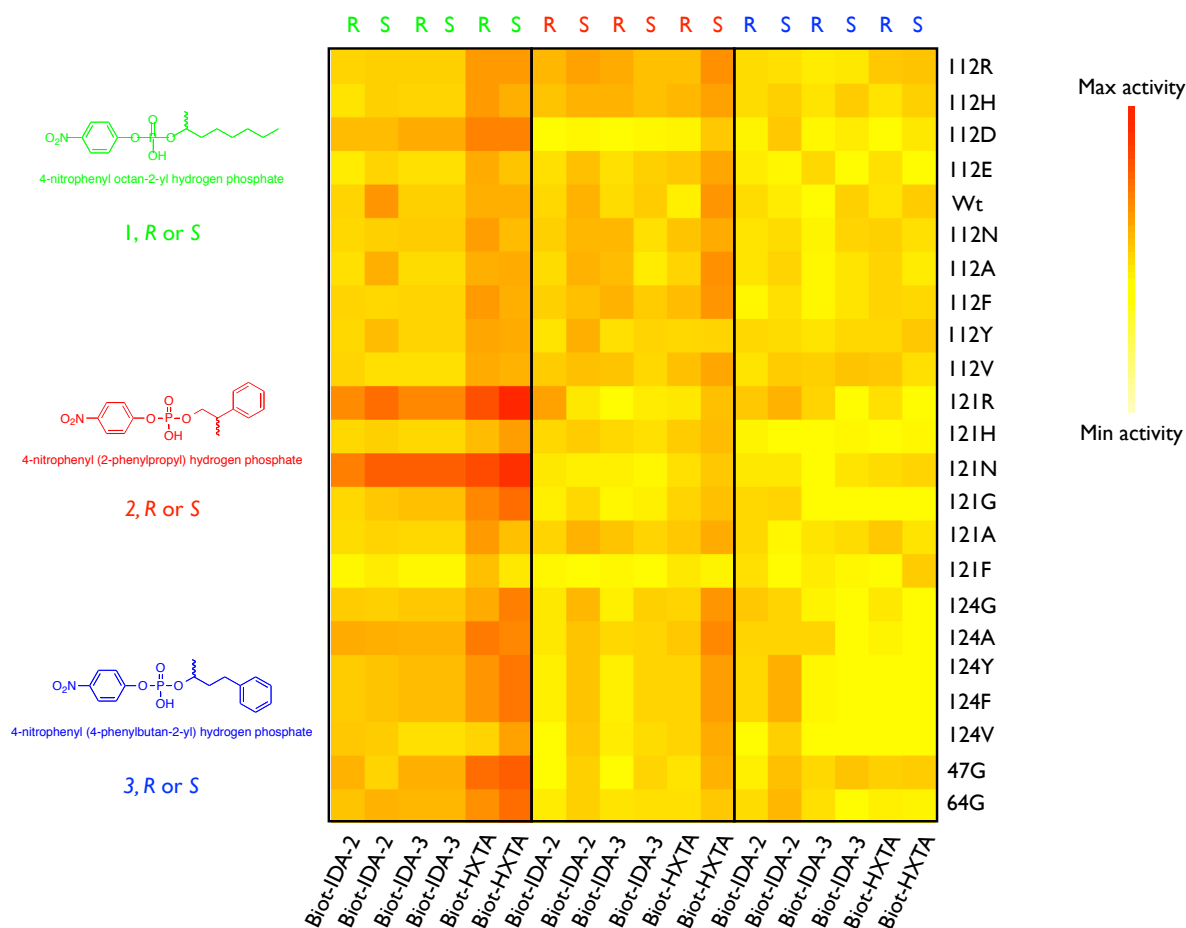
Figure 5 Mapping of the TON (turnover number) of the catalyst for phosphodiester hydrolysis of substrate 1, 2 and 3 after 3 h of reaction. The *R* and *S* substrates were tested with Sav mutants without complexes to establish the background reaction. The background reaction was subtracted to the catalytic runs performed with the artificial metalloenzymes.

Annex

Table 1: Selected best TON of the screening

Entry	Complex	Substrate	Enantiomer	Mutant	TON
1	$\{(\textbf{Biot-HXTA})Ce_2\}^{3+}$	**1**	*S*	K121R	2.09
2	$\{(\textbf{Biot-HXTA})Ce_2\}^{3+}$	**1**	*S*	K121N	1.84
3	$\{(\textbf{Biot-HXTA})Ce_2\}^{3+}$	**1**	*S*	V47G	1.37
4	$\{(\textbf{Biot-HXTA})Ce_2\}^{3+}$	**1**	*S*	K121G	1.24
5	$\{(\textbf{Biot-HXTA})Ce_2\}^{3+}$	**1**	*S*	P64G	1.22
6	$\{(\textbf{Biot-HXTA})Ce_2\}^{3+}$	**2**	*S*	S112R	1.14
7	$\{(\textbf{Biot-HXTA})Ce_2\}^{3+}$	**1**	*S*	L124Y	1.13
8	$\{(\textbf{Biot-HXTA})Ce_2\}^{3+}$	**1**	*R*	L124A	1.1
9	$\{(\textbf{Biot-HXTA})Ce_2\}^{3+}$	**1**	*S*	L124G	1.06
10	$\{(\textbf{Biot-HXTA})Ce_2\}^{3+}$	**2**	*R*	S112A	0.89
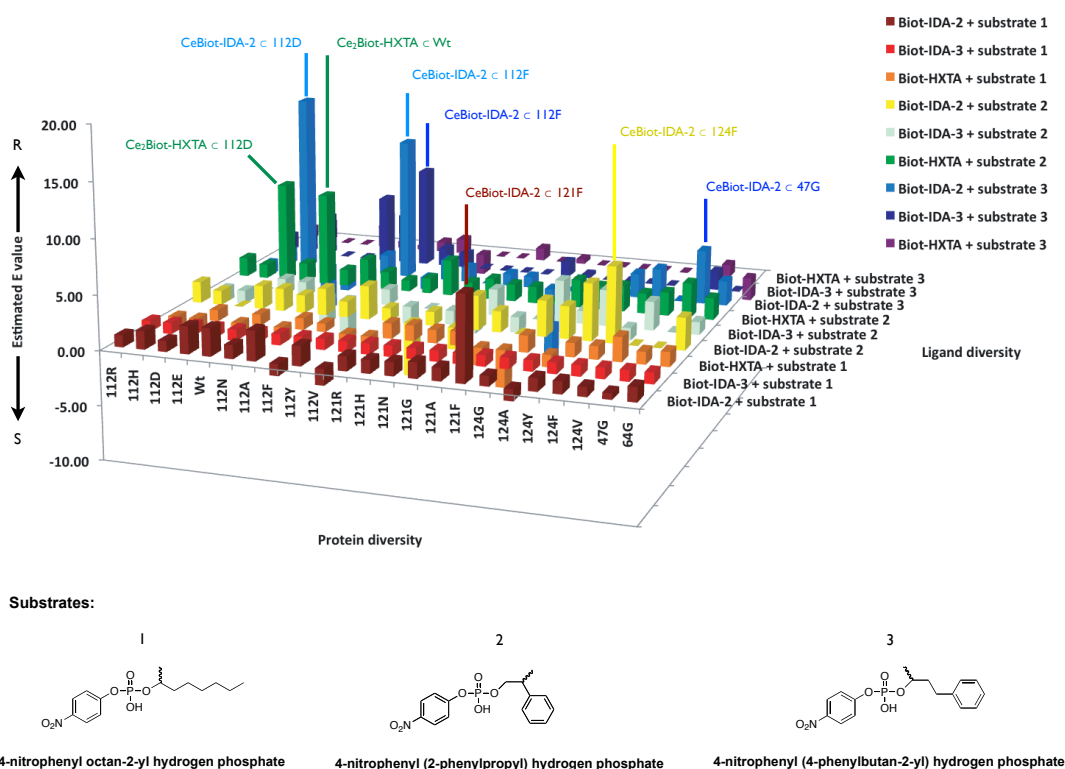
Figure 6 Chart of the estimated *E* for phosphodiester hydrolysis of substrate (**1**), (**2**) and (**3**) after 3 h reaction time. The background reactions were substracted from the data obtained with artificial metalloenzymes.

Table 2: Selected best estimated E values from the screening

Entry	Complex	Mutant	Substrate	estimated E value
1	{(**Biot-2-IDA**)Ce}$^{2+}$	S112D	3	16.5
2	{(**Biot-2-IDA**)Ce}$^{2+}$	S112F	3	13.2
3	{(**Biot-HXTA**)Ce$_2$}$^{3+}$	S112D	2	9.3
4	{(**Biot-HXTA**)Ce$_2$}$^{3+}$	Wt	2	8.6
5	{(**Biot-2-IDA**)Ce}$^{2+}$	K121F	1	7.8
6	{(**Biot-2-IDA**)Ce}$^{2+}$	L124F	2	6.7
7	{(**Biot-2-IDA**)Ce}$^{2+}$	L124Y	2	5.3
8	{(**Biot-2-IDA**)Ce}$^{2+}$	V47G	3	5.0
9	{(**Biot-2-IDA**)Ce}$^{2+}$	S112E	3	-4.2
10	{(**Biot-2-IDA**)Ce}$^{2+}$	K121A	3	-7.2

9.2.4 Substrate-protein interactions

In order to determine if streptavidin interacts with the substrate, immobilization experiments of the protein on the substrate were performed (see figure 7). The substrate was added to water to form micelles and a solution of streptavidin was added on it. The biphasic mixture was shaken for 30 minutes and the reaction centrifuged to separate the precipitate from the supernatant. The pellet and supernatant were loaded into a 12% SDS-PAGE gel to determine whether the protein interacts strongly with the micelles formed by the substrate. (B$_4$F was added to reveal the presence of streptavidin)
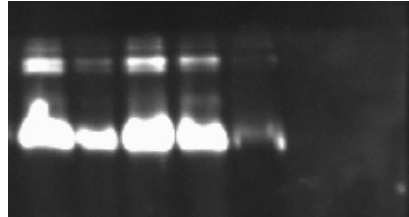
Annex

Pellet:

1 2   3   4   5   6

1 = S112K pellet with (*R*)-4-nitrophenyl (4-phenylbutan-2-yl) hydrogen phosphate
2 = S112K pellet with (*S*)-4-nitrophenyl (4-phenylbutan-2-yl) hydrogen phosphate
3 = S112K pellet with (*R*)-4-nitrophenyl (2-phenylpropyl) hydrogen phosphate
4 = S112K pellet with (*S*)-4-nitrophenyl (2-phenylpropyl) hydrogen phosphate
5 = positive control with Wt
6 = positive control with S112K

Supernatant :

1   2   3   4   5   6

1 = S112K pellet with (*R*)-4-nitrophenyl (4-phenylbutan-2-yl) hydrogen phosphate
2 = S112K pellet with (*S*)-4-nitrophenyl (4-phenylbutan-2-yl) hydrogen phosphate
3 = S112K pellet with (*R*)-4-nitrophenyl (2-phenylpropyl) hydrogen phosphate
4 = S112k pellet with (*S*)-4-nitrophenyl (2-phenylpropyl) hydrogen phosphate
5 = positive control with Wt
6 = positive control with S112K

Figure 7 Immobilization of streptavidin on different substrates forming micelles indicating that streptavidin strongly interacts with the anionic substrate.

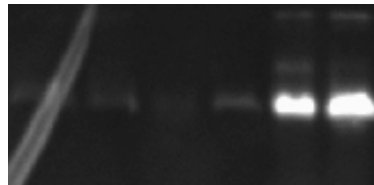In nature, phospholipases adhere to the substrate to react with the substrate. SDS-PAGE shows that streptavidin interacts with the micelles and mimics the phospholipases binding to the insoluble substrate. When complexes are added to streptavidin, the global positive charge of the metalloenzyme increases further which could give rise to Coulomb interactions with the phosphate moiety of the phospholipidic substrate. In this context, ionic interaction of the catalyst directly with the substrate significantly increases the effective molarity.

9.3 Conclusion

The screening of the 207 metal $\subset$ protein combinations using a 96 well plate format allowed to chemo-genetically optimize a heterogeneous hydrolytic reaction. The position and nature of the mutations around the catalyst-binding pocket were crucial for the optimization of the artificial phospholipase and to enantioselectivity. As in the active site of natural enzymes, tuning the environment of the catalyst improved the overall kinetic characteristics of the system. Furthermore, interactions of the streptavidin with the insoluble substrates allowed its "immobilization" of an artificial enzyme on substrates.

Part 2: Artificial restriction enzymes

9.4 Introduction

{(**Biot-HXTA**)Ce$_2$}$^{3+}$ has been reported in literature to cleave phosphosdiesters such as the model substrate BNPP (**2**).[9] In the first part of the research, efforts were devoted to phosphodiester hydrolysis to create artificial phosphodiesterase. A model substrate for RNA (HPNP, **1**) was used to investigate the kinetic properties of the hybrid catalyst.[10] One of the major challenges in this field is to create highly active and selective artificial phosphodiesterases in order to create artificial restriction enzymes for medical applications such as cancer therapeutics.[7] Such artificial catalysts

may be able to recognize a specific DNA or RNA target and cleave it. Both DNA and RNA can be found in a single strand form[12] and are a potential target for artificial restriction enzymes. Designing an active site of such an enzyme is particularly challenging and many artificial catalysts have been tailored to improve their activity by chemical means.[13] Streptavidin presents the advantage to offer both a defined active site in the vicinity of the anchored complex and an enormous potential for amino acid shuffling as a protein.

Tailoring the active site is of interest to improve specific interactions of the complex to the substrate. It would be a first step towards the development of a new generation of artificial phosphatases for gene silencing, cancer treatments or new biotechnological applications.[13b]

9.5 Results and discussion

In order to investigate the cleavage of single stranded DNA, a biotinylated single stranded DNA, containing six nucleotides (poly A) was designed, and a fluorescent tag (FAM) added. The biotinylated substrate was added to WT streptavidin. The presence of a biotin anchor ensured its localization within streptavidin.

Thanks to the dimer of dimer nature of Sav with close lying biotin binding sites, it was anticipated that, in the presence of both Biot-AAAAAA-FAM and $\{(\textbf{Biot-HXTA})Ce_2\}^{3+}$, the polyA substrate may be bought in close proximity to the biotinylated Lewis acid. This could thus improve the hydrolytic efficiency, to liberate FAM which could be detected by fluorescence (see figure 8).

General concept of a artificial restriction pseudoenzyme
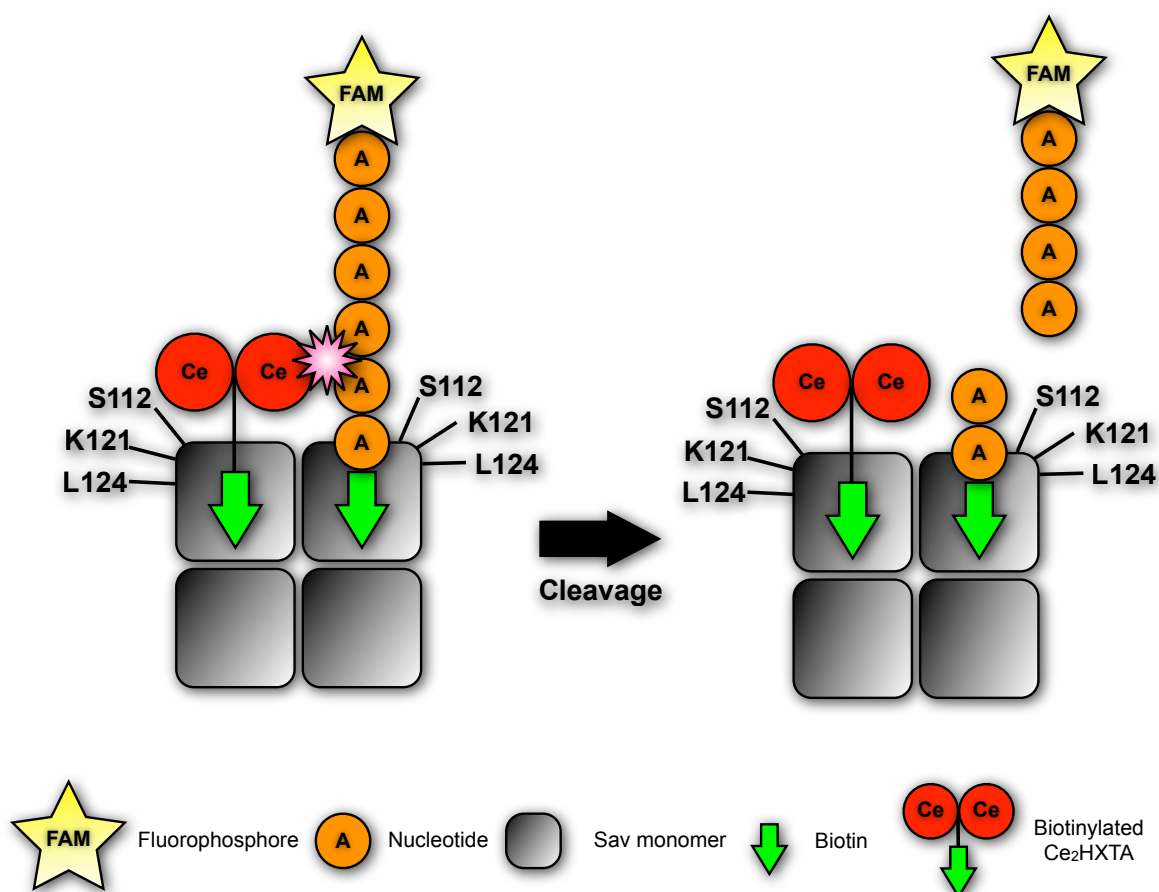
Figure 8 A biotinylated single stranded DNA, composed of 6 adenosines bases and bearing at the end an FAM, was designed. This substrate was anchored into WT streptavidin. Upon addition of {(**Biot-HXTA**)Ce$_2$}$^{3+}$, cleavage occurs and liberates the FAM moiety.

SDS-PAGE

Biot-AAAAAA-FAM ⊂ Sav
= not migrating

cleaved FAM
= migrating

without spiking with Sav WT

Spiking with
Sav WT after 3h

non-hydrolysed substrate

hydrolysed substrate

Gel 1: {(**HXTA**)Ce$_2$}$^{3+}$ and {(**BiotHXTA**)Ce$_2$}$^{3+}$
cleaves efficiently single stranded DNA

Sav WT prevents
the cleavage

Cleavage occurs with
{(BiotHXTA)Ce$_2$}$^{3+}$

Gel 2: Sav WT prevents the hydrolysis of the
single stranded DNA from {(**HXTA**)Ce$_2$}$^{3+}$

30min   1h   1h30   2h   2h30

Gel 3: The reaction occurs rapidly

Figure 9 Cleavage of the Biot-AAAAAA-FAM with {(**Biot-HXTA**)Ce$_2$}$^{3+}$ in the presence of WT streptavidin.

1) **Gel 1** (see figure 9) demonstrates that Sav binds to the biotinylated nucleotide. Futhermore cleavage occured with {(**Biot-HXTA**)Ce$_2$}$^{3+}$ and with {(**HXTA**)Ce$_2$}$^{3+}$ (spiking of the substrate with Wt Sav after 3h) but not with CAN alone, it demonstrated that a dinuclear complex is necessary for cleavage.

2) **Gel 2** (see figure 9) demonstrates that Sav Wt prevents the cleavage of the biotinylated nucleotide from {(**HXTA**)Ce$_2$}$^{3+}$ but not for {(**Biot-HXTA**)Ce$_2$}$^{3+}$. Avidin, which is positively charged

Annex

at pH = 8 and adheres to DNA, shows the same activity for the cleavage of biotinylated single stranded DNA.

3) **Gel 3** (see figure 9) demonstrates that the reaction occurs quickly, within 30 min.

Only close contact between the catalytic center and the single stranded DNA leads to cleavage: no cleavage occurs with CAN or with $\{(\textbf{HXTA})Ce_2\}^{3+}$, it demonstrates that the biotinylated DNA is protected against hydrolysis by streptavidin. With $\{(\textbf{Biot-HXTA})Ce_2\}^{3+}$, cleavage occurs due to the close proximity of the metal center to single stranded DNA. It permits the hydrolysis of the polynucleotide with high efficiency thus liberating the fluorophore.

9.6 Conclusion

A new method for selective single stranded DNA cleavage has been developed with a pseudo artificial metalloenzyme. The active site of the artificial metalloenzyme can be modulated in order to provide specific interactions and cleavage of the substrate.

Annex

9.7 Bibliography

[1]   U. Bornscheuer, R. Kazlauskas, *Hydrolases in organic synthesis: regio-and stereoselective biotransformations*, 2nd edition ed., WILEY-VCH Verlag GmBH & Co.kGaA, **2006**.

[2]   H. Ping, M. A. Frohman, *Expert Opin. Ther. Targets* **2007**, *11*.

[3]   G. M. Jenkins, M. A. Frohman, *Cell. Mol. Life Sci.* **2005**, *62*, 2305.

[4]   a)M. Jones, *Adv. Colloid Interface Sci.* **1995**, *54*, 93; b)P. Walde, K. Cosentino, H. Engel, P. Stano, *ChembioChem*, *11*, 848; c)A. M. Dopico, *Methods in Membrane Lipids*, Humana Press, **2007**.

[5]   M. Grandbois, H. Clausen-Schaumann, H. Gaub, *Biophys. J.* **1998**, *74*, 2396.

[6]   a)G. Schenk, L. R. Gahan, L. E. Carrington, N. Mitlic, M. Valizadeh, S. E. Hamilton, J. de Jersey, L. W. Guddat, *Proc. Natl. Acad. Sci. U. S. A.* **2004**, *102*, 273; b)J. E. Coleman, *Annu. Rev. Biophys. Biomol. Struct* **1992**, *21*, 441.

[7]   J. Cowan, *Curr. Opin. Chem. Biol.* **2001**, *5*, 634.

[8]   M. Wilson, G. Whitesides, *J. Am. Chem. Soc.* **1978**, *100*, 306.

[9]   M. E. Branum, A. K. Tipton, S. Zhu, L. Que, *J. Am. Chem. Soc.* **2001**, *123*, 1898.

[10]   D. Brown, D. Usher, *J. Chem. Soc.* **1965**, 6558.

[11]   a)M. Creus, A. Pordea, T. Rossel, A. Sardo, C. Letondor, A. Ivanova, I. Letrong, R. E. Stenkamp, T. R. Ward, *Angew. Chem. Int. Ed.* **2008**, *47*, 1400; b)G. Klein, N. Humbert, J. Gradinaru, A. Ivanova, F. Gilardoni, U. E. Rusbandi, T. R. Ward, *Angew. Chem. Int. Ed.* **2005**, *44*, 7764; c)J. Pierron, C. Malan, M. Creus, J. Gradinaru, I. Hafner, A. Ivanova, A. Sardo, T. R. Ward, *Angew. Chem. Int. Ed.* **2008**, *47*, 701; d)A. Pordea, M. Creus, J. Panek, C. Duboc, D. Mathis, M. Novic, T. R. Ward, *J.Am.Chem.Soc.* **2008**, *130*, 8085; e)M. Creus, T. R. Ward, *Org. Biomol. Chem.* **2007**, *5*, 1835.

[12]   a)M. Orita, H. Iwahana, H. Kanazawa, K. Hayashi, T. Sekiya, *PNAS* **1989**, *86*, 2766; b)J. M. Berg, J. L. Tymoczko, L. Stryer, *Biochemistry*, fifth ed., Freeman, W H, **2002**.

[13]   a)R. Bonomi, G. Saielli, U. Tonellato, P. Scrimin, F. Mancin, *J. Am. Chem. Soc.* **2009**, *131*, 11278; b)F. Mancin, P. Scrimin, P. Tecilla, U. Tonellato, *Chem. Commun.* **2005**, 2540.

[14]   F. Rosati, G. Roelfes, *ChemCatChem* **2010**, *2*, 916.

CV

Education

2006-2011	**PhD student in chemistry**

Department of Chemistry, University of Basel (CH)

2004-2006	**Master in science, mention very good, Jean Landry Prize**

University of Neuchâtel (CH)

2001-2004	**Bachelor in science**

University of Neuchâtel (CH)

1999-2001	**Maturity type C (scientific)**

High School Denis-de-Rougemont, Neuchâtel (CH)

Research experience

PhD Thesis, University of Basel   2006 to 2010

Artificial Metalloenzymes Laboratory (AMEL), University of Basel

Thesis: Artificial Phosphate Transferases and Hydrogen Transferases Based on Biotin-Streptavidin Technology.

Supervisor: Prof Thomas R. Ward

Summary: The work consisted of developing artificial metalloenzymes for enantioselective catalysis by incorporation of a catalytically active metal fragment within streptavidin. We have developed immobilized artificial hydrogenases for ketone and imine reduction and artificial phosphodiesterases for kinetic resolution of chiral phosphodiesters.

Technical skills:

- Synthesis background: multi-step synthesis, work under controlled atmosphere (Schlenk techniques)

- Catalysis background: asymetric homogeneous organometallic catalysis, enzymatic catalysis, parallel catalyst screening using a multireactor, high throughput screening methods in ELISA plates.

- Standard purification and characterization methods: flash chromatography, NMR, MS, UV-Vis, analytical HPLC and GC.

- Protein production and characterisation

Master thesis   2005 to 2006

Laboratory of molecular parasitology, University of Neuchâtel

Master thesis: Surface treatment of polymers with an ionic beam to ameliorate human cell adhesion, proliferation and differentiation.

Annex

Supervisor: Prof Bruno Betschart, Dr Serguei Mikhaïlov, Dr Martha Liley

Summary: The work consisted of identifying human cell lines capable of specific interactions to ionic beam irradiated nanostructured surfaces. The topography and the chemistry of treated surfaces were in this context characterized.

Technical skills:

- Human cell line cultures under sterile conditions
- Tissue colorations
- ELISA techniques
- Gel techniques
- Microscopy techniques
- Immunofluorescence techniques

Training, University of Neuchâtel February to June 2005

Molecular Parasitology Laboratory under the supervision of Professor Bruno Betschart

Technical skills:

- Human cell line cultures under sterile conditions

Training, Bern Hospital   August to October 2004

Clinical Pharmacology Laboratory under the supervision of Professor Jean-François Dufour

Techinical skills:

- Protein expression
- PCR and RT-PCR
- Gel techniques
- Human cell line cultures under sterile conditions

Awards

- Jean Landry Prize for the master thesis (5.62/6)

Publications

«Artificial Transfer Hydrogenases for the Enantioselective Reduction of Cyclic Imines». M. Dürrenberger, Tillmann Heinisch, Yvonne M. Wilson, Thibaud Rossel, Elisa Nogueira, Livia Knörr, Annette Mutschler, Karoline Kersten, Malcolm Jeremy Zimbron, Julien Pierron, Tilman Schirmer and Thomas R. Ward**. *Manuscript accepted by Angewandte Chemie International Edition.*

«Designed Evolution of an Artificial Transfer Hydrogenase Based on the Biotin-Streptavidin Technology». A. Pordea, M. Creus, T. Rossel, A. Sardo, C. Letondor, A.Ivanova, I. LeTrong, R. E.Stenkamp, T. R. Ward, *Angew. Chem, Int. Ed.,* **2008**, *47,* 1400.

«Surface Treatment of Polymers by Ion Beam Irradiation to Control the Human Osteoblast Adhesion: Fluence and Current Density». G. Guibert, T. Rossel, G. Weder, B. Betschart, C. Meunier and S. Mikhailov. *AIP Proceedings,* **2009**, *1099*, 511.

Skills

Languages:

French: mother tongue

English: fluent

German: high school level (2 years laboratory teaching in German)

Teaching:

- An apprentice in chemistry for one year

- Three undergraduate students on three different research projects for 6 months each.

- Laboratory section of analytical chemistry for undergraduate students in biology and pharmacy.

Informatics:

Scientific software: Scifinder, Chemdraw, Isisdraw, WeblabviewerPro, DS Visualizer, Prism, Fingerprinting

Office software: Word, Excel, Powerpoint, Kaleidagraph

Drawing software: CS Illustrator, CS Photoshop, Graphic converter

Maintenance of the informatic systems of the group during the PhD.

Conferences and posters

Conferences:

- CUSO's summerschool, Villars, Switzerland, September 2006
- CUSO's summerschool, Villars, Switzerland, September 2007
- Biocat, Hamburg, Germany, September 2008
- Biotrans, Bern, Switzerland, July 2009

Posters:

- Swiss Chemical Society 2007, 2008, 2009, 2010 (Poster prize)
- Biotrans, Bern, Switzerland, July 2009